ISSN: 2687-2153

IJEIR

International Journal of Engineering & Innovative Research

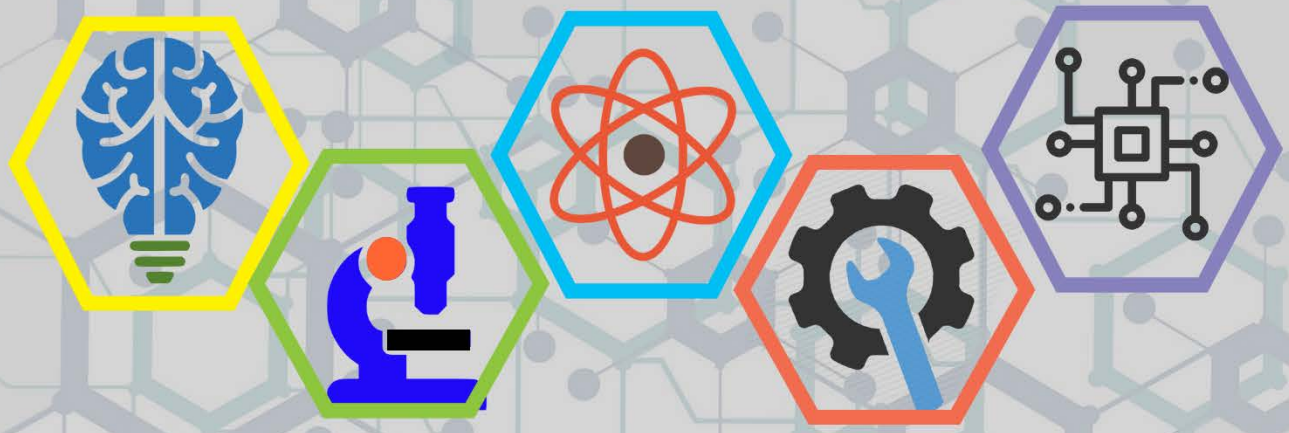

Volume: 3 Issue: 3

International Journal of Engineering and Innovative Research (IJEIR)

Year: 2021 **Volume:** 3 **Issue:** 3

Correspondence Address

International Journal of Engineering and Innovative Research (IJEIR)
Secretaries Office
Isparta University of Applied Sciences
Isparta / Turkey

Phone and e-mail
Tel: +90 0246 531 26 21 - 0246 531 26 22
E-mail: ijeirturkey@gmail.com

e-ISNN: 2687-2153

International Journal of Engineering and Innovative Research (IJEIR)

Year: 2021 **Volume:** 3 **Issue:** 3

International Journal of Engineering and Innovative Research (IJEIR)

Year: 2021 **Volume:** 3 **Issue:** 3

CONTENTS **PAGE**

Research Articles

Research Article

MODELLING AND EXPERIMENTAL INVESTIGATION OF COPPER-ZINC ALLOY USING SPLIT-SPLIT PLOT DESIGN

Authors: Dickson David OLODU, Okagbare, G.O

To cite to this article: Olodu, D. D. Okagbare, G.,O,. (2021). MODELLING AND EXPERIMENTAL INVESTIGATION OF COPPER-ZINC ALLOY USING SPLIT-SPLIT PLOT DESIGN. International Journal of Engineering and Innovative Research , 3(3), p:175-186 . DOI: 10.47933/ijeir.905756

DOI: 10.47933/ijeir.905756

International Journal of Engineering and Innovative Research

http://dergipark.gov.tr/ijeir

MODELLING AND EXPERIMENTAL INVESTIGATION OF COPPER-ZINC ALLOY USING SPLIT-SPLIT PLOT DESIGN

[1*] Dıckson Davıd OLODU, [1]OKAGBARE, G.O

[1] Benson Idahosa University, Faculty of Engineering, Department of Mechanical Engineering, PMB 1100, Benin City, Edo State, NIGERIA.

Corresponding Author E-mail: dolodu@biu.edu.ng

https://doi.org/10.47933/ijeir.905756

(**Received:** 30.03.2021; **Accepted:** 22.05.2021)

ABSTRACT: This study focused on the modelling and experimental investigation of Copper-Zinc alloy using Split-split plot design. The effects of process parameters such as percentage by volume of material, material type (copper and zinc), pressure and their interactions on the mechanical properties of the produced copper-zinc alloy using split-split plot design was investigated. The mechanical properties examined in this study include; tensile strength, modulus of elasticity, shear modulus and hardness. The values obtained from the evaluation of these mechanical properties were imputed into the analytical design of the split-split plot to obtain its numerical designs. Interactive model for the process parameters were also developed for this study. The sum of squares (SS) and the mean of squares (MS) were calculated from the numerical designs of split-split plot to obtain the Fisher's ratio (F_{cal}) values. The results of the calculated Fisher's ratio at significant value of 0.05 for the process parameters and their interactions ranges from -57.70 to 8.50, and were presented on analysis of variance (ANOVA) table. The results obtained shows that there is strong interaction between pressure, percentage by volume of zinc and copper in the production zinc-copper alloy in alloy manufacturing industries.

Keywords: Copper-Zinc Alloy, Mechanical Properties, Modelling, Process Parameters, Split-Split Plot Design.

1. INTRODUCTION

Brass is an alloy of copper and zinc in proportions which can be varied to achieve varying mechanical and electrical properties. Brass is an alloy of 70% copper and 30% zinc [1]. However, 'the proportions of copper and zinc can be varied to obtain a range of brasses with varying mechanical properties. Brass has higher malleability and low melting point (900ºC to 940°C) depending on its composition. By varying the proportions of copper and zinc, the properties of the brass can be changed, allowing hard and soft brasses to be produced. Brass has the desirable properties that make it ideal for use as a rolling element material, such as good frictional properties against hardened steel components, copper-zinc alloy also have reasonable strength, high toughness and excellent thermal conductivity'. In addition, brass has good machining and joining characteristics that make it cost-effective [2]. The malleability of copper-zinc alloy has made it the metal of choice [3]. This alloy had applications where low friction are required such as locks, gears,

bearings, doorknobs, ammunition, and valves. Improper analysis of process parameters such as percentage by volume of copper and zinc, pressure and their interaction in the manufacture of copper-zinc alloy had poses great challenges in alloy manufacturing. Moreover, the split-plot design which is an experiment design includes at least one hard-to-change factor that is difficult to completely randomize because of time or cost constraints [4]. According to Olodu and Osarenmwinda [4], stated that in a split-plot experiment, levels of the hard-to-change factor were held constant for several experimental runs, which were collectively treated as a whole plot. 'The easy-to-change factors were varied during these runs, each combination of which is considered a sub-plot within the whole plot. In addition, they randomize the order in which they run both the whole plots and the sub-plots within whole plots. In simple terms, a split-plot experiment is a blocked experiment, where the blocks themselves serve as experimental units for a subset of the factors. Thus, there were two levels of experimental units, the blocks are referred to as whole plots; while the experimental units within blocks are called split plots, split units, or subplots. According to them [4], one randomization was conducted to determine the assignment of block-level treatments to whole plots. Then, as always in a blocked experiment, a randomization of treatments to split-plot experimental units occurred within each block or whole plot.' Olodu and Osarenmwinda [4] examined the effect of process parameters such as temperature in the production of polypropylene-grass composite using split-split plot experimental design, their results show that temperature contributes significantly to the production of composites in polymeric industries. Aviles and Pinheiro [5] examined the experiments that have complete randomization order of runs which was not feasible or might be too expensive to use when performed. They concluded from their study that the use of split-plot designs and models are feasible, efficient and cheap. Goldsmith and Gaylor [6]' carried out extensive investigation on optimal designs for estimating variance components in a completely random nested classification. Loeza-Serrano and Donev [7] 'constructed D-Optimal design for variance components estimation in a three-stage crossed and nested classification. For experiments that include both crossed and nested factor in the same model, no assumption of a complete random model has been made. Ankenman et al; Aviles and Pinheiro [8,5] investigations indicate that experiments involving complete randomization of order of runs which is not feasible or too expensive to use is performed using split plot models. Chunping *et al* [9] carried out a study aimed to model fundamental bonding characteristics and performance of composite materials. In their work, mathematical model and a computer simulation model were developed to predict the variation of inter-element (strand) contact during mat consolidation. The mathematical predictions and the computer simulations agree well with each other'. Their results showed that the relationship between the inter-element contact and the mat density was highly nonlinear and was significantly affected by the wood density and the element thickness.

This study therefore focused on the modelling and experimental investigation of Copper-zinc alloy using Split-split plot design.

2. MATERIALS AND METHODS

2.1 Materials

The materials used in this study were zinc and copper. These materials were subjected to various production pressures (hot pressures) ranging from 20GPa to 78 GPa respectively. These materials produced at various pressures were evaluated for mechanical properties after cooling.

2.2 Method of Data Collection

The various samples of the developed copper-zinc alloy that were produced at various pressure were tested according to American Standard of Testing Machine (ASTM) using the tensometer and Charpy Impact Test machines respectively. The data obtained were further evaluated for mechanical properties for the developed copper-zinc alloy. Furthermore, Samples were tested on a 10-ton DAK tensile testing machine at a constant cross head speed of 1 mm/min. Standard samples of tensile specimens ASTM-E8M are prepared for testing. A total of 6 samples were tested in each case and average values were obtained.

2.3 Evaluation of Developed Copper-Zinc Alloy for Mechanical Properties at Various Pressures

The developed copper-zinc alloy samples were evaluated for mechanical strength (tensile strength, modulus of elasticity, Brinell hardness and shear modulus) using Equation 1 to 4 respectively [10].

$$\text{Tensile strength} = \frac{\text{Maximum Load}}{\text{Original Cross - Sectional Area}} \quad (1)$$

$$\text{modulus of Elasticity, E} = \frac{Stress}{Strain} = \frac{FL_o}{L_m - L_o} \quad (2)$$

Where F= applied force, l_o=original length; l_m=Final length

$$\text{shear modulus} = \frac{\text{shear stress}}{\text{shear strain}} = \frac{\frac{F}{A}}{\frac{x}{y}}. \quad (3)$$

Where F= applied force: A=Cross-sectional Area; x=extension; y-original length

$$\text{Brinell Hardness Number (BHN)} = \frac{2P}{\pi D[D - \sqrt{D^2 - d^2}}} \quad (4)$$

Where P is the load in kilogram, D is the steel ball diameter in millimeter, and d is the depression diameter or indentation diameter.

2.4 The Split-Split Plot Design

The split-split plot design which is an experimental design was used to investigate the interaction between material type, percentage by volume of material and pressure on the mechanical properties of the produced copper-zinc alloy. In simple terms, a split-split plot experiment is a blocked experiment, where the blocks themselves serve as experimental units for a subset of the factors [11]. Analytical and numerical designs using split-split plot design was carried out to investigate the effects of process parameters in the developed copper-zinc alloy.

2.4.1 The F-Test

The F-test is used for comparing the factors of the total deviation. Statistical significance is tested for by comparing the F test statistic.

$$F = \frac{Variance\ between\ treatments}{Variance\ within\ treatments} \quad (5)$$

$$F = \frac{MS_{Treatments}}{MS_{Error}} = \frac{SS_{Treatments/(I-1)}}{SS_{Error}/(nT-1)} \quad (6)$$

2.5 Hypothesis Statements for Copper-Zinc Alloy

The null hypothesis with its alternative was formulated for copper-zinc alloy as follows:

Null Hypothesis (H_o)***:*** The percentage by volume of material, material type, pressure and their interactions contribute significantly to the mechanical properties of the developed copper-zinc alloy at a significant value (α-value) of 0.05.

Alternate Hypothesis (H_1)***:*** The percentage by volume of material, material type, pressure and their interactions does not contribute significantly to the mechanical properties of copper-zinc alloy produced at α-value of 0.05.

3. RESULTS AND DISCUSSION

3.1 The Interactive Model Developed for Copper-Zinc Alloy

The split-split plot design which is an experimental design was used to investigate the interaction between mechanical strength of copper-zinc alloy, material type, percentage by volume of material and pressure. The results obtained from the evaluation of mechanical properties are shown appendix A1, A2, A3 and A4 respectively. These results were imputed into the analytical design of the split-split plot design to obtain its numerical design, this was furtherly presented on ANOVA Table 1.

The Interactive model developed is depicted as:

$$X_{ijkl} = \mu + \gamma_i + \beta_j + \delta_l + y_k + \gamma\beta_{ij} + \gamma y_{ik} + \beta y_{jk} + \gamma\delta_{il} + \beta\delta_{jl} + y\delta_{lk} + \gamma\beta y_{ijk} + \gamma\beta\delta_{ijl} + \gamma y\delta_{ikl} + \beta y\delta_{jkl} + \gamma\beta\delta y_{ijkl} + \varepsilon_{ijkl} \quad (7)$$

Where:

μ = Mean response; γ_I= Block variable (mechanical properties); β_j = Block variable (pressure); δ_l = Treatment Variable (percentage by volume of material); y_k= Treatment Variable (type of material); $\gamma\beta_{ij}$= Block interaction (mechanical properties and pressure interaction); γy_{ik}= Block and Treatment interaction (mechanical properties and type of material interaction); βy_{jk}=Treatment Interaction (pressure and type of material interaction); $\gamma\delta_{il}$= Block and Treatment interaction (mechanical properties and percentage by volume of material interaction); $\beta\delta_{jl}$= Block and Treatment interaction (pressure and percentage by volume of material interaction); $y\delta_{lk}$= Treatment Interaction (percentage by volume of material and type of material interaction); $\gamma\beta y_{ijk}$= Block and Treatment interaction (mechanical properties, pressure and type of material interaction); $\gamma\beta\delta_{ijl}$= Block and Treatment interaction (mechanical properties, pressure and Percentage by volume of material interaction); $\gamma y\delta_{ikl}$= Block and Treatment interaction (mechanical properties, type of material and Percentage by volume of material interaction); $\beta y\delta_{jkl}$ = Block and Treatment interaction (pressure, type of material and Percentage by volume of material interaction); $\gamma\beta\delta y_{ijkl}$= Block and Treatment interaction (mechanical properties, pressure, type of material and percentage by volume of material interaction); X_{ijkl}= Response Variable; ε_{ijkl}= Error term

3.2 Statistical Computations of Sum of Squares for Copper-Zinc Alloy

Equations 8 to 22 were used to calculate for the sum of squares for the process parameters and their interactions which were used to investigate the effects of pressure and its interactions on copper-zinc alloy using Split-Split Plot experimental design analysis, the obtained results were presented on ANOVA Table 1 shown below.

A) Total Sum of Squares (SS_T)

$$SS_T = \sum_{i=1}^{I=4}\sum_{j=1}^{J=11}\sum_{k=1}^{K=2}\sum_{l=1}^{L=7} X_{ijkl}^2 - \frac{X_{....}^2}{IJLK} \quad (8)$$

Where I=4, J=11, K=2, L=7

B) Sum of Squares for Materials (SS_A)

$$SS_A = \sum_{k=1}^{K=2} \frac{X^2_{\cdot\cdot K\cdot}}{IJL} - \frac{X^2_{\cdot\cdot\cdot\cdot}}{IJLK} \quad (9)$$

C) Sum of Squares for the Percentage by Volume of Materials (SS_B)

$$SS_B = \sum_{l=1}^{L=7} \frac{X^2_{\cdot\cdot\cdot l}}{IJK} - \frac{X^2_{\cdot\cdot\cdot\cdot}}{IJLK} \quad (10)$$

D) Sum of Squares for Mechanical Strength (SS_C)

$$SS_C = \sum_{i=1}^{I=4} \frac{X^2_{i\cdot\cdot\cdot}}{JKL} - \frac{X^2_{\cdot\cdot\cdot\cdot}}{IJLK} \quad (10)$$

E) Sum of Squares for Pressure (SS_D)

$$SS_D = \sum_{j=1}^{J=11} \frac{X^2_{\cdot j\cdot\cdot}}{IKL} - \frac{X^2_{\cdot\cdot\cdot\cdot}}{IJLK} \quad (11)$$

F) (Material Type) X (Percentage by Volume of Material) Interaction (SS_{AB})

$$SS_{AB} = \sum_{k=1}^{K=2}\sum_{l=1}^{L=7} \frac{X^2_{\cdot\cdot k\, l}}{IJ} - \sum_{k=1}^{K=2} \frac{X^2_{\cdot\cdot k\cdot}}{IJK} - \sum_{l=1}^{L=7} \frac{X^2_{\cdot\cdot\cdot l}}{IJK} + \frac{X^2_{\cdot\cdot\cdot\cdot}}{IJLK} \quad (12)$$

G) (Material type) X (Mechanical Strength) Interaction (SS_{AC})

$$SS_{AC} = \sum_{i=1}^{I=4}\sum_{k=1}^{K=2} \frac{X^2_{i\cdot k\cdot}}{JL} - \sum_{i=1}^{I=4} \frac{X^2_{i\cdot\cdot\cdot}}{JKL} - \sum_{k=1}^{K=2} \frac{X^2_{\cdot\cdot k\cdot}}{IJL} + \frac{X^2_{\cdot\cdot\cdot\cdot}}{IJLK} \quad (13)$$

H) (Material type) X (Pressure) Interaction (SS_{AD})

$$SS_{AD} = \sum_{k=1}^{K=2}\sum_{j=1}^{J=11} \frac{X^2_{\cdot j\, k\cdot}}{IL} - \sum_{k=1}^{K=2} \frac{X^2_{\cdot\cdot k\cdot}}{IJL} - \sum_{j=1}^{J=11} \frac{X^2_{\cdot j\cdot\cdot}}{IKL} + \frac{X^2_{\cdot\cdot\cdot\cdot}}{IJLK} \quad (14)$$

I) (Percentage by Volume of Material) X (Mechanical Strength) Interaction (SS_{BC})

$$SS_{BC} = \sum_{i=1}^{I=4}\sum_{l=1}^{L=7} \frac{X^2_{i\cdot\cdot l}}{JK} - \sum_{i=1}^{I=4} \frac{X^2_{i\cdot\cdot\cdot}}{JKL} - \sum_{l=1}^{L=7} \frac{X^2_{\cdot\cdot\cdot l}}{IJK} + \frac{X^2_{\cdot\cdot\cdot\cdot}}{IJLK} \quad (15)$$

J) (Percentage by volume of material) X (Pressure) Interaction (SS_{BD})

$$SS_{BD} = \sum_{j=1}^{J=11}\sum_{l=1}^{L=7} \frac{X^2_{\cdot j\cdot l}}{IK} - \sum_{j=1}^{J=11} \frac{X^2_{\cdot j\cdot\cdot}}{IKL} - \sum_{l=1}^{L=7} \frac{X^2_{\cdot\cdot\cdot l}}{IJK} + \frac{X^2_{\cdot\cdot\cdot\cdot}}{IJLK} \quad (16)$$

K) (Mechanical Strength) X (Pressure) Interaction (SS_{CD})

$$SS_{CD} = \sum_{i=1}^{I=4}\sum_{j=1}^{J=11} \frac{X^2_{i\, j\cdot\cdot}}{KL} - \sum_{i=1}^{I=4} \frac{X^2_{i\cdot\cdot\cdot}}{JKL} - \sum_{j=1}^{J=11} \frac{X^2_{\cdot j\cdot\cdot}}{IKL} + \frac{X^2_{\cdot\cdot\cdot\cdot}}{IJLK} \quad (17)$$

L) (Material type) X (Percentage by Volume of Material) X (Mechanical Strength) Interaction (SS_{ABC})

$$SS_{ABC} = \sum_{i=1}^{I=4}\sum_{k=1}^{K=2}\sum_{l=1}^{L=7} \frac{X^2_{i\cdot k\, l}}{J} - \sum_{i=1}^{I=4}\sum_{k=1}^{K=2} \frac{X^2_{i\cdot k\cdot}}{JL} - \sum_{k=1}^{K=2}\sum_{l=1}^{L=7} \frac{X^2_{\cdot\cdot k\, l}}{IJ} + \sum_{k=1}^{K=2} \frac{X^2_{\cdot\cdot k\cdot}}{IJL} \quad (18)$$

M) (Material type) X (Percentage by Volume of Material) X (Pressure) Interaction (SS_{ABD})

$$SS_{ABD} = \sum_{j=1}^{J=11}\sum_{k=1}^{K=2}\sum_{l=1}^{L=7} \frac{X^2_{\cdot j\, k\, l}}{I} - \sum_{j=1}^{J=11}\sum_{k=1}^{K=2} \frac{X^2_{\cdot j\, k\cdot}}{IL} - \sum_{k=1}^{K=2}\sum_{l=1}^{L=7} \frac{X^2_{\cdot\cdot k\, l}}{IJ} + \sum_{k=1}^{K=2} \frac{X^2_{\cdot\cdot k\cdot}}{IJL}$$

(19)

N) (Material type) X (Mechanical strength) X (Pressure) Interaction (SS_{ACD})

$$SS_{ACD} = \sum_{i=1}^{I=4}\sum_{j=1}^{J=11}\sum_{k=1}^{K=4}\frac{X^2_{i\ j\ k\ .}}{L} - \sum_{i=1}^{I=4}\sum_{j=1}^{J=11}\frac{X^2_{i\ j\ .\ .}}{KL} - \sum_{j=1}^{J=11}\sum_{k=1}^{K=7}\frac{X^2_{.\ j\ k\ .}}{IL} + \sum_{j=1}^{J=11}\frac{X^2_{.\ j\ .\ .}}{IKL} \quad (20)$$

O) (Percentage by Volume of Material) X (Mechanical strength) X (Pressure) Interaction (SS_{BCD})

$$SS_{ACD} = \sum_{i=1}^{I=4}\sum_{j=1}^{J=11}\sum_{l=1}^{L=7}\frac{X^2_{i\ j\ .\ l}}{K} - \sum_{i=1}^{I=4}\sum_{j=1}^{J=11}\frac{X^2_{i\ j\ .\ .}}{KL} - \sum_{j=1}^{J=11}\sum_{l=1}^{L=7}\frac{X^2_{.\ j\ .\ l}}{IK} + \sum_{j=1}^{J=11}\frac{X^2_{.\ j\ .\ .}}{IKL} \quad (21)$$

P) Error Sums of Squares $(\mathbf{SS_E}) = SS_T - SS_A - SS_B - SS_C - SS_D - SS_{AB} - SS_{AC} - SS_{AD}$

$- SS_{BC} - SS_{CD} - SS_{ABC} - SS_{ABD} - SS_{ACD}$. (22)

3.2.1 Result for Effects of Pressure on Copper-Zinc Alloy Using Split-Split Plot Design

Table 1 shows Analysis of Variance (ANOVA) results for the effects of process parameters and their interactions on produced Copper-Zinc alloy.

Table 1. Analysis of Variance (ANOVA) Results for Effects of Pressure on Copper-Zinc Alloy

Sources of Variation	Sum of Squares (SS)	Degree of freedom	Mean of Squares (MS)	Fisher's Ratio F_{cal} α=0.05	Fisher's Ratio F_{Table}	Decision
SS_A	2.45	K-1=1	2.45	$\frac{MS_A}{MS_B} =$ 2.45	5.99	$F_{cal} < F_{Table}$, no enough evidence to reject null hypothesis.
SS_B	459.00	L-1=6	76.50	$\frac{MS_B}{MS_{AB}} = 3.89$	4.28	$F_{cal} < F_{Table}$, no enough evidence to reject null hypothesis..
SS_C	2786.10	I-1=3	928.70	$\frac{MS_C}{MS_{AC}} =$ 7.43	9.28	$F_{cal} < F_{Table}$, no enough evidence to reject null hypothesis..
SS_D	2315.00	J-1=10	231.5	$\frac{MS_D}{MS_{AD}} =$ 2.00	2.98	$F_{cal} < F_{Table}$, no enough evidence to reject null hypothesis..
SS_{AB}	685.80	(K-1)(L-1)=6	114.3	$\frac{MS_{AB}}{MS_C} =$ 8.50	8.94	$F_{cal} < F_{Table}$, no enough evidence to reject null hypothesis..

SS_{AC}	337.50	(K-1)(I-1)=3	112.5	$\frac{MS_{AC}}{MS_{BC}} = 2.50$	3.16	$F_{cal} < F_{Table}$, no enough evidence to reject null hypothesis..
SS_{AD}	224.50	(K-1)(J-1)=10	22.45	$\frac{MS_{AD}}{MS_{BD}} = 2.50$	1.99	$F_{cal} > F_{Table}$, there was enough evidence to reject null hypothesis..
SS_{BC}	693.00	(L-1)(I-1)=18	38.50	$\frac{MS_{BC}}{MS_{ABC}} = 1.00$	2.01	$F_{cal} < F_{Table}$, no enough evidence to reject null hypothesis..
SS_{BD}	-15030.00	(L-1)(J-1)=60	-250.50	$\frac{MS_{BD}}{MS_{ABD}} = -57.70$	0.51	$F_{cal} < F_{Table}$, no enough evidence to reject null hypothesis..
SS_{CD}	3168.00	(I-1)(J-1)=30	105.60	$\frac{MS_{CD}}{MS_{ACD}} = 1.02$	1.37	$F_{cal} < F_{Table}$, no enough evidence to reject null hypothesis..
SS_{ABC}	1809	(K-1)(L-1)(I-1)=18	100.50	$\frac{MS_{ABC}}{MS_{D}} = 2.23$	2.98	$F_{cal} < F_{Table}$, no enough evidence to reject null hypothesis..
SS_{ABD}	-6.60	(K-1)(L-1)(I-1)=60	-0.11	$\frac{MS_{ABD}}{MS_{CD}} = -0.01$	0.17	$F_{cal} < F_{Table}$, no enough evidence to reject null hypothesis..
SS_{ACD}	6642	(K-1)(I-1)(J-1)=30	221.40	$\frac{MS_{ACD}}{MS_{BCD}} = 1.50$	1.93	$F_{cal} < F_{Table}$, no enough evidence to reject null hypothesis..
SS_{BCD}	7290.00	(L-1)(I-1)(J-1)=180	40.50	$\frac{MS_{BCD}}{MS_{E}}$=5.65	6.57	$F_{cal} < F_{Table}$, no enough evidence to reject null hypothesis..
SS_{E}	0.05	(I-1)(J-1)(K-1)(L-1)=180	9.00			
SS_{T}	11375.80	IJKL-1=615				

3.3 Discussion of the Results

Table 1 Shows that the fourteen null hypothesis H_o^1, H_o^2, H_o^3, H_o^4, H_o^5, H_o^6, H_o^7, H_o^8, H_o^9, H_o^{10}, H_o^{11}, H_o^{12}, H_o^{13}, H_o^{14}, are respectively not rejected at α-value of 0.05, suggesting that there appears to be no differential treatment and block effects. Also, interaction appears to exist between treatment and block effects.

(a)Examination of Treatment Effect of Materials (Copper-Zinc Alloy) (SS_A)

Since $F_{cal}=2.45<F_{Table}=5.99$, the F_{cal} is less than the F_{Table} in the statistical table, our experimental data do not furnish enough evidence for us to reject the null hypothesis H_o^1 treatment at α-value of 0.05. Our conclusion therefore is that the materials (copper and zinc) parameters contribute significantly to the mechanical property of the copper-zinc alloy produced in industries.

(b) Examination of Treatment Effect of Percentage by Volume of Materials (SS_B)

Since $F_{cal}=3.89<F_{Table}=4.28$, the F_{cal} is less than the F_{Table} in the statistical table, our experimental data do not furnish enough evidence for us to reject the null hypothesis H_o^2 treatment at α-value of 0.05. Our conclusion therefore is that the percentage by volume of materials parameter contributes significantly to the mechanical property of the copper-zinc alloy produced in industries.

(c) Examination of Block Effect of Mechanical Properties (SS_C)

Since $F_{cal}=7.43<F_{Table}=9.28$, the F_{cal} is less than the F_{Table} in the statistical table, our experimental data do not furnish enough evidence for us to reject the null hypothesis H_o^3 at α-value of 0.05. Our conclusion therefore is that the mechanical strength parameters contribute significantly to copper-zinc alloy produced in industries.

(d) Examination of Block Effect of Pressure (SS_D)

Since $F_{cal}=2.00<F_{Table}=2.98$, the F_{cal} is less than the F_{Table} in the statistical table, our experimental data do not furnish enough evidence for us to reject the null hypothesis H_o^4 of block effect at α-value of 0.05. Our conclusion therefore is that the pressure parameters contribute significantly to the mechanical property of the copper-zinc alloy produced in industries.

(e) Examination of Treatment Effect of Material Type and Percentage by Volume of Material Interaction (SS_{AB})

Since $F_{cal}=8.50<F_{Table}=8.94$, the F_{cal} is less than the F_{Table} in the statistical table, our experimental data do not furnish enough evidence for us to reject the null hypothesis H_o^5 of interaction effect of material type and percentage by volume of material interaction at α-value of 0.05. Our conclusion therefore is that the material type and percentage by volume of material interaction parameters contribute significantly to the mechanical property of the copper-zinc alloy produced in industries.

(f) Examination of Treatment Effect of Material Type and Block Effect Mechanical Strength Interaction (SS_{AC})

Since $F_{cal}=2.50<F_{Table}=3.16$, the F_{cal} is less than the F_{Table} in the statistical table, our experimental data do not furnish enough evidence for us to reject the null hypothesis H_o^6 interaction at α-value of 0.05. Our conclusion therefore is that the materials (copper-zinc alloy) and Mechanical Strength interaction parameters contribute significantly to copper-zinc alloy produced in industries.

(g) Examination of Treatment Effect of Material Type and Block Effect (Pressure) Interaction (SS_{AD})

Since $F_{cal}=2.50>F_{Table}=1.99$, the F_{cal} is greater than the F_{Table} in the statistical table, our experimental data therefore furnish enough proof for us to reject the null hypothesis H_o^7 interaction at α-value of 0.05. Our conclusion therefore is that the treatment effect of material type and blocks effect (pressure) interaction parameters do not contribute significantly to the mechanical property of the copper-zinc alloy produced in industries.

(h) Examination of Treatment Effect of (Percentage by Volume of Material) and Block Effect (Mechanical Strength) Interaction (SS_{BC})

Since F_{cal}=1.00<F_{Table}=2.01, the F_{cal} is less than the F_{Table} in the statistical table, our experimental data do not furnish enough evidence for us to reject the null hypothesis H_o^8 interaction at α-value of 0.05. Our conclusion therefore is that the treatment effect of (percentage by volume of material) and block effect (mechanical strength) interaction parameters contribute significantly to copper-zinc alloy produced in industries.

(i) Examination of Treatment Effect (Percentage by Volume of Material) and Block Effect (Pressure) Interaction (SS_{BD})

Since F_{cal}=-57.70<F_{Table}=0.51, the F_{cal} is less than the F_{Table} in the statistical table, our experimental data do not furnish enough evidence for us to reject the null hypothesis H_o^9 interaction at α-value of 0.05. Our conclusion therefore is that the treatment effect (percentage by volume of material) and block effect (pressure) interaction parameters contribute significantly to the mechanical property of the copper-zinc alloy produced in industries.

(j) Examination of Treatment Effect of (Mechanical Strength) X (Pressure) Interaction (SS_{CD})

Since F_{cal}=1.02>F_{Table}=1.37, the F_{cal} is less than the F_{Table} in the statistical table, our experimental data do not furnish enough evidence for us to reject the null hypothesis H_o^{10} interaction at α-value of 0.05. Our conclusion therefore is that the treatment effect (mechanical strength) and block effect (pressure) interaction parameters contribute significantly to copper-zinc alloy produced in industries.

(k) Examination of Treatment Effect of Material type, Percentage by Volume of Material and Block Effect (Mechanical Strength) Interaction (SS_{ABC})

Since F_{cal}=2.23<F_{Table}=2.98, the F_{cal} is less than the F_{Table} in the statistical table, our experimental data do not furnish enough evidence for us to reject the null hypothesis H_o^{11} interaction at α-value of 0.05. Our conclusion therefore is that the treatment effect of material type, percentage by volume of material and block effect (mechanical strength) interaction parameters contribute significantly to copper-zinc alloy produced in industries.

(l) Examination of Treatment Effect of Material Type, Percentage by Volume of Material and Block Effect (Pressure) Interaction (SS_{ABD})

Since F_{cal}=-0.01<F_{Table}=0.17, the F_{cal} is less than the F_{Table} in the statistical table, our experimental data do not furnish enough evidence for us to reject the null hypothesis H_o^{12} interaction at α-value of 0.05. Our conclusion therefore is that the treatment effect of material type, percentage by volume of material and block effect (Pressure) interaction parameters contribute significantly to the mechanical property of the copper-zinc alloy produced in industries.

(m) Examination of Treatment Effect of Material Type, and Block Effect of Both Mechanical strength and Pressure Interaction (SS_{ACD})

Since F_{cal}=1.50<F_{Table}=1.93, the F_{cal} is less than the F_{Table} in the statistical table, our experimental data do not furnish enough evidence for us to reject the null hypothesis H_o^{13} interaction at α-value of 0.05. Our conclusion therefore is that the treatment effect of material type, and block effect of both mechanical strength and pressure interaction parameters contribute significantly to the strength of the copper-zinc alloy alloy produced in industries.

(n) Examination of Treatment Effect of Percentage by Volume of Material, and Block Effect of Both Mechanical Strength and Pressure Interaction (SS_{BCD})

Since F_{cal}=5.65<F_{Table}=6.57, the F_{cal} is less than the F_{Table} in the statistical table, our experimental

data do not furnish enough evidence for us to reject the null hypothesis H_o^{14} interaction at α-value of 0.05. Our conclusion therefore is that the treatment effect of percentage by volume of material, and block effect of both mechanical strength and pressure interaction parameters contribute significantly to the strength of copper-zinc alloy produced in industries.

4. CONCLUSION

The study on the modelling and experimental investigation of copper-zinc alloy using split-split plot design had been achieved. The results obtained shows that the calculated Fisher's ratio ranges from -57.70 to 8.50 at significant value of 0.05 for the process parameters and their interactions. The results obtained from the interactive model developed using the split-split plot design indicates that there was strong interaction between pressure, type of material and percentage by volume of material on mechanical properties (tensile strength, modulus of elasticity, shear modulus and hardness) for the produced copper-zinc alloy. Hence, these process parameters contribute significantly to the production of copper-zinc alloy in alloy manufacturing industries. Decisions made based on the hypothesis statements also shows that there was no enough evidence to reject the null hypothesis at α-value of 0.05 for developed copper-zinc alloy. Finally, the developed interactive model will also be useful to researcher, industrialist and small-scale manufacturer to ease the production of alloys in alloy manufacturing industries.

REFERENCES

[1] Gaspar, I. S., Pasko, J. Analysis of Fracture Process and Common Defects in Casting Alloys EN43100 Manufactured by Die Casting Technology. *Advanced Materials Research.* **2014**, 1077: 39-43.

[2] Bahloul, B., Ahmed, M. M; Samuel, M; Fadhil, A. Abdulsalam, A. Copper-Zinc-Lead Alloys, Common Defects Through Production Stages and Remedy Methods. *Turkish Online Journal of Science & Technology*. **2015**, 4(1): 23-32.

[3] Zhang Y. Dezincification and Brass Lead Leaching in Premise Plumbing Systems: Effects of Alloy, Physical Conditions and Water Chemistry. *Virginia Polytechnic Institute and State University*. **2009**, 5(2): 17-22.

[4] Olodu D.D and Osarenmwinda J.O. Empirical Modelling of Developed Polyvinyl Chloride-Grass Composite. *Journal of Energy Technology and Environment*. **2019**, 1(1): 29-37.

[5] Avilles, A.I and Pinheiro, J.C. Optimal Design for Mixed Effects Models with two Random Nested Factors. *Journal of Statistical Sinica.* **2015**, 13: 385-401.

[6] Goldsmith, C.H and Gaylor, D.W. Three Stage Nested Designs for Estimating Variance Components. *Journal of Technometrics*. **1970**, 12: 487-498.

[7] Loeza, S and Donev, A.N. Construction of Experimental Design to estimate Variance Components. *Journal of Computational Statistics and Data Analysis.* **2014**, 71: 1168–1177.

[8] Ankenman, B.E; Liu, H; Karr, AF and Picka, J.D. A Class of Experimental Designs for Estimating a Response Surface and Variance Components. *Journal of Technometrics.* **2001,** 44: 45-54.

[9] Chunping, D; Changing. Y; and Cheng, Z. Theoretical Modeling of Bonding Characteristics and Performance of Wood Composites of Inter-element Contact. *Journal of Wood and Fiber Science.* **2007,** 39: 48-55.

[10] Olodu, D.D and Osarenmwinda, J.O. Effects of Process Parameters in the Production of High-Density Polyethylene-Grass Composite. *Journal of Applied Sciences and Environmental management*. **2018**, 22(9): 1479-1483.

[11] Goos, P. and Vandebroek, M., (2003). D-optimal Split-Plot Designs with Given Numbers and Sizes of Whole Plots. *Journal of Technometrics*. **2003**, 45: 235-245.

APPENDIX

Table A1: The Tensile Strength of Copper-Zinc Alloy at Various Pressure and Percentage Composition

Mechanical Property	Zinc	Copper	Pressure (GPa)										
			130	150	170	190	210	230	250	270	290	310	330
Tensile Strength (Mpa)	50	50	345	334	331	310	301	287	276	288	265	287	264
	45	55	321	334	267	278	256	268	278	298	311	299	340
	55	45	289	341	323	318	290	297	310	324	331	309	332
	54	46	321	234	234	256	342	312	267	324	289	278	269
	58	42	288	278	298	328	329	339	289	276	265	254	300
	60	40	300	264	274	298	312	267	296	278	325	319	312
	63	37	286	277	311	349	297	300	316	327	334	309	284

Table A2: The Modulus of Elasticity of Copper-Zinc Alloy at Various Pressure and Percentage Composition

Mechanical Property	**Percentage by Volume of Copper %**	**Percentage by Volume of Zinc %**	**Pressure (GPa)**										
			130	150	170	190	210	230	250	270	290	310	330
Modulus of Elasticity (GPa)	50	50	84	90	94	92	91	116	117	104	108	80	82
	45	55	81	99	88	111	98	117	112	89	89	79	78
	55	45	83	98	87	112	111	113	114	98	85	88	90
	54	46	78	103	89	104	102	110	118	87	76	98	97
	58	42	89	105	93	109	105	99	109	79	87	112	103
	60	40	91	108	95	110	106	102	107	80	87	98	102
	63	37	94	107	98	116	107	111	103	85	78	90	100

Table A3: The Shear Modulus of Copper-Zinc Alloy at Various Pressure and Percentage Composition

Mechanical Property	**Percentage by Volume of Copper (%)**	**Percentage by Volume of Zinc (%)**	**Pressure (GPa)**										
			130	150	170	190	210	230	250	270	290	310	330

Shear Modulus (Gpa)	50	50	18	22	19	25.5	24	23	17	14	18.5	20	26
	45	55	17	20	20	23.4	22.2	24	21	16	19	19	24
	55	45	19	21	21	22.5	21.7	22	18	17	18	20	23
	54	46	18	19	22	23	20	19	19	16.2	16	17	25
	58	42	20	21	22	24	21.6	18.7	20	18	17.4	18	26.2
	60	40	22	23	24	20	19	17	18.6	17	19	21	20
	63	37	19.6	34	23	22	21	20	19	15	19	20	19

Table A4: The Brinell Hardness Number of Copper- Zinc Alloy at Various Pressure and Percentage Composition

Mechanical Property	**Percentage by Volume of Copper (%)**	**Percentage by Volume of Zinc (%)**	**Pressure (GPa)**										
			130	150	170	190	210	230	250	270	290	310	330
Brinell Hardness Number (BHN)	50	50	52	54	53	60	61	58	61	54	48	45	53
	45	55	47	45	46	49	54	61	58	57	54	58	60
	55	45	58	57	52	45	61	58	47	55	54	61	56
	54	46	54	50	56	51	48	45	60	58	56	51	52
	58	42	49	53	51	56	58	47	58	60	55	53	57
	60	40	48	52	55	53	54	50	56	58	50	52	51
	63	37	50	48	49	54	59	61	54	51	45	46	48

Research Article

OPTIMIZATION OF REMOVAL EFFICIENCY AND ABSORPTION CAPACITY OF DYESTUFFS BY ASPERGILLUS SP. USING MANOVA

Authors: Semra Malkoç , Berna Yazıcı , Mukaddes Şimşek

To cite to this article: Malkoç, S., Yazıcı, B. & Şimşek, M. (2021). OPTIMIZATION OF REMOVAL EFFICIENCY AND ABSORPTION CAPACITY OF DYESTUFFS BY ASPERGILLUS SP. USING MANOVA . International Journal of Engineering and Innovative Research, 3(3), p:187-200. DOI: 10.47933/ijeir.931772

DOI: 10.47933/ijeir. 931772

To link to this artice: https://dergipark.org.tr/tr/pub/ijeir/archive

International Journal of Engineering and Innovative Research

http://dergipark.gov.tr/ijeir

OPTIMIZATION OF REMOVAL EFFICIENCY AND ABSORPTION CAPACITY OF DYESTUFFS BY *ASPERGILLUS SP.* USING MANOVA

Semra Malkoç[1], Berna Yazıcı[2], Mukaddes Şimşek[2]

[1]Eskisehir Technical University, Faculty of Engineering, Department of Environmental Engineering, Eskişehir, Turkey

[2]Eskisehir Technical University, Faculty of Science, Department of Statistics, Eskişehir, Turkey

[*]Corresponding Author: bbaloglu@eskisehir.edu.tr

https://doi.org/10.47933/ijeir.931772

(**Received:** 03.05.2021; **Accepted:** 23.05.2021)

ABSTRACT: Fungi is widely found on air, soil, water and organic substances in nature. Unlike single-celled bacteria, fungi form multicellular structures, sometimes even visible to the naked eye. In studies of *Aspergillus* sp. removal and dye removal in order to obtain information, examinations are made by painting. Basic dyes, when ionized, are charged with positive electricity. Basic dyes include malachite green (MG), methyl violet (MV), crystal violet (CV), and basic fuchsin (BF). The aim of this research is to determine the effects of different factors on the parameters of absorption capacity and the removal efficiency of malachite green (MG), methyl violet (MV), crystal violet (CV) and basic fuchsin (BF) from *Aspergillus* sp. The data analyzed using Minitab statistical software. MANOVA used as the statistical analysis. It is concluded that the temperature and initial concentration have significant effect on removal efficiency and absorption capacity.

Keywords: *Aspergillus* sp., Dyestuff, Multifactorial Experiments, MANOVA

1. INTRODUCTION

Fungi are among the most widely distributed organisms on Earth and are of great environmental and medical importance. Fungi is a plural form of fungus. Fungus is any of about 144,000 known species of organisms of the kingdom Fungi, which includes the yeasts, rusts, smuts, mildews, molds, and mushrooms. Many fungi are free-living in soil or water; others form parasitic or symbiotic relationships with plants or animals. Fungi are everywhere in very large numbers-in the soil and the air, in lakes, rivers, and seas, on and within plants and animals, in food and clothing, and in the human body. Together with bacteria, fungi are responsible for breaking down organic matter and releasing carbon, oxygen, nitrogen, and phosphorus into the soil and the atmosphere. Humans have been indirectly aware of fungi since the first loaf of leavened bread was baked and the first tub of grape must be turned into wine. Fungi are essential to many household and industrial processes, notably the making of bread, wine, beer, and cheese. Fungi are also used as food; for example, some mushrooms, morels, and truffles are epicurean delicacies and mycoproteins (fungal proteins), derived from the mycelia of certain species of fungi, and are used to make foods that are high in [1-4].

Dyestuffs are a group of organic pollutants and their industrial use is common. Dyestuffs is the general name of intensely colored and complex organic compounds that dissolve in certain environments and permanently give their color to the applied material. In order for a substance to be named as a dye, it must provide a continuous coloring on another substance. Unlike pigments, almost all of the dyestuffs are soluble compounds and are generally applied after being made into an aqueous solution in order to ensure a homogeneous color distribution [5]. Dyestuffs consist of two main components. The first is the functional groups that bind the dye to the yarn; the second is the chromophore groups that give color. Chromophore means coloring. A chromophore is an atom, group of atoms or electrons that provide a colored appearance in an organic molecule. It contains one or more links. These bonds are variable and provide the bright colored appearance of the paint by absorbing the light. Aromatic ring compounds containing chromophores in the dyestuff are called chromogen. Dyestuffs are generally complex, synthetic, high molecular weight and organic compounds. It is classified by considering various characteristics such as solubility, chemical structure and dyeing properties. Due to their chemical structure, they can resist heat, water and many chemicals, and color removal is very difficult due to their complex synthetic structure. Examples of dyestuffs include MG, MV, CV, and BF. These dyestuffs cause serious harm to people and the environment. For this reason, it is important to remove these dyestuffs [6-12].

In the present study, determining the factors and levels affecting the removal efficiency and absorption capacity of MG, MV, CV, and BF, which are dyestuffs, are examined. So, with *Aspergillus* sp., it is examined whether the factors and interactions, namely the independent variables, have a significant effect on the removal efficiency and absorption capacity of MG, MV, CV, and BF from fungi and dyestuffs. Thus, the effects of different factors on the parameters of MG, MV, CV, and BF removal efficiency and absorption capacity will be determined. It is considered to eliminate or minimize negative factors for removal efficiency and absorption capacity. Thus, by optimizing the removal efficiency and absorption capacity, with fungi of *Aspergillus* sp., it is aimed to see and analyze the results of the experiment of removing fungi and dyestuffs. So, the treatment combinations which give the maximum removal efficiency and maximum absorption capacity will be obtained. Multivariate analysis of variance (MANOVA) will be applied with the Minitab package program to determine the effects of different factors on the parameters of the removal efficiency and absorption capacity. In this way, it is aimed to make the necessary analyzes for the removal efficiency and absorption capacity of these dyestuffs as well as reducing the negative effects on people and the environment. For this purpose, it was planned to use 4 factors (initial concentration (mg/L), biosorbent amount (g/L), temperature (°C), time (minute)) in the experiment, and different levels for each factor. These levels; 50-100-150-200 mg/L for initial concentration, 0.1 - 0.2 - 0.4 - 0.6 - 0.8 - 1 g/L for biosorbent amount, 25-35-45 °C for temperature and 30-60-90-120-150-180 minutes for time. In our study, since there is more than one dependent variable, MANOVA (Multivariate ANOVA), that is, multivariate analysis of variance is used.

2. METHODS

2.1. Multivariate Analysis of Variance (MANOVA)

In Multivariate analysis of variance (MANOVA), the number of response variables is increased to two or more. In multivariate variance analysis, Wilks 'Lambda, Lawley - Hotelling Trace, Pillai' s Trace and Roy's Largest Root statistics are used [13].

In this study, MANOVA of the results of the experiments made by applying the necessary conditions will be done with Minitab. In addition to that, with Minitab, it is planned to draw the

necessary graphics according to the analysis of the observations obtained [14]. The best way to understand or improve a process is to measure that process accurately and analyze the measurement data correctly.

3. EXPERIMENTAL STUDY

Malachite green (MG), methyl violet (MV), basic fuchsin (BF) and crystal violet (CV) can be given as examples of dyestuffs, which are common and organic pollutants for industrial use. MG is a green-colored form that does not contain malachite minerals and is a toxic chemical substance used in dyeing. MV is the name given to the group consisting of similar pH indicators and dye chemicals. MV types are mostly used in textile, for dyeing products with purple color. BF magenta dye, it is a mixture of rosaniline, pararosaniline, novel fuchsin and magenta II [15-19]. In the experiments in this study, there are 4 factors and the levels of these factors. Factors and levels for the removal efficiency (%) and absorption capacity (mg/g) are as follows: 50-100-150-200 mg/L for initial concentration, 0.1 - 0.2 - 0.4 - 0.6 - 0.8 - 1 g/L for biosorbent amount, 25-35-45 °C for temperature and 30-60-90-120-150-180 minutes for time.

With *Aspergillus* sp., the factors affecting the removal efficiency and absorption capacity of dyestuffs such as MG, MV, CV, and BF are examined. With *Aspergillus* sp., necessary experiments for the removal efficiency and absorption capacity of MG, MV, CV, and BF from the dyestuffs by using fungi microorganism will be carried out with the help of a team.

4. RESULTS

There are 4 factors in the experiment. These factors are initial concentration (mg/L), amount of biosorbent (g/L), temperature (°C), time (minutes). Different levels will be used for each factor. These levels; 50-100-150-200 mg/L for initial concentration, 0.1, 0.2, 0.4, 0.6, 0.8, 1 g/L for biosorbent amount, 25-35-45 °C for temperature and for time 30, 60, 90, 120, 150, 180 minutes. In addition, there are two dependent variables in this experiment. These dependent variables; removal efficiency (%) and absorption capacity (mg/g).

Table 1. Variables and their levels

Factor	Units	Levels
Biosorbent Amount (A)	g	0.1 - 0.2 - 0.4 - 0.6 - 0.8 - 1
Time (B)	min	30 - 60 - 90 - 120 - 150 - 180
Temperature (C)	°C	25 - 35 - 45
Initial Concentration (D)	mg / L	50 - 100 - 150 - 200

4.1. Results for the Malachite Green (MG)

Minitab uses s, m and n to calculate the F-statistics for Wilks, Lawley-Hotelling, and Pillai's tests. The F-statistic is exact if s=1 or 2. If $s \neq 1$ or 2, the F-statistic is approximate. The formulas for calculating s, m and n in Minitab are as follows:

s $\quad \min(p, q)$
m $\quad .5(|p - q| - 1)$
n $\quad .5(v - p - 1)$

p number of responses
q df of the hypothesis
v df for E
E error matrix

Table 2. MANOVA Tests for Temperature (°C)

Criterion	Test Statistic	F	Num	Denom	P
Wilks'	0.73394	1.42	4	34	0.25
Lawley-Hotelling	0.36036	1.44	4	32	0.24
Pillai's	0.26765	1.39	4	36	0.26
Roy's	0.35426				

s = 2 m = -0.5 n= 7.5

Since the results of four different multivariate statistics for the temperature variable are p>0.05, it is not significant at the 0.05 level. There is no significant difference in terms of dependent variables. In other words, changes in temperature levels do not make a significant difference on the removal efficiency and absorption capacity of MG.

Table 3. MANOVA Tests for Initial Concentration (mg/L)

Criterion	Test Statistic	F	Num	Denom	P
Wilks'	0.0835	13.9	6	34	0
Lawley-Hotelling	7.77342	20.7	6	32	0
Pillai's	1.18387	8.7	6	36	0
Roy's	7.33701				

s = 2 m = 0 n = 7.5

Since the results of four different multivariate statistics for the initial concentration variable are p<0.05, it is significant at the 0.05 level. There is significant difference in terms of dependent variables. In other words, the change in the initial concentration levels creates a significant difference in the removal efficiency and absorption capacity of MG.

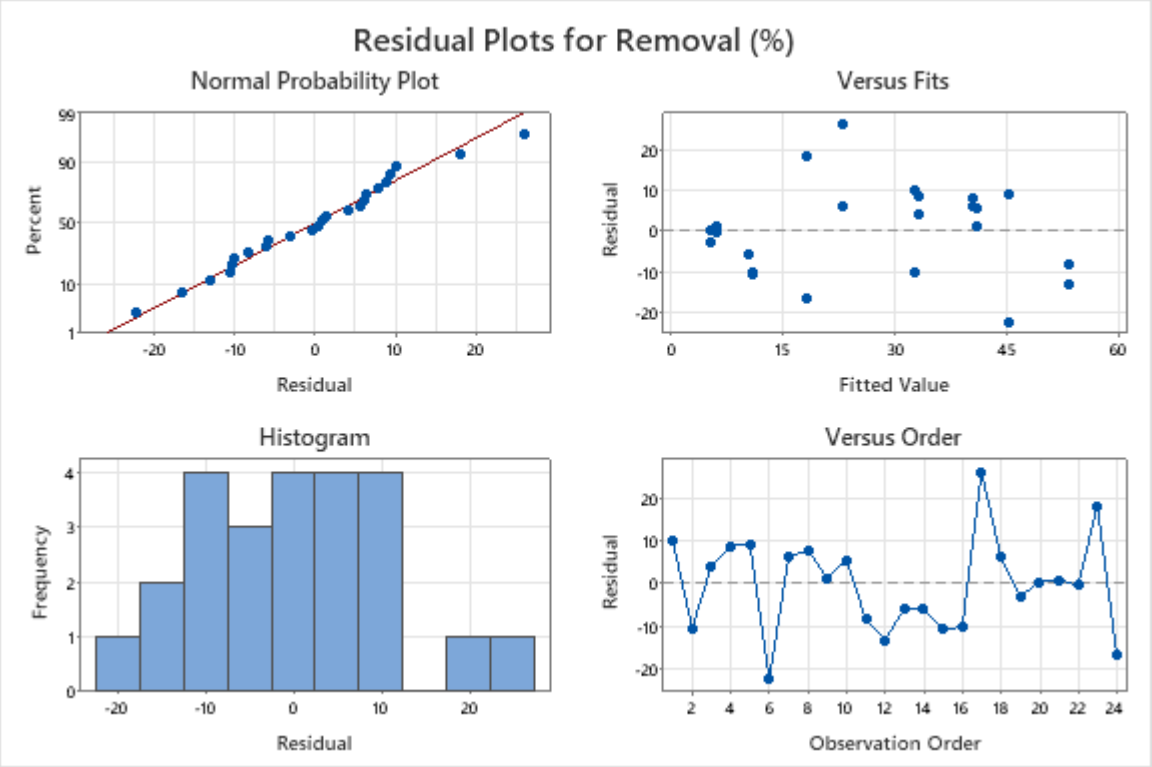

Fig. 1 Residual Plots for Removal Efficiency (%) for Malachite Green (MG)

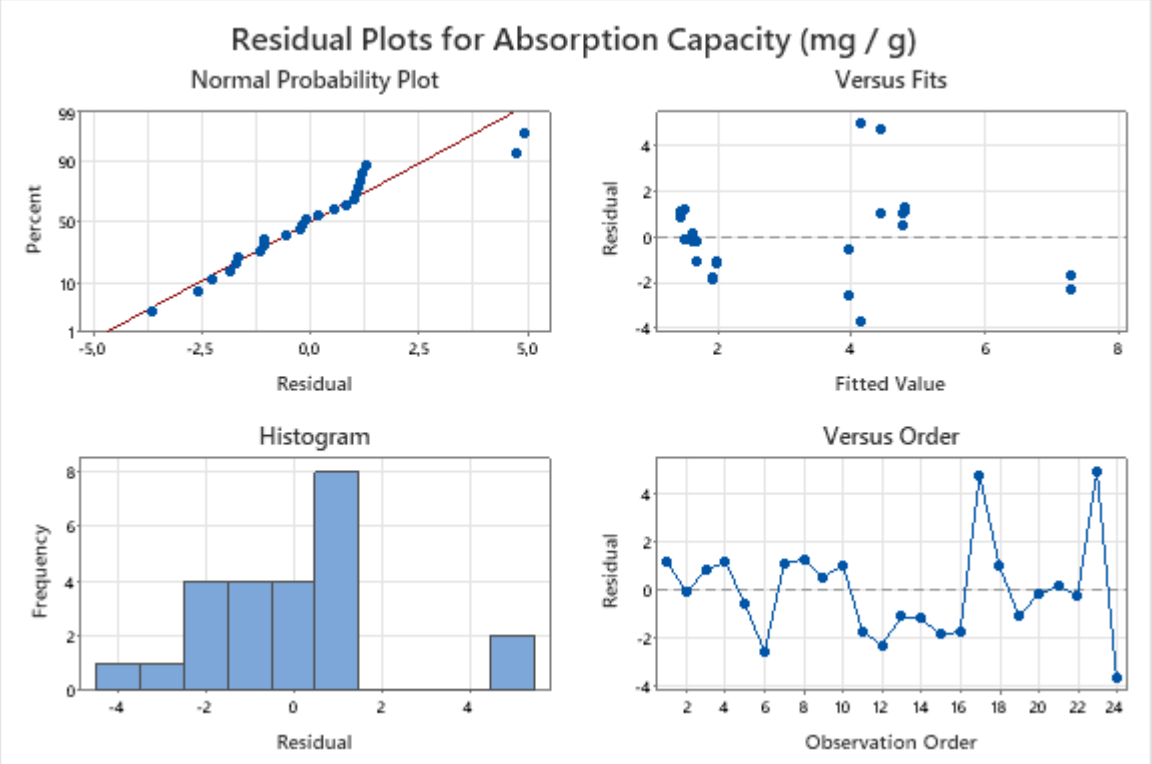

Fig. 2 Residual Plots for Absorption Capacity (mg/g) for Malachite Green (MG)

Table 4. Means for Initial Concentration (mg/L)

Initial Concentration (mg / L)	N	Mean	StDev	95 % CI
50	6	37.03	12.5	(25.43, 48.64)

100	6	45	3.07	(33.39, 56.61)
150	6	14.8	20.08	(3.19, 26.41)
200	6	9.9	13.19	(-1.71, 21.51)

Pooled St. Dev. = 13.6282

When we analyze the factors given in Table 1, the factor that is significant is the initial concentration and there are 4 levels related to it. These levels are 50, 100, 150 and 200 mg/L. When the initial concentration levels are examined, it is seen that the removal efficiency and absorption capacity is higher at the level of 100 mg/L. That is, the factor that is significant is the initial concentration and the corresponding removal at the 100 mg/L level is high and should be adopted.

It was observed that the removal efficiency and absorption capacity of 0.8 g amount of biosorbent was high in the single factor experiment performed in two repetitions.

It was observed that the removal efficiency and absorption capacity of 120 minutes was high in the single factor experiment performed in two repetitions.

4.2. Results for the Methyl Violet (MV)

MANOVA conducted for temperature and the results are given in Table 5.

Table 5. MANOVA Tests for Temperature (°C)

Criterion	Test Statistic	F	Num	Denom	P
Wilks'	0.26251	14	2	10	0
Lawley-Hotelling	2.80935	14	2	10	0
Pillai's	0.73749	14	2	10	0
Roy's	2.80935				

s = 1 m = 0 n = 4

Since the results of four different multivariate statistics for the temperature variable are $p<0.05$, it is significant at the 0.05 level. There is significant difference in terms of dependent variables. In other words, the change in the temperature levels creates a significant difference on the removal efficiency and absorption capacity of MV.

Table 6. MANOVA Tests for Initial Concentration (mg/L)

Criterion	Test Statistic	F	Num	Denom	P
Wilks'	0.00182	74.8	6	20	0
Lawley-Hotelling	47.4563	71.2	6	18	0
Pillai's	1.91	77.8	6	22	0
Roy's	31.59829				

s = 2 m = 0 n = 4

Since the results of four different multivariate statistics for the initial concentration variable are $p<0.05$, it is significant at the 0.05 level. There is significant difference in terms of dependent variables. In other words, the change in the initial concentration levels creates a significant difference in the removal efficiency and absorption capacity of MV.

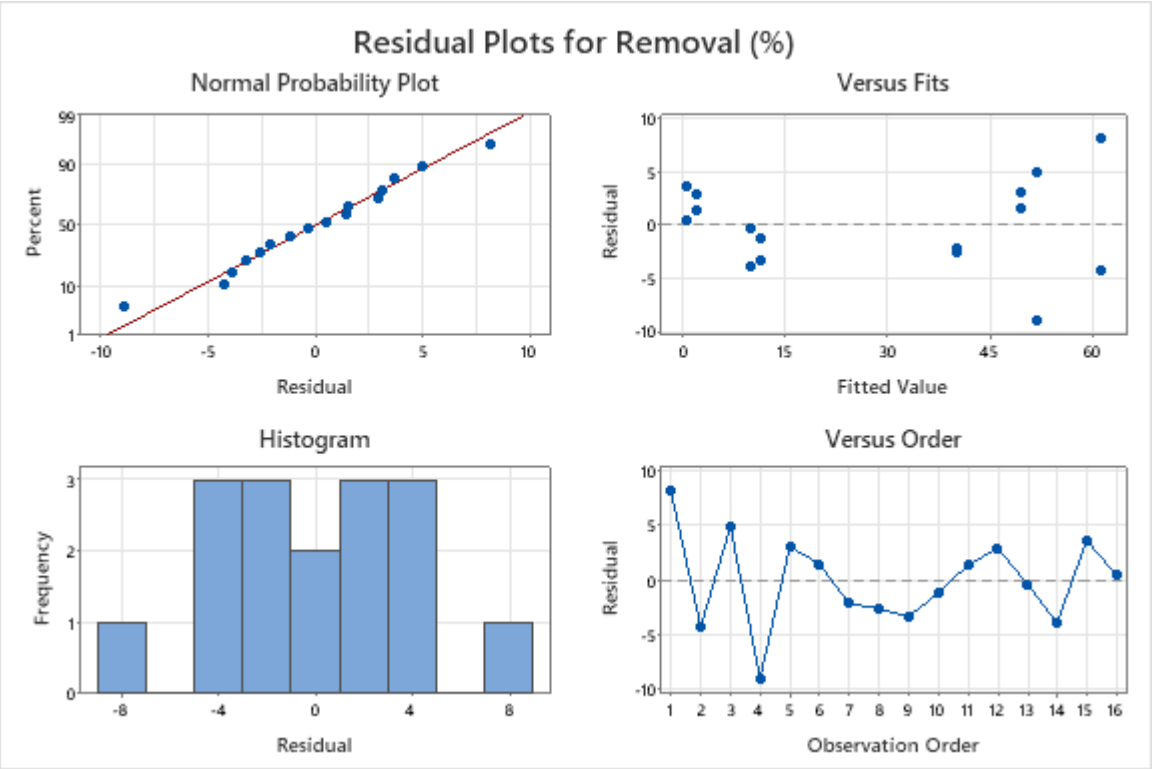

Fig. 3 Residual Plots for Removal Efficiency (%) for Methyl Violet (MV)

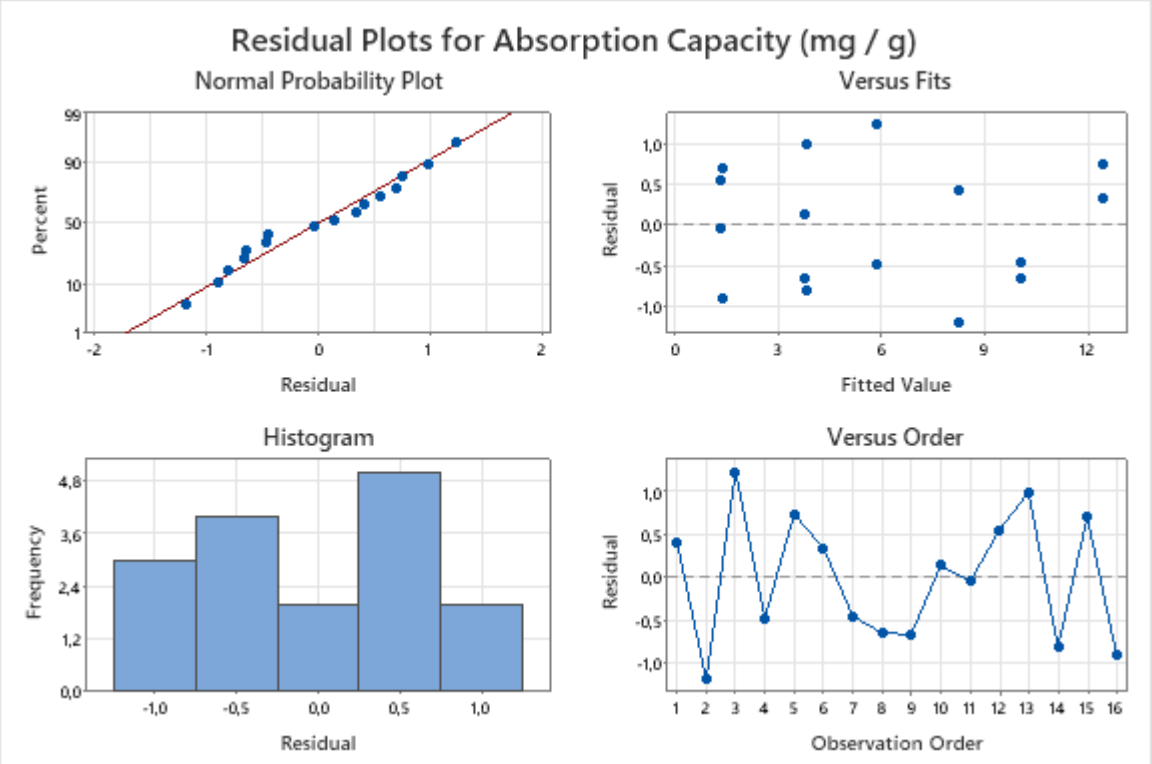

Fig. 4 Residual Plots for Absorption Capacity (mg/g) for Methyl Violet (MV)

Table 7. Means for Temperature (°C)

Temperature (°C)	N	Mean	StDev	95 % CI
35	8	33.16	26.82	(14.41, 51.92)
45	8	23.66	22.45	(4.91, 42.42)

Pooled St. Dev. = 24.7331

Temperature is found significant factor for removal efficiency and absorption capacity. Temperature has 2 levels; 35 °C and 45 °C. When the temperature levels are examined, it is seen that the removal efficiency and absorption capacity is higher at the level of 35 °C. That is, the factor that is significant is the temperature and the corresponding removal efficiency and absorption capacity at the 35 °C level is high and should be adopted.

Table 8. Means for Initial Concentration (mg/L)

Initial Concentration (mg/L)	N	Mean	StDev	95 % CI
50	4	56.67	10.87	(48.81, 64.54)
100	4	44.92	8.2	(37.06, 52.79)
150	4	6.8	3.13	(-1.06, 14.66)
200	4	5.25	3.64	(-2.61, 13.11)

Pooled St. Dev. = 7.21714

Initial concentration is also found significant factor for removal efficiency and absorption capacity. It has 4 levels; 50, 100, 150 and 200 mg/L. When the initial concentration levels are examined, it is seen that the removal is higher at the level of 50 mg/L. That is, the factor that is significant is the initial concentration and the corresponding removal at the 50 mg/L level is high and should be adopted.

It was observed that the removal efficiency and absorption capacity of 0.4 g amount of biosorbent was high in the single factor experiment performed in two repetitions.

It was observed that the removal efficiency and absorption capacity of 180 minutes was high in the single factor experiment performed in two repetitions.

It was observed that the removal efficiency and absorption capacity of 150 mg/L initial concentration was high in the single factor experiment performed in two repetitions.

4.3.Results for the Crystal Violet (CV)

Table 9. MANOVA Tests for Temperature (°C)

Criterion	Test Statistic	F	Num	Denom	P
Wilks'	0.42645	6.73	2	10	0.01
Lawley-Hotelling	1.34493	6.73	2	10	0.01
Pillai's	0.57355	6.73	2	10	0.01
Roy's	1.34493				

s = 1 m = 0 n = 4

Since the results of four different multivariate statistics for the temperature variable are $p<0.05$, it is significant at the 0.05 level. In other words, the change in the temperature levels creates a significant difference in the removal efficiency and absorption capacity of CV.

Table 10. MANOVA Tests for Initial Concentration (mg/L)

Criterion	Test Statistic	F	Num	Denom	P
Wilks'	0.00132	88.3	6	20	0
Lawley-Hotelling	261.70315	393	6	18	0
Pillai's	1.65095	17.3	6	22	0
Roy's	259.80641				

s = 2 m = 0 n = 4

Since the results of four different multivariate statistics for the initial concentration variable are $p<0.05$, it is significant at the 0.05 level. In other words, the change in the initial concentration levels creates a significant difference in the removal efficiency and absorption capacity of CV.

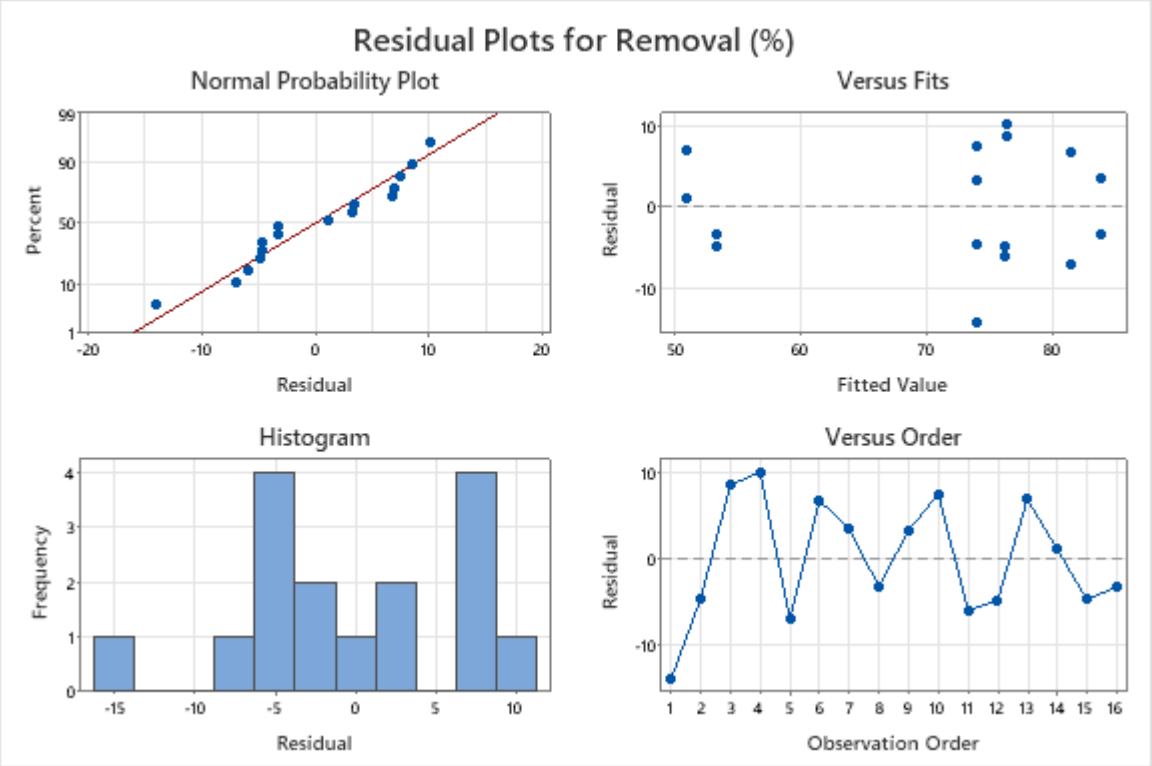

Fig. 5 Residual Plots for Removal Efficiency (%) for Crystal Violet (CV)

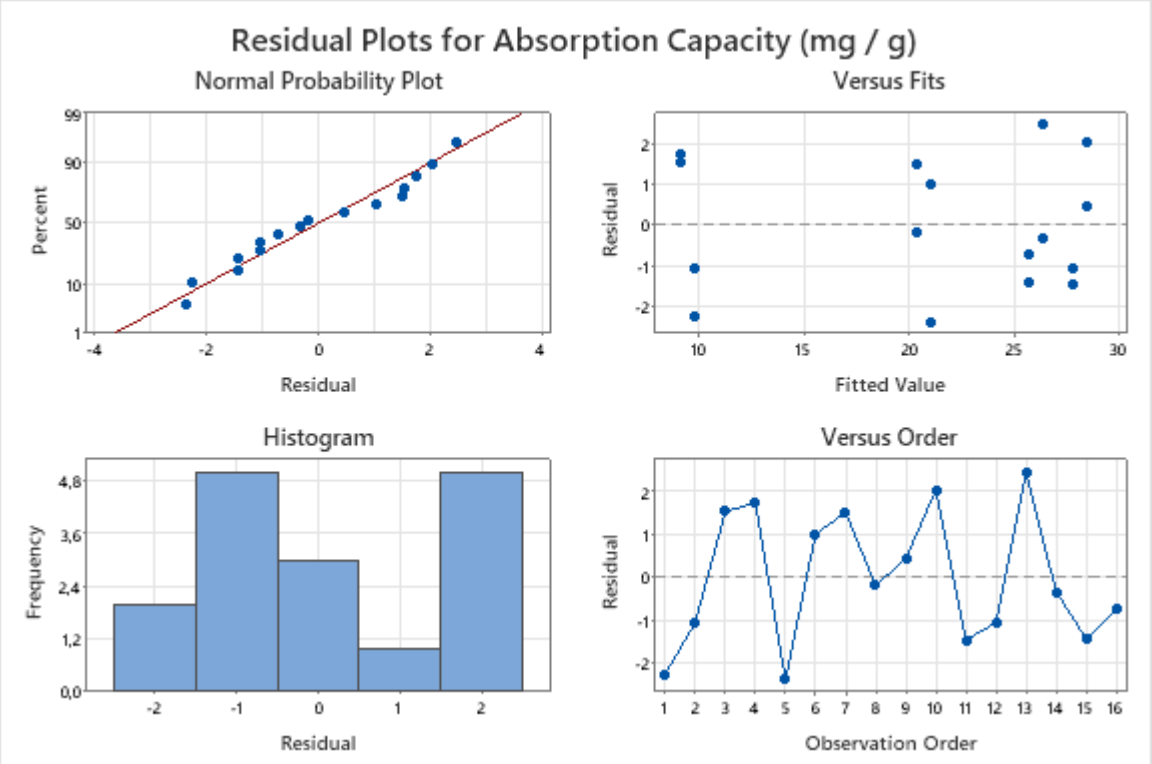

Fig. 6 Residual Plots for Absorption Capacity (mg/g) for Crystal Violet (CV)

Table 11. Means for Temperature (°C)

Temperature (°C)	N	Mean	StDev	95 % CI
35	8	70.14	12.58	(59.35, 80.92)
45	8	72.51	15.7	(61.73, 83.30)

Pooled St. Dev. = 14.2252

Temperature is found significant factor for removal efficiency and absorption capacity. Temperature has 2 levels; 35 °C and 45 °C. When the temperature levels are examined, it is seen that the removal efficiency and absorption capacity is higher at the level of 45 ° C. That is, the factor that is significant is the temperature and the corresponding removal efficiency and absorption capacity at the 45 °C level is high and should be adopted.

Table 12. Means for Initial Concentration (mg/L)

Initial Concentration (mg/L)	N	Mean	StDev	95 % CI
50	4	75.22	12.76	(66.66, 83.79)
100	4	82.75	6.4	(74.18, 91.32)
150	4	75.18	5.19	(66.61, 83.74)
200	4	52.15	4.09	(43.58, 60.72)

Pooled St. Dev. = 7.86646

Initial concentration is also found significant factor for removal efficiency and absorption capacity. It has 4 levels; 50, 100, 150 and 200 mg/L. When the initial concentration levels are examined, it is seen that the removal efficiency and absorption capacity is higher at the level of 100 mg/L. That is, the factor that is significant is the initial concentration and the corresponding removal efficiency and absorption capacity at the 100 mg/L level is high and should be adopted.

It was observed that the removal efficiency and absorption capacity of 0.6 g amount of biosorbent was high in the single factor experiment performed in two repetitions.

It was observed that the removal efficiency and absorption capacity of 90 minutes was high in the single factor experiment performed in two repetitions.

It was observed that the removal efficiency and absorption capacity of 100 mg/L initial concentration was high in the single factor experiment performed in two repetitions.

4.4.Results for the Basic Fuchsin (BF)

MANOVA is conducted for temperature and the results are given in Table 13.

Table 13. MANOVA Tests for Temperature (°C)

Criterion	Test Statistic	F	Num	Denom	P
Wilks'	0.78544	1.09	4	34	0.38
Lawley-Hotelling	0.26427	1.06	4	32	0.39
Pillai's	0.22155	1.12	4	36	0.36
Roy's	0.22468				

s = 2 m = -0.5 n = 7.5

Since the results of four different multivariate statistics for the temperature variable are $p>0.05$, it is not significant at the 0.05 level. There is no significant difference in terms of dependent variables. In other words, changes in temperature levels do not make a significant difference in the removal efficiency and absorption capacity of BF.

Table 14. MANOVA Tests for Initial Concentration (mg/L)

Criterion	Test Statistic	F	Num	Denom	P
Wilks'	0.00479	76.2	6	34	0
Lawley-Hotelling	82.35769	220	6	32	0
Pillai's	1.59598	23.7	6	36	0
Roy's	80.80533				

$s = 2 \quad m = 0 \quad n = 7.5$

Since the results of four different multivariate statistics for the initial concentration variable are $p<0.05$, it is concluded that concentration is significant ($p<0.05$). In other words, the change in the initial concentration levels creates a significant difference in the removal efficiency and absorption capacity of BF.

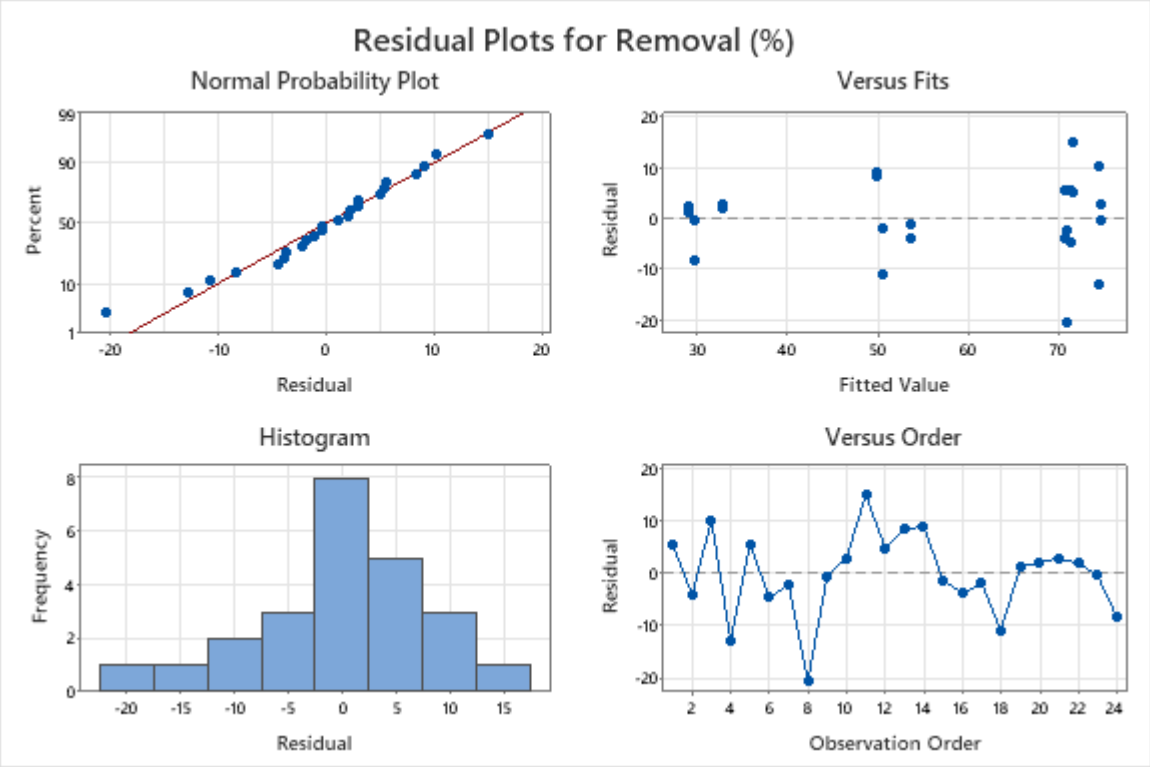

Fig. 7 Residual Plots for Removal Efficiency (%) for Basic Fuchsin (BF)

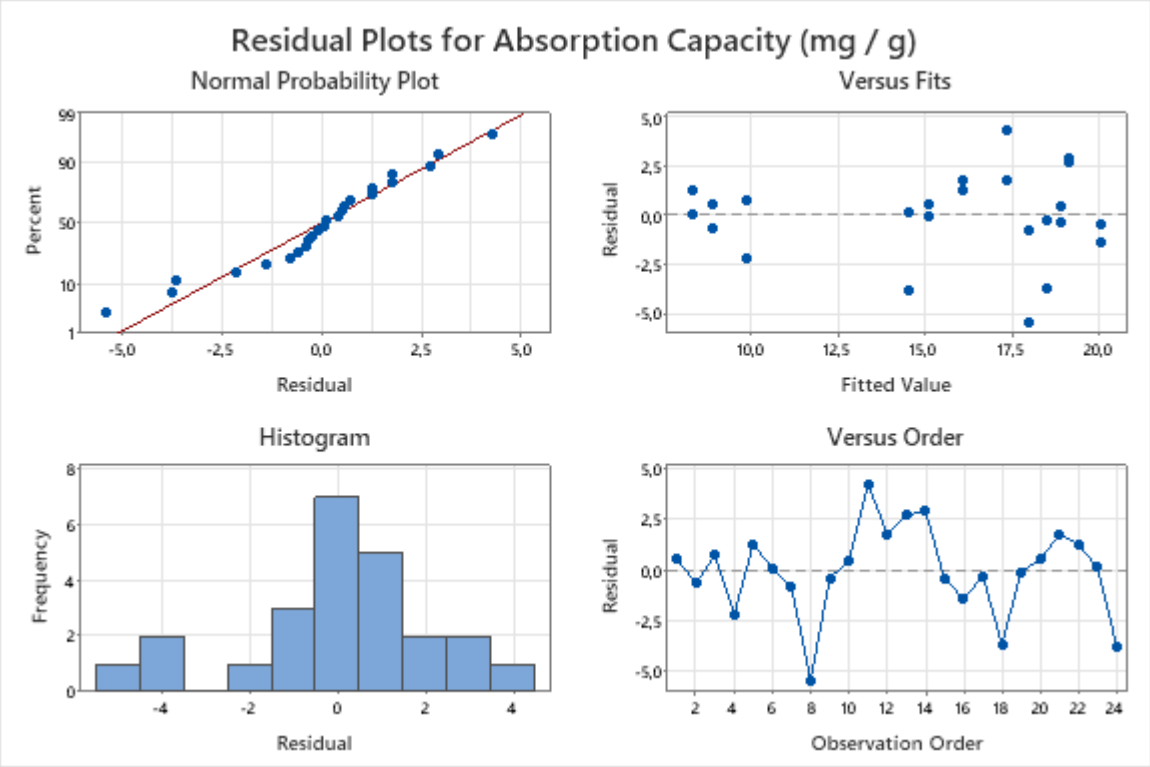

Fig. 8 Residual Plots for Absorption Capacity (mg/g) for Basic Fuchsin (BF)

Table 15. Means for Initial Concentration (mg/L)

Initial Concentration (mg/L)	N	Mean	StDev	95 % CI
50	6	72.12	8.52	(64.76, 79.47)
100	6	72.43	12.22	(65.08, 79.79)
150	6	51.3	7.09	(43.95, 58.65)
200	6	30.57	5.1	(23.21, 37.92)

Pooled St. Dev. = 8.63422

When we analyze the factors above, the factor that is significant is the initial concentration and there are 4 levels related to it. These levels are 50, 100, 150 and 200 mg/L. When the initial concentration levels are examined, it is seen that the removal efficiency and absorption capacity is higher at the level of 100 mg/L. That is, the factor that is significant is the initial concentration and the corresponding removal efficiency and absorption capacity at the 100 mg/L level is high and should be adopted.

It was observed that the removal efficiency and absorption capacity of 0.6 g amount of biosorbent was high in the single factor experiment performed in two repetitions.

It was observed that the removal efficiency and absorption capacity of 120 minutes was high in the single factor experiment performed in two repetitions.

5. RESULTS AND DISCUSSION

In this study, the effects of the factors on the removal efficiency and absorption capacity of MG, MV, CV, and BF from *Aspergillus* sp. were examined. We defined the dependent variables, factors and the levels of these factors in the experiments. Multivariate Analysis of Variance (MANOVA) with Minitab was used for optimum removal efficiency and optimum absorption capacity combination with these factors.

The factor that is significant for MG is the initial concentration and there are 4 levels related to it. These levels are 50, 100, 150 and 200 mg/L. When the initial concentration levels are examined, it appears that the removal efficiency and absorption capacity is 45 % at the 100 mg/L level. It is seen that the removal efficiency and absorption capacity are higher at the level of 100 mg/L. That is, the factor that is significant is the initial concentration and the corresponding removal efficiency and absorption capacity at the 100 mg/L level are high and should be adopted.

The factors that are significant for MV are the temperature and the initial concentration. Temperature levels are 35 °C and 45 °C. When the temperature levels are examined, it appears that the removal efficiency and absorption capacity is 33.16 % at the 35°C level. It is seen that the removal efficiency and absorption capacity are higher at the level of 35 °C. The temperature is significant factor and the corresponding removal efficiency and absorption capacity at the 35 °C are high and should be adopted. Initial concentration has 4 levels and these levels are 50, 100, 150 and 200 mg/L. When the initial concentration levels are examined, it appears that the removal efficiency is 56.67% at the 50 mg/L level. It is seen that the removal efficiency and absorption capacity are higher at the level of 50 mg/L. The initial concentration and temperature are found as significant factors. Hence, the corresponding removal efficiency and absorption capacity at the 50 mg/L level are high and should be adopted. So, 50 mg/L initial concentration and 35 °C temperature should be adopted for MV.

The factors that are significant for CV are the temperature and initial concentration. Temperature has 2 levels related to it. These levels are 35°C and 45 °C. When the temperature levels are examined, it appears that the removal efficiency is 72.51 % at the 45 °C level. It is seen that the removal efficiency and absorption capacity is higher at the level of 45 °C. The factor that is significant is the temperature and the corresponding removal efficiency and absorption capacity at the 45 °C are high and should be adopted. Initial concentration has 4 levels which are 50, 100, 150 and 200 mg/L. When the initial concentration levels are examined, it appears that the removal efficiency 82.75% at the 100 mg/L level. It is seen that the removal efficiency and absorption capacity are higher at the level of 100 mg/L. The factor that is significant is the initial concentration and the corresponding removal efficiency and absorption capacity at the 100 mg/L level is high and should be adopted. So, 100 mg/L initial concentration and 45 °C temperature should be adopted for CV.

The factor that is significant for BF is the initial concentration with 4 levels. These levels are 50, 100, 150 and 200 mg/L. When the initial concentration levels are examined, it appears that the removal efficiency is 72.43 % at the 100 mg/L level. That is, the factor that is significant is the initial concentration and the corresponding removal efficiency and absorption capacity at the 100 mg/L level are high and should be adopted.

As a result, with this study, MG, MV, CV, and BF which are dyestuffs, it is put forward reveal the relationship between the factors and levels as a result of the analyzes for the removal efficiency and absorption capacity. Temperature and initial concentration will be useful for removal efficiency and absorption capacity. It is thought that the temperature and initial concentration parameters determined during the experiment will be useful for the subsequent studies for removal efficiency and absorption capacity.

ACKNOWLEDGEMENTS

This work was financially supported by the Unit of the Scientific Research Projects of Eskişehir Technical University under grant no. [19ADP109] and also financially supported by Scientific and Technological Research Council of Turkey [2209].

REFERENCES

[1] Aydin Kurç, M., Güven, K., Korcan, E., Malkoç, S., Güven, A. (2016). Lead biosorption by a moderately Halophile *Penicillium* sp. Isolated from Çamalti Saltern in Turkey. Anadolu University Journal of Science and Technology–C–Life Science and Biotechnology. 5(1), 13–21.

[2] Malkoç, S. (2017). Removal of remazol red dye with live cell *Aspergillus terreus.* Anadolu University Journal of Science and Technology A: Applied Sciences and Engineering. 18(3), 654-662.

[3] Hasgul, E., Malkoç, S., Güven, A., Dede, A., Güven, K. (2019). Biosorption of cadmium and copper by *Aspergillus* spp. isolated from industrial ceramic waste sludge, Biological Diversity Conservation. 12(3), 44-56.

[4] Malkoc, S., Anagun, A. S., Deniz, N. (2021) A Novel Sustainable Biosorbent (*Ulocladium Consortiale*) Proposal with Central Composite Design to Reduce Water Pollution, Iranian Journal of Science and Technology, Transactions A: Science. 1-11.

[5] Durmaz B. (2009). Bakteriyel Boyalar ve Boyama Yöntemleri, Yüksek İhtisas Üniversitesi, Ankara.

[6] Kumar, C. G., Mongolla, P., Joseph, J., Sarma, V. U. M. (2012). Decolorization and biodegradation of triphenylmethane dye, brilliant green, by *Aspergillus* sp. isolated from Ladakh, India. Process Biochemistry. 47(9), 1388–1394.

[7] Chen, S.H., Yien Ting, A.S. (2015). Biosorption and biodegradation potential of triphenylmethane dyes by newly discovered *Penicillium simplicissimum* isolated from indoor wastewater sample. International Biodeterioration & Biodegradation. 103, 1-7.

[8] Chen, S. H., Yien Ting, A. S. (2015). Biodecolorization and biodegradation potential of recalcitrant triphenylmethane dyes by *Coriolopsis* sp. isolated from compost. Journal of Environmental Management. 150, 274-280.

[9] Munck, C., Thierry, E., Grable, S., Chen, S. H., Yien Ting, A. S. (2018). Biofilm formation of filamentous fungi *Coriolopsis* sp. on simple muslin cloth to enhance removal of triphenylmethane dye. Journal of Environmental Management. 214, 261-266.

[10] Cardoso, B. K., Linde, G. A., Colauto, N., Valle, J. S. (2018). *Panus strigellus* laccase decolorizes anthraquinone, azo, and triphenylmethane dyes. Biocatalysis and Agricultural Biotechnology. 16, 558-563.

[11] Rybczyńska-Tkaczyk, K., Święciło, A., Szychowski, K. A., Korniłłowicz-Kowalska T. (2018). Comparative study of eco- and cytotoxicity during biotransformation of anthraquinone dye Alizarin Blue Black B in optimized cultures of microscopic fungi. Ecotoxicology and Environmental Safety. 147, 776-787.

[12] Shanmugam, L., Naikawadi, V. B., Ahire, M. L., Nikam, T. D. (2018). Decolorization and detoxification of reactive azo dyes using cell cultures of a memory tonic herb *Evolvulus alsinoides* L. Journal of Environmental Chemical Engineering. 6, 6479-6488.

[13] Multivariate Analysis of Variance (MANOVA), NCSS Statistical Software

[14] Minitab İstatistik Yazılımı, https://sigmacenter.com.tr/minitab/ (Date of access: 24.03.2021)

[15] Sani, R. K., Banerjee, U. C. (1999). Decolorization of triphenylmethane dyes and textile and dye-stuff effluent by *Kurthia* sp. Enzyme and Microbial Technology. 24, 433-437.

[16] Chen, C. C., Liao, H. J., Cheng, C. Y., Yen, C. Y., Chung, Y. C. (2007). Biodegradation of crystal violet by *Pseudomonas putida*. Biotechnology Letters. 29(3), 391–396.

[17] Chen, C. Y., Kuo, J. T., Cheng, C. Y., Huang, Y. T., Ho, I. H., Chung, Y. C. (2009). Biological decolorization of dye solution containing malachite green by *Pandoraea pulmonicola* YC32 using a batch and continuous system. Journal of Hazardous Materials. 172(2–3), 1439–1445.

[18] Du, L. N., Zhao, M., Li, G., Xu, F. C., Chen, W. H., Zhao, Y. H., 2013. Biodegradation of malachite green by Micrococcus sp. strain BD15: biodegradation pathway and enzyme analysis. International Biodeterioration & Biodegradation. 78, 108–116.

[19] Przystas, W., Zabłocka-Godlewska, E., Grabinska-Sota, E. (2018). Efficiency of decolorization of different dyes using fungal biomass immobilized on different solid supports, Brazilian journal of microbiology. 49, 285–295.

Research Article

COLOR SEPARATION WITH COMPUTER VISION

Authors: Hüseyin CEYLAN , Ömer ÇOKAKLI

To cite to this article: Ceylan, H. and Çokaklı, Ö. (2021). COLOR SEPARATION WITH COMPUTER VISION . International Journal of Engineering and Innovative Research ,3(3), p: 201-208DOI: 10.47933/ijeir.945265

DOI: 10.47933/ijeir. 945265

To link to this artice: https://dergipark.org.tr/tr/pub/ijeir/archive

International Journal of Engineering and Innovative Research

http://dergipark.gov.tr/ijeir

COLOR SEPARATION WITH COMPUTER VISION

Hüseyin CEYLAN[*], Ömer ÇOKAKLI [2]

[1] Kırıkkale University, Kırıkkale Vocational School, Kırıkkale, Turkey.
[2] Ermes BTK, Product Engineer, Konya, Turkey.

[*]Corresponding Author: huseyinceylan@kkk.edu.tr
https://doi.org/10.47933/ijeir.945265

(**Received:** 30.05.2021; **Accepted:** 26.07.2021)

ABSTRACT: From the first day of existence human beings have been carrying out various production activities to meet their basic needs. Today, the majority of products are produced within factories. The identification, differentiation or classification of these products plays an extremely important role in factory operation and efficiency. Human factors and mechanical systems in factories cause a waste of time, defects or faulty separation of products. According to these requirements and problems, the methods used in factories have necessarily become more functional. Various cases such as whether the products produced in the factories comply with the required standards or their classification are determined according to varying parameters. One of these parameters is the color of the product (or the color of some part on the product). In this study, different product images will be browsed through the Matlab environment with a camera and this image will see colors (Red, Green, Blue) in Matlab environmental visual planning techniques and its separation is the main purpose of the study.

Keywords: Computer Vision, Color Detection, Product Separation, Image Processing

1. INTRODUCTION

Human beings have been led to research and develop faster methods of supply in order to meet the consumption of the rapidly increasing world population and the increasing demand accordingly. Today, the identification, differentiation, or classification of all products, from the heaviest to the lightest one, is carried out economically and quickly thanks to the color detection field. Thanks to modern technology, color separation systems are preferred in many sectors, where industrial automation systems are used, such as food, agriculture, automotive, chemistry, cosmetics. With the increasing demand of human beings, new demands like the identification, control, counting and sorting of products produced in factories have arisen. Due to these demands, color detection systems have now become more functional.

Color separation systems in the automation industry provide an alternative option for processes such as identification, sorting or control of different products. Color recognition systems allow easy identification, sorting or control of products according to their own colors, other labels, packages or texts. Especially in the packaging industry, color control on products is used extensively. Besides, it provides a significant advantage in the sifting of products that are out of the standard due to the detection of packages and bottles.

In this study, firstly, color detection studies carried out previously will be mentioned. Theoretical information about computer vision, image processing and color detection will be given. Products separating process in Matlab environment according to their colors will be explained in a detailed way. As a result, the designed interface will be tested and the results will be announced.

Gürcan, in his study titled - "Computer Vision in Industrial Automation", has designed an economical, modern and real-time vision system that can meet the industrial automation needs by using camera and computer image processing techniques [1].

Öztürk, in his study titled - "Detecting eggshell defects on white eggs with image processing techniques", used computer vision techniques in the quality classification of eggs [2].

Arslan, in his study titled - "Real-Time Forest Fire Smoke Detection in Motion Camera", used computer vision techniques in detecting the presence of possible smoke in the images obtained from a moving camera that can monitor a wide area of 3600 [3].

Çelik, in his study titled - "Mouse Design Using Image Processing for Disabled", discussed the issue of developing a mouse that can be controlled with the help of a camera [4].

Senthilkumar, in his study titled - "Traffic Analysis and Control Using Image Processing", used the computer vision method to develop a highly efficient work as an alternative to existing solutions to manage traffic congestion and accidents especially in big cities [5].

Ebraheem, in his study titled - "Using Digital Image Processing to Make an Intelligent Gate", has brought a new perspective to the field of home security by using image processing techniques preferred in many sectors (medical, social life,… etc.) [6].

Bayrakdar in his study titled – "An accelerated approach for facial expression analysis on video files", an approach is proposed for the accelerated facial expression analysis of video files[7].

The main purpose of this study is products separation according to their colors (Red, Green, Blue) delicately and without using human power. Firstly, the products images in different colors (red, green and blue) will be obtained by the camera and then they will be separated according to their color using computer vision techniques.

2. COMPUTER VISION

According to the study conducted by Chang Shu [8], computer vision (CV) is a field of study that offers assistive techniques for interpretation and understanding of images with useful information extracted from the contents of digital images such as images and videos, by computer modeling the perception way with eyes of living beings. According to the studies by Szeliski [9] and Adrien [10], the algorithms used in this field studies are divided into three groups: those that improve the noise or missing data in the image, learn the image in real time, and those that allow the use of limited resources such as power and memory. Existing research has been carried out on studies in grouped titles to make algorithms more robust and efficient [11]. Computer Vision has taken its place in various mathematical methods such as statistics, optimization and differential equations, and its use in the fields of robotics, graphics and security has started to increase gradually [8].

The first fruits of computer vision are based on the 1970s. In the beginning, only very simple shapes such as writings could be perceived. Processing lines by labeling or showing the shape with a circuit were a few of them. In the following 1980s, objects began to be defined by looking at their shapes and boundaries and decisions were made based on these defined objects. These algorithms were based on methods such as corner detection, shading, and physically based modeling. In the 1990s, not only one image but many images from different angles were processed. More familiar methods such as face recognition, factorization-based structure from motion, image segmentation were started to be used. In the 2000s, three-dimensional modeling has been one of the most interesting subjects of today [11].

Operation order in the computer vision field consists of image acquisition, image processing, feature extraction, preparation, recognition, interpretation, and understanding stages [11]. The operation order is shown in Figure 1. The subject of image processing will be explained in 2.1 in a detailed way.

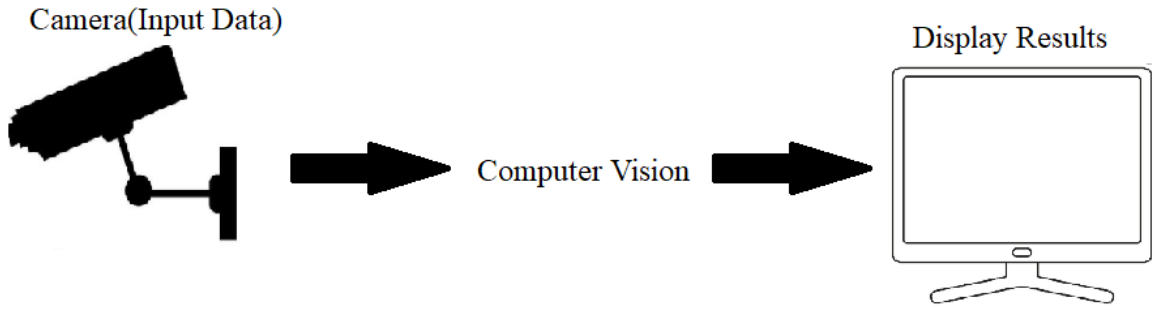

Figure 1. Computer vision processing steps

The image source is determined via image acquisition process, which is the first step of the cycle in Figure 1. The image source contents can be taken by optical intervention or digital photography. Image sources' contents can be images or videos as well. Thus, the image acquisition phase is completed by executing the image capture process. After the image acquisition stage, the converting process of the images into digital data starts, which is the second step in Figure 1. Various tools are used in this process. The digital data obtained through those tools are evaluated with digital methods such as various signal processing methods and statistics, allowing them to produce measurable throughput, analyze and interpret them. Computer graphics are obtained from the image data which becomes digital data by using computer vision techniques and image processing methods with the image processing stage shown in Figure 1. This stage is the last step of the Computer Vision process, which plays a role in the decision-making process by making the actual analysis of the data. In the other steps, low-level information and image data are calculation process is carried out. In this step, high-level algorithms are applied on the calculated data. Feature extraction methods that provide high-level information extraction from the image such as color and shape, classification of information extracted from the image, and algorithms including image recognition processes that enable objects recognition are applied to the image at this step. The obtained image data becomes ready for the application of machine learning methods.

2.1. Image Processing

Image processing is one of the forms of signal processing in which an "image" is used as the input signal. It is a method of obtaining a new image by changing the features and appearance by processing images that have been transformed into a digital image in different ways due to various needs [12]. Image processing is one of the forms of signal processing in which an "image" is used as the input signal; and it is a method of obtaining a new image as a result of processing images transformed into a digital image in different ways within the framework of various needs and purposes, changing their features and appearance [12].

Image processing stages vary depending on the purpose for which the image will be processed. However, the basic stages in image processing can be sorted as noise removal and image editing (image enhancement, image sharpening, etc.), color editing (brightening, sharpness adjustment, color conversion), edge detection, corner detection, segmentation (dividing the image into objects or areas), image recognition, detection by classification (creating a concept related to seeing with the help of image analysis of recognized objects) [12-15]. These levels are also an image processing method.

Today, the application scope of image processing is more in comparison with past and this diversity is increasing day by day.

Fundamentally, image processing is used in almost all fields, as well as in medicine and biology (detection of bone fractures, tumor detection, biomedical imaging, etc.), astronomy (satellite images, etc.), industrial applications and engineering (film industry, TV, material testing, remote sensing, inspection of moving surfaces, robotics. , textile and food industries process and product inspection, barcode reading, document processing, etc.), security, defense and law (fingerprint recognition, plate recognition system, iris, face recognition, symbol recognition, hand gesture and sign recognition, paper money recognition. Picture or image recognition, target identification, GPR-mine scanning, night vision, smart rocket systems, etc.), sports (finding the speed of the athlete, detecting whether the ball crosses the goal line, etc.), banking, commerce, art, geography (forecasting via air and satellite images, etc.), biology, physics (spectrometers, electron microscope images), game programming (computer vision, 3-D modeling, etc.), space science (satellite, microwave radar images, etc.) r images etc.)[14-19].

The methods used for image processing can be developed optionally. Applications may require combined use of various methods, inclusion of some criteria, and transaction speeds increase. Image processing contains a lot of methods like Fourier transform, which is used for different purposes, Histogram equalization, Median (Medium) filters, Gabor filter method, wavelet transform method, Topological Independent Component Analysis (TICA), etc.

Perihanoğlu [21,24] divided image processing methods into 3 groups. They are point processing techniques, image enhancement methods and morphological processes.

Karakoç [22,25] divided image processing methods into seven groups. They are:

- ✓ Image transforms (Fast Fourier Transform, Hadamard Transform, Cosine Transform),
- ✓ Image enhancement (Spatial Enhancement, Frequency Enhancement),
- ✓ Image restoration (Distortion Models, Block-Circulant Matrices, Inverse Filtering),

- ✓ Image segmentation (Discontinuity-Capturing [Point capture, line capture, edge detection], Threshold/Field Detection,
- ✓ Image compression (Lossy Compression, Error-Free Compression),
- ✓ Image presentation (Border Recognition, Area Recognition) and
- ✓ Image interpretation (Decision-Theory Methods, Structural Methods).

3. METHOD AND EXPERİMENT

The products separating process according to their colors by using computer vision techniques is shown in the block diagram in Figure 2.

Figure 2. By using a block diagram

Products images of different colors were exported to Matlab environment via camera. The camera has 6 layers of high quality CMOS optical 5-Glass lenses, 2.0 megapixels and a picture resolution of 2304x1728 pixels [23]. The camera that has been used is shown in Figure 3, the sample image obtained from that camera is given in Figure 4.

Figure 3. Camera used in image acquisition

Figure 4. Image obtained from the camera

After camera acquisition of products in different colors, the computer vision stage in Matlab environment starts. At this stage, the conversion process in an image to a gray scale, pixel determining of the red, green and blue (RGB) combination in the gray scale image, applying the extraction process to the image from the red, green and blue color space forms respectively, converting the obtained images to binary and counting the white pixels were carried out. Products color determination is done after the counting process. Flow chart of computer vision stage applied in Matlab environment is shown in Figure 5.

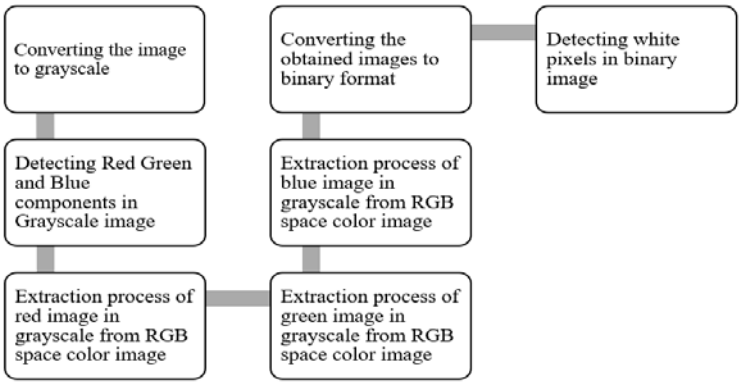

Figure 5. Flow chart of the computer vision process applied to images in Matlab environment.

The flow chart in Figure 5 has been randomly applied to three products of different colors. These products are shown in Figure 6.

Figure 6. Products that Computer Vision process is applied.

4. DISCUSSION AND SUGGESTIONS

To test the algorithm, images of 3 different products were exported to the Matlab environment via camera as shown in Figure 6. These products are a screwdriver (red color), a pencil (green color) and a key ring (blue color). These images were separately subjected to the flow diagram given in chapter 3, figure 5. The products have been converted from RGB color space to gray scale. The red, green and blue pixels of the gray scale products have been detected. The gray scale image has been extracted from the RGB space color image. The white pixel areas in the new images were detected. These detected regions have enabled the products to be distinguished according to their colors.

Color classification of the products in three different colors has been completed successfully and the study has achieved its goal. The obtained results are shown in Figures 7, 8 and 9.

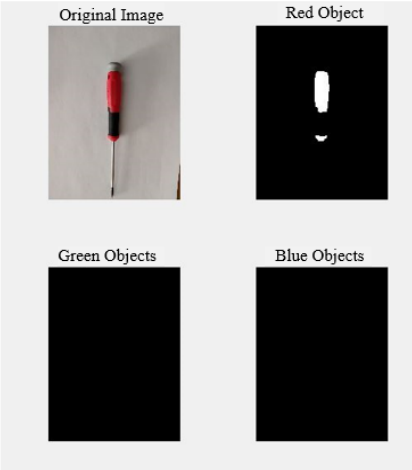

Figure 7. Red product color separation result

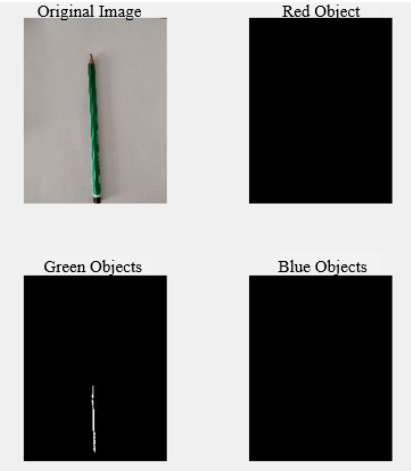

Figure 8. Green product color separation result

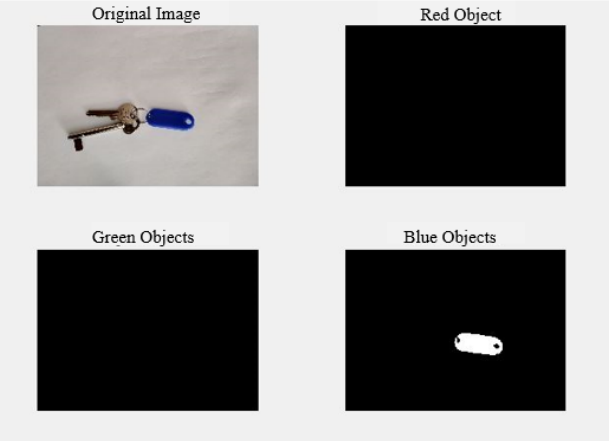

Figure 9. Blue product color separation result

In order to develop this system, this can be integrated in factories, where belt conveyors are used for production, calibration can be made for other colors and the color recognition scale can be increased or the work carried out in the quality control sector can be used. Other programming languages such as PYTHON, C# can be used instead of the Matlab interface. STM, Little Panda, Beaglebone, NVIDIA etc. development cards can be used in industrial applications of computer vision.

REFERENCES

[1] Gürcan, E. "Computer Vision in Industrial Automation." Master Thesis, Yildiz Technical University, 2008.

[2] Öztürk, N. "Eggshell Defects Detection on White Eggs Using Image Processing Techniques." Master Thesis, Karadeniz Technical University, 2014.

[3] Arslan, İ. "Real Time Wildfire Smoke Detection On Moving Camera." Master Thesis, Hacettepe University, 2015.

[4] Çelik, Y. "Mouse Design Using Image Processing for Disabled. "Kahramanmaras Sutçu Imam University Journal of Engineering Sciences 20//3 ,2017: 49-55.

[5] Senthilkumar K. "Traffic Analysis and Control Using Image Processing." IOP Conference Series Materials Science and Engineering 263//4(2017):042047.
[6] Ebraheem S. "Using Digital Image Processing to Make an Intelligent Gate." International Journal of Advanced Computer Science and Applications 5//5, 2014.
[7] Bayrakdar S, Akgün D, Yücedağ İ., "An accelerated approach for facial expression analysis on video files". Pamukkale University Journal of Engineering Sciences. 23(5).2017
[8] Shu C. and Gerhardrothrogerscom G. R., "Introduction to Computer Vision What is Computer Vision? The goal of computer vision is to develop Machine Vision General visual perception is hard, " pp. 1–12, 2008.
[9] Szeliski R., "Computer Vision, Algorithms and Applications", Springer, pp. 1–25, 2010.
[10] Bishop M., "What is Computer Vision?, " Security & Privacy, IEEE, 2003. [Online]. Available: https://hayo.io/computer-vision/
[11] Disun. "What is Computer Vision." https://www.disun.com.tr/index.php/sayfa1/
[12] Karakoç M. "Image Processing Technologies and Applications", Akademik Bilisim Conference 2012 (1-3 February 2012), Usak University, Usak, 2012.
[13] Aydın İ., Bölüm:0 "Introduction Digital Image Processing.", Elazığ, 2013. http://web.firat.edu.tr/iaydin/bmu357/bmu357_bolum0.pdf , 2016.
[14] Sevgen S., "Stable Template Design For Cellular Neural Network With Applications To Image Processing", Unpublished Ph.D. Thesis, Istanbul University, Istanbul, 2009.
[15] Kısa M., "Detection Of Vehicles On The Road", Unpublished Ph.D. Thesis, Selcuk University, Konya, 2014.
[16] Alçın M., "Image Processing Based Fingerprint Verification Reliable", Unpublished Master Thesis, Marmara University, Istanbul, 2007.
[17] Özalp M., 2015, Image Enhancement, http://documents.tips/documents/imgeiyilestirme-sunu.html , (03.11.2016).
[18] Yetik İ.Ş., ELE 473-573 "Digital Image Processing - Projects", 2015, http://syetik.etu.edu.tr/ele573/projects.html , 2016.
[19] Huang J., Kumar S.R., Mitra M., Zhu W.J., Zabih R., "Spatial color indexing and applications", International Journal of Computer Vision, Volume:35, Number:3, pp.245–268. 1999, http://www.cs.cornell.edu/~rdz/Papers/jing-IJCV99.pdf, 2016.
[20] Akan H., "A System Design For Control Of The Processes Based On Digital Image Analysis", Unpublished Master Thesis, Marmara University, Istanbul, 2007
[21] Perihanoğlu G.M., "Feature Extraction from Images By Using Digital Image Processing Techniques", Unpublished Master Thesis, Istanbul Technical University, Istanbul, 2015
[22] Karakoç M., "Image Searching Inside Another Image Processing Techniques And Artificial Intelligence Methods", Unpublished Master Thesis, Pamukkale University, Denizli, 2011.
[23] Artes Camera. "Property of Camera." http://artescorp.com/store/ProductDetails.aspx?productid=85513
[24] Perihanoğlu G.M., "Feature Extraction from Images By Using Digital Image Processing Techniques", Unpublished Master Thesis, Istanbul Technical University, Istanbul, 2015.
[25] Karakoç M., "Image Searching Inside Another Image Processing Techniques And Artificial Intelligence Methods", Unpublished Master Thesis, Pamukkale University, Denizli, 2011.

Research Article

DEVELOPMENT AND EFFICIENCY OF SMART MOBILE DEVICE APPLICATION: EXAMPLE OF HEAT AND TEMPERATURE INSTRUCTION

Authors: Okan ORAL, Volkan GÖK

To cite to this article: Gök, V. & Oral, O. (2021). DEVELOPMENT AND EFFICIENCY OF SMART MOBILE DEVICE APPLICATION: EXAMPLE OF HEAT AND TEMPERATURE INSTRUCTION . International Journal of Engineering and Innovative Research, 3(3), p:209-221 DOI: 10.47933/ijeir.902543

DOI: 10.47933/ijeir.902543

To link to this artice: https://dergipark.org.tr/tr/pub/ijeir/archive

International Journal of Engineering and Innovative Research

http://dergipark.gov.tr/ijeir

DEVELOPMENT AND EFFICIENCY OF SMART MOBILE DEVICE APPLICATION: EXAMPLE OF HEAT AND TEMPERATURE INSTRUCTION

Okan ORAL[1*], Volkan GÖK[1]

[1]Akdeniz University, Department of Engineering, Antalya, Turkey.

[*]Corresponding Author: okan@akdeniz.edu.tr

https://doi.org/10.47933/ijeir.902543

(**Received:** 25.03.2021; **Accepted:** 04.07.2021)

ABSTRACT: The versatility of mobile devices, such as availability, portability, adaptability, and the ability to personalize individual experiences, makes them valuable and makes their use mandatory. Rapid developments in mobile devices have had an impact on the field of education as well as in all areas. This situation has revealed mobile learning in the education system. Mobile learning is seen as a field of research that attracts practitioners at different stages of education to facilitate learning. The use of mobile technologies in learning has a number of advantages in terms of providing learning opportunities anywhere and anytime. This superiority, more mobility and expanded functionality, allows for faster, student-faculty interactions in flexible times and locations. In addition, when mobile technologies are used as part of active learning, they can increase students' motivation and satisfaction, and contribute to the learning of the taught content. The aim of this study is to develop mobile applications for the subject of heat and temperature, which students find hard to understand, and to use the developed applications in the lecture and to measure their impact on learning. For this purpose, mobile applications of the planned scenarios were created using Crazy Talk Animator and Adobe Flash CS6. Mobile applications were applied to the students as pre-test-post-test with control group and as half-experimental in the lessons. When the results were evaluated, it was observed that educational materials consisting of mobile applications were significantly more effective in increasing students' level of knowledge on the subject compared to normal lectures.

Keywords: Mobile Application Development, Mobile Learning, Content Design, Heat and Temperature.

1. INTRODUCTION

Today, as a result of efforts to integrate rapidly developing technology into almost every field, use of mobile technologies has become indispensable in our lives. The expansion of mobile device use has introduced the concept of mobile learning as a new dimension to distance learning. In mobile learning, a person can flexibly and quickly reach the needed information, regardless of time and space. [23].

Mobile learning is an educational approach that aims to close the individual's deficiencies in education with mobile devices. It has become very popular as a result of the widespread use of mobile devices [2]. In the use of mobile training tools and applications in some studies, many users find the teaching technique with mobile devices interesting [3]. In addition, parallel with the development of mobile devices with students whose use is widespread, it is seen that the

level of attitude towards mobile learning is high. [11]. The benefits of mobile learning are listed as follow:

- The ability to continue the learning activity outside the classroom without interruption,
- The prediction that education systems can be expanded by making them suitable for mobile devices,
- Providing equal opportunity for disabled students,
- Increasing the audio and visual interaction between students, academicians, and other users,
- Increasing the student's interest and motivation.

Physics teaching is perceived as a lesson full of formulae among learners. This attitude towards the lesson, makes physics lesson difficult in the eyes of the learner. Students, in their minds, try to revive these concepts and incidences in physics in their own way. Because of the wrong perception created, this situation causes great misconceptions on students. [23].
The biggest reason for misconceptions about heat and temperature, definition of heat and temperature, used in daily life or as a result of individual observation, consists of wrong terms. What is the difference between heat and temperature? A student who thinks about questions from his/her experiences in life enters a confusion of concepts when he/she evaluates these questions with their interpretation. If theoretical knowledge is supported by practical training, the student will be able to get rid of this conceptual confusion.[6]

The biggest deficiency of applied training is the inability of experiments that are difficult and expensive to be done at any time. Also, while doing the experiment, dangerous situations that may occur with the test materials used are among the challenges of practical training.

For this reason, computer-aided virtual experiments, applied with animation and simulations, can be done more effectively. With mobile applications prepared on the subject, students will be able to learn the cases that cannot be concluded with observations. With simulations prepared, broader learning experiences will be provided. Training using computer animations can be as functional as activity-assisted teaching. [13]. This study is aimed to produce interactive contents for mobile devices and to measure teaching effectiveness on physics lesson heat and temperature where confusion of concepts and difficulty of perception is experienced.

2. METHODS AND EXPERIMENTAL

2.1. Research Pattern

This study is a semi-experimental study examining the effectiveness of educational materials developed based on computer and instructional technologies in relation to heat and temperature in ninth grade high school students in physics lesson. Pre-test, post-test and quasi-experimental design with control group were used in the study. Pre-test, post-test and quasi-experimental design with control group are considered as one of the most effective quasi-experimental designs used to ensure internal reliability. Also, it provides a high level of statistical power to the researcher regarding testing the effect of the experimental procedure on the dependent variable, allowing the conclusions to be interpreted in the context of cause and effect. It is known as a powerful pattern that is frequently used in both educational sciences and computer and educational technologies [4,5,7,8,14,15,21,22].

The view for this pattern is shown in Table 1.

Tablo 1. Research Pattern

Groups	Pre-test	Process	Post-test
Experimental Group	Personel Information Form Heat and Temperature Achievement Test	Heat and Temperature Lecture Based on Computer and Instructional Technologies	Personel Information Form Heat and Temperature Achievement Test
Control Group	Personel Information Form Heat and Temperature Achievement Test	Classical Heat and Temperature Lecture	Personel Information Form Heat and Temperature Achievement Test

As seen in Table 1, ninth grade students in the experimental group and the control group, before teaching the subject of Heat and Temperature, a Personal Information Form, an achievement test on Heat and Temperature was applied to both groups. While lecturing heat and temperature based on computer and instructional technologies to students in the experimental group by the same teacher, classical lectures were made to the students in the control group. While there is no difference in the pre-test scores of both groups, an increase in the post-test scores is expected in both groups after the lecture. However, if the increase in the posttest scores is statistically higher in the individuals in the experimental group than the individuals in the control group, this will show that the program developed based on computer and instructional technologies is more effective in increasing the academic achievement than the classical lecture method in the teaching of heat and temperature.

2.2. Working Group

The study group of the study consists of 58 ninth grade students who are attending a multi-program high school, selected through appropriate sampling. In this high school, ninth grade students are taught in two grades. Students studying in these classes are assigned to the control or experimental group by lot. 34.5% of the students are women and 65.5% are men. The average age range of students varies between 14 and 16 years old, with an average age of 14.71. More detailed information about the students in the experimental and control groups can be seen in Table 2.

Table 2. Descriptive statistics for students in the experimental and control groups.

Variable	experiment		Control		χ^2	p
	n	%	n	%		
Gender					.31	.581
Girl	11	37.9	9	31		
Male	18	62.1	20	69		
Mother Education Level					3.70	.158
İlliterate	6	20.7	2	6.9		
only literate	5	17.2	10	34.5		
elementary school graduate and above	18	62.1	17	58.6		
Father Education Level					.09	.760
İlliterate	0	0	1	3.4		
only literate	5	17.2	4	13.8		

elementary school graduate and above	24	82.8	24	82.8		
	Ort	S.s	Ort	S.s	z	p
Age	14.76	.64	14.66	.61	.62	.535
Income	1151.72	1075.58	981.03	1032.63	.60	.551
Teog Score	253.27	56.28	244.98	56.76	.55	.581

Note:The number of students who were illiterate at the father's education level was not included in the analysis since there was only one person in the experimental group. The assumptions of the tests are met. z: Mann-Whitney test result statistics, χ2: Chi-Square test result statistics.

As seen in Table 2, 37.9% of the students in the experimental group are women and 62.1% are men. While the mothers of 20.7% of the students in the experimental group were illiterate, 17.2% were only literate, 62.1% had a primary or higher education level. When the students in the experimental group were examined in terms of the education level of their fathers, 17.2% were only literate, while 82.8% had a primary education or higher education level. While the average age of students in the experimental group is 14.76, their average income level is 1151.72 Turkish lira. Finally, the average Teog score of the students in the experimental group is 253.27. On the other hand, 31% of the students in the control group are women and 61% are men. While the mothers of 6.9% of the students in the control group were illiterate, 34.5% were only literate, 58.6% had a primary or higher education level. When the fathers were examined in terms of education level, 3.4% of the fathers of the students in the control group were illiterate, 13.8% were only literate and 82.8% had primary education and higher education level. While the average age of the students in the control group is 14.66, their average income level is 981.03 Turkish lira. Finally, the average Teog score of the students in the control group is 244.98. The number of women and men in the control and experimental groups are similar in terms of mother's education level, father's education level, and transition score from basic education to secondary education, average monthly income level of the family and average age (Table 2).

2.3. Data Collection Tools

2.3.1. Personal Information Form

It was developed by the researcher to gather information about the students' name, surname, gender, age, mother-education level, father's education level, and average monthly income. Information on students' TEOG placement scores, was obtained from the e-School Management Information System of the Ministry of National Education by the researchers with the help of a school administrator, after obtaining permission from the students and the school administration.

2.3.2. Heat and Temperature Subject Achievement Test

Heat and Temperature subject success test has been developed in order to determine the level of knowledge students have about heat and temperature. The test development stages proposed by DeVellis [10] were followed in the development of the test. First, the heat and temperature subject curriculum in the ninth-grade textbook was examined by the Ministry of National Education and the achievements that students should have, were determined.

In accordance with these achievements in the second stage, a 25-question success test from the auxiliary textbooks recommended by the Ministry of National Education was prepared by two different physics teachers working at the school where one of the researchers was working. This form was examined by a faculty member with experience in physical education and the final form of the success test was given. The success test was then applied as part of the pilot

study to five students attending ninth grade outside the school where the application was performed. As a result of the pilot study, students stated that there was no expression that they had difficulty understanding.

Here is a sample question in the success test.

Question: On hot days, the environment cools if the places are frequently watered. According to this;

I- Cooling of water in water tests
II- If the cut watermelon is kept in the sun for a short time, the watermelon cools down.
III- If ice is put in the lemonade glass on a hot day, the outside of the glass sweats.

Which of its events can be explained by the same principle?

a) Only I b) Only III c) I and II d) II and III e) I, II, III

Students were given 1 point for each correct answer given in the test; wrong answers were ignored. For this reason, the scores that can be obtained from the achievement test vary between 1 and 25. The increase in the scores of the students in the achievement test indicates that the level of knowledge about heat and temperature has increased.

2.4. Mobile Application Preparation Process

2.4.1. Storyboard

Storyboard is the form of the stream (animation, video) that will be used in the prepared e-content, which has been cast into the picture. Animation or video montage are structures that require difficult processes, and the animator or video editor "Does the scenario give the desired effect?" searches for an answer to the question on the storyboard. After the fiction is put into a picture, to what extent the story to be told or the information to be given is effective, whether there is any disconnection in the fiction, and the integrity of the animation tests are also examined on the storyboard. The animation or video is then brought to life. Storyboard preparation is used in the design phase of e-content creation. [13]

2.4.2. User Interface

Application user interface screen has been prepared using Adobe Flash CS 5.5 and Action Script 3.0 (Figure 1). The interface is designed to link all documents to be used by the student as separate files from the program background using the extensible markup language (XML). In this way it plays by calling the animation file and the sound file from the database file and depending on whether the user is on, the program provides a lecture about the subject. As a result, the application developed within the scope of the study does not occupy much space in the memory of the user's mobile device, and its performance is high and it can work comfortably on devices that are not powerful in terms of hardware.

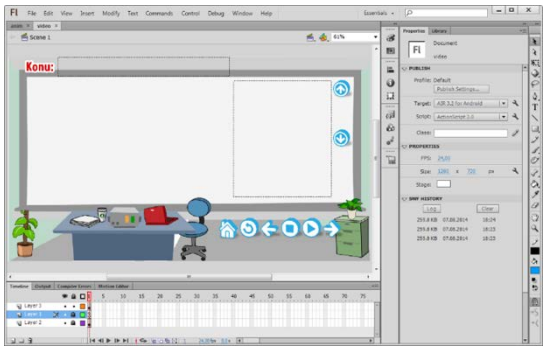

Figure 1. Adobe flash CS 5.5 application screen

The application is designed to work horizontally in full screen on mobile devices. In order to be user friendly, other educational software prepared in the Google market were examined and according to the results, application control buttons, text area, animation area were placed on the stage. The application has been prepared to be very colorful to attract attention.

The stage consists of 6 main parts (Figure 2);
1. Subject title section,
2. Animation section,
3. Summary lectures section,
4. Summary subject checks section,
5. Application controls section,
6. Volume controls section.

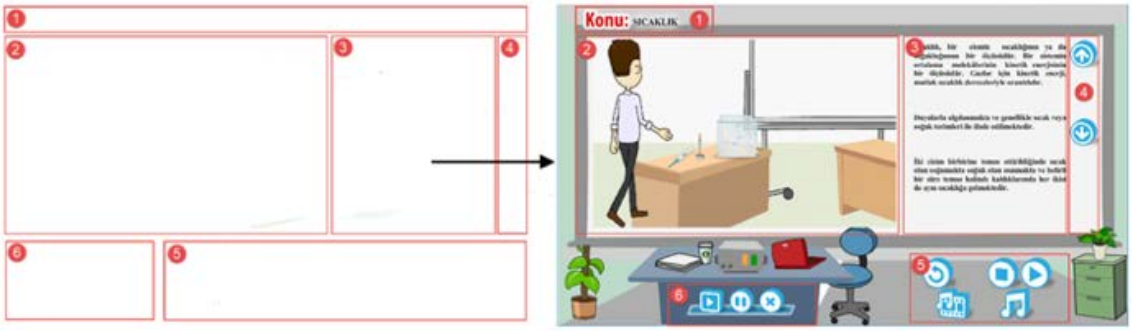

Figure 2. Scene parts

2.4.3. Animation Preparation Process

Animations were prepared using Crazy Talk Animator (Figure 3) program. Crazy Talk Animator is a program developed on character animation. With this application, modeling, dressing, and animating the character, and creating harmonious animations between scenes can be easily done. In the application, the objects placed on the stage, where they should be in the flow of the animation with the timeline, they perform the desired behaviors (Figure 4). For each object, individual change, visibility, transparency, and motion properties can be adjusted in this section to provide interaction between objects. While animating characters, the 2 and 3 dimensional properties to be used can also be adjusted over the timeline.

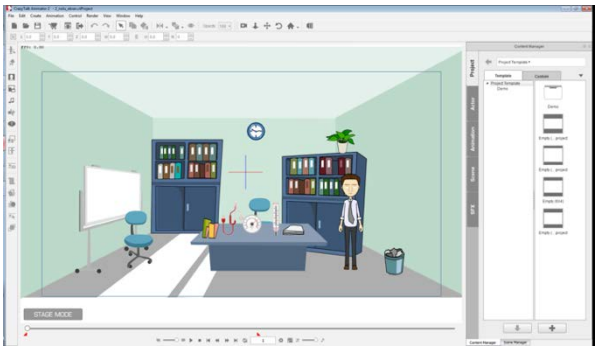

Figure 3. Crazy talk animation program application screen

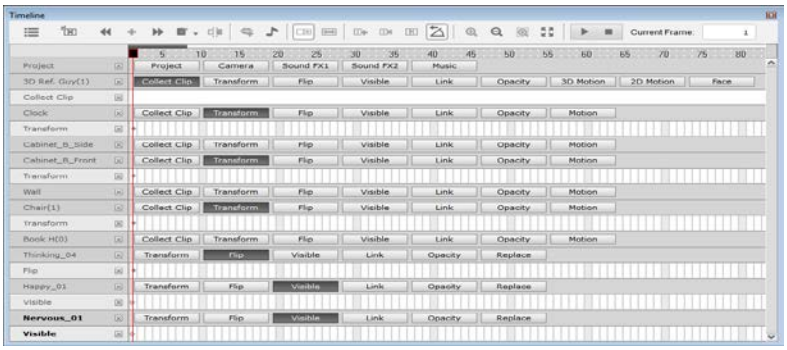

Figure 4. Timeline panel

3D motion Key editor panel, it enables the animation to be viewed from every angle by allowing the created character to be examined in three-dimensional plane (Figure 5).

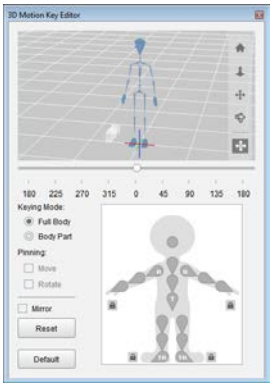

Figure 5. 3d Motion key editor

2.4.4. Packaging of the Application

In order to enable the completed training software to run on android-based mobile devices, using the publish button from the file menu in the animation software, a dialog window with the necessary settings is opened (Figure 6). After the publishing window approval, the created Apk file will be ready for use.

Figure 6. Apk publishing screen

Apk is a short form for Android Package Kit and is the equivalent of executable EXE (Executable File Format) files in the Windows operating system in the android operating system. Apk files are used to install applications on mobile devices using the Android operating system without using the Play market. Manually installing applications in this way is called "sideloading" [1]

2.4.5. Application Examples

The scene in Figure 7 shows the melting of some ice and the freezing of the water. During the process, heat was given to the ice to melt the ice, and heat was taken from the water to freeze the water. At the end of this section, it is aimed that students learn how heat exchange occurs in melting and freezing.

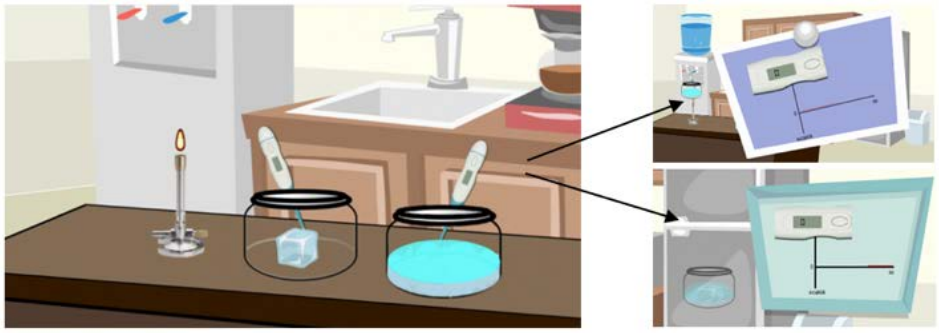

Figure 7. "Melting and freezing temperature" animation

In the scene shown in Figure 8, there are water and steam at 100 degrees Celsius in two containers. The pot with water in it is placed on the cooker and heat is given, and the temperature at which the water boiling does not change is shown on the temperature graph. The second container is put on ice and heat is taken from the water vapor. In this case, the temperature at which the water vapor condenses into a liquid does not change and again it is shown on the heat-temperature graph. At the end of this section, it is aimed that students comprehend the relationship between heat and temperature during boiling and condensation state changes.

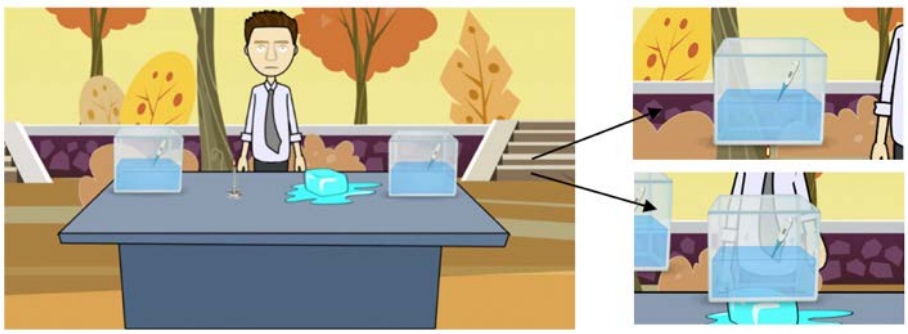

Figure 8. "Boiling and condensation temperature" animation

An animation screen shot prepared for the scenario is shown in Figure 9. In this scene, it has been shown that a heated sphere increases with the expansion of its volume and as a result, it cannot pass after heat is given from the ring through which it can pass before heat is given. In daily life, the volumes of the objects that receive heat generally increase in direct proportion to their temperatures. For example, inflated balls harden in hot environments and their volume increases as a result of this situation. At the end of this section, it is aimed that students learn the direct proportion between temperature increase and volumetric expansion.

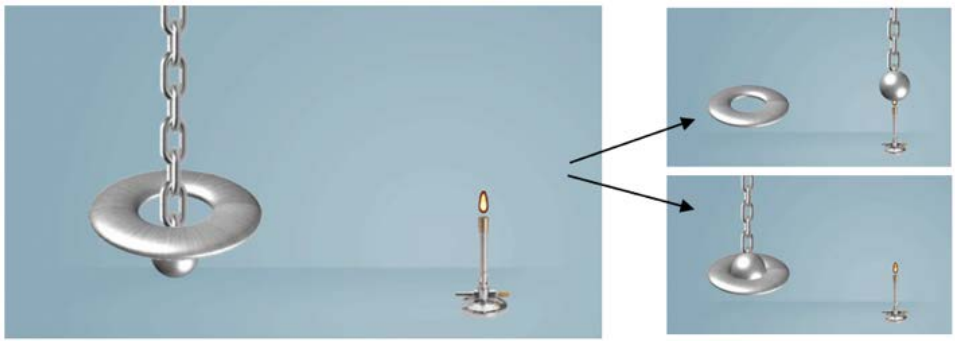

Figure 9. "Expansion by volume" animation

In this scene (Figure 10), the melting of the ice mass at -10 degrees by applying heat is shown. At the same time giving a graph of heat and temperature, the graphic relationship between state change and temperature was presented. While the temperature of the objects that are given heat increases in daily life, there is no increase in temperature even though heat is given during the process. The reason for this is that heat energy is spent on process change instead of temperature increase. At the end of this chapter, it is aimed that students learn the relationship between process and temperature.

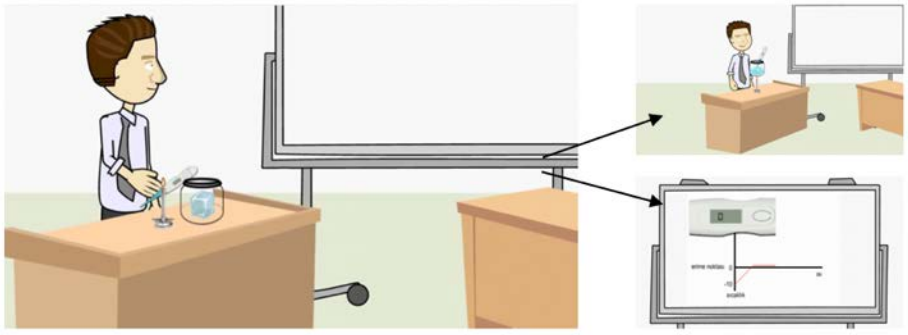

Figure 10. State change (melting and freezing) animation.

In this scene (Figure 11), there is an increase in the temperature of an object of mass m, given heat. The temperature rise of objects is the difference between their final temperature and their initial temperature. At the end of this section, it is aimed that students learn how to calculate temperature change.

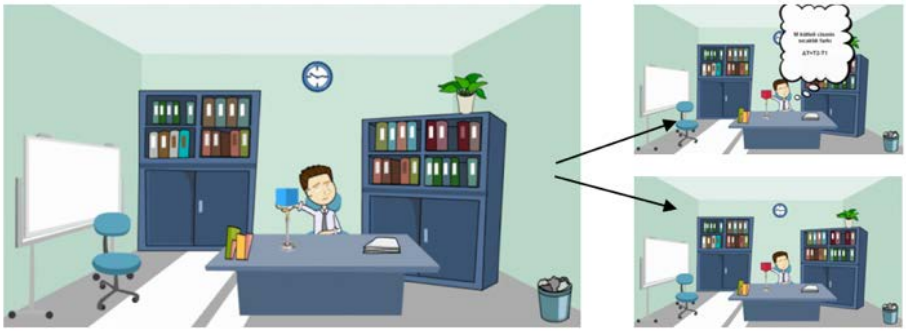

Figure 11. "Heat" animation

2.5. Process and Application

In research, the general purpose of researching information about the examination of the research, the principles of confidentiality and voluntarism have been explained and informed. The applications were carried out in a spacious and quiet classroom environment and the application was carried out in two groups by the physics teacher working at the school. While the physics teacher gave normal lectures to the class in the control group, he taught the class in the experimental group with the necessary materials in computer and instructional technologies and in accordance with the necessary acquisitions in the Physics Textbook of the Ministry of National Education. The students answered the pre-tests one week before the application, and the post-tests were carried out one day after the application.

2.6. Data Analysis

The data collected in accordance with the purpose of the research were scored and analyzed through the appropriate statistics program. The assumptions of the statistical techniques used before the analysis were examined. Firstly, normality assumption was examined in order to determine whether parametric or non-parametric statistics will be used in the analysis of data. In this study, the assumption of normality was evaluated by using Shapiro-Wilk test skewness and kurtosis values and graphical approaches. The Shapiro-Wilk test is used when the sample size in each group is 50 and below [12,17,19,20]. This test tests the hypothesis that sample data come from a normal distribution. While the test results show that the data are not from a normal distribution, the insignificant test results indicate that the data show a normal distribution. It was seen from the data that only the pre-test scores of the control group were not normally distributed. However, when the graphs of skewness and kurtosis values and control group pre-test scores were examined, it was decided to use parametric tests because the data showed a distribution close to normal [12,17,20]

Group differences between the pre-test before the application and the post-test scores after the application of the individuals in the control and experimental groups. T-test was used for independent samples for comparison, and t-test for dependent samples was used to compare the scores of individuals in each group before and after receiving education.

The t-test for independent samples has the assumption of homogeneity of variances as well as the assumption of normality. This assumption was checked by the Levine test and found to be met in all analyzes. Levine [18] suggests that statistical analysis results should be given together with effect size estimates. The effect size simply shows how meaningful the results obtained are in practice. The effect size classification proposed by Cohen [8] was used to interpret the differences between groups. When trying to compare the difference between averages, the most frequently used effect size statistic is Cohen's d. According to Cohen [8], the d value of 0.20 and below is low, the d value of around 0.50 is medium, and the d value of 0.80 and above indicates a high level of effect size. In all analyzes 0.05 margin of error was determined as the upper limit.

3. RESULTS AND DISCUSSION

Table 3 shows the mean and standard deviation values of the pre-test results and the t-test results for independent samples before the lectures to the students in the experimental and control groups.

Table 3. The achievement test pre-test results of the individuals in the experimental and control groups

Variable	Experiment		Control		sd	t	p	Cohen's d
	Avg.	S.s	Avg.	S.s				
Pretest Success Score	5.59	1.86	6.24	2.40	56	1.16	250*	.30

Note: *p > .05**

Table 3 shows that there is no statistically significant difference in the pre-test scores of the individuals in the experimental and control groups. However, as can be seen from the Cohen d effect size, the achievement test mean scores of the individuals in the control group are 0.30 standard deviations higher than the mean scores of the students in the experimental group. **Table 4** shows the average of achievement test scores and standard deviation values applied to the experimental and control groups before and after the training. In order to determine whether these score differences show a statistically significant difference, a series of dependent samples t-test was conducted. Table 4 shows the results for this test.

Table 4. t-test for dependent samples performed for pre-test-post-test scores

Variable	Pretest		Lasttest		sd	t	p	Cohen's d
	Avg.	S.s	Avg.	S.s				
Control Group	6.24	2.40	9.34	3.10	28	9.19	.000*	1.07
Experimental Group	5.59	1.86	11.14	2.72	28	11.82	.000*	2.36

Note: *p < .001**

Table 4 shows that there was a significant increase in the temperature and temperature knowledge levels of the individuals in the control and experimental groups. However, when the effect sizes are examined, there is an increase of approximately one standard deviation in the knowledge level of the individuals in the control group in the classroom where the normal lecture is given, there was an increase of approximately 2.4 standard deviations in the knowledge level of the individuals in the experimental group.

In other words, compared to normal lectures, the education in the experimental group with computer and instructional technology-based materials is more effective in teaching the information about heat and temperature than the education in the control group with normal lecture. **Table 5** shows the mean and standard deviation values for the test results after the lectures of the students in the experimental and control groups of the students and the t-test results for independent samples.

Table 5. The achievement test posttest results of the individuals in the experimental and control groups

	Experiment		Control		sd			
	Avg.	S.s	Avg.	S.s				
Post-Test Success Score	11.14	2.72	9.34	3.10	56	2.34	.023*	.65

Table 5 shows that while there is no significant difference between the pre-test results of the groups, there is a significant difference in favor of the individuals in the experimental group as a result of the post-tests.

4. CONCLUSIONS

This study consists of 2 parts. In the first part, physics lesson, in order to prevent confusion about heat and temperature, the subject was examined, scripted, and animated with Crazy Talk Animator and Flash CS 5.5 applications, audio narrations were created. The animations, the audio files containing the lectures and the lectures on the subject were packaged in 35 scenes to be controlled through the prepared interface and arranged to work on mobile devices using Android operating system. The mobile application prepared in the second part was applied to the control and experimental groups, and the results were evaluated with the tests. with the application prepared, students were able to understand the difference between the terms of heat and temperature, which they frequently used interchangeably in daily life, in visual and audio expressions, and get rid of the confusion of concepts. The prepared application is available for Android devices. If the interface is prepared for devices using the IOS operating system, it will be accessible by a wider user audience. Using the mobile application developed as a result of the study, animations of similar topics that are difficult to understand by students can be developed and their use in mobile devices can be expanded. In addition, when the results are evaluated as a whole, it shows that educational materials developed based on computer and instructional technologies are significantly more effective in increasing students' level of knowledge about the subject compared to normal lectures. This research was conducted only within the scope of ninth grade students and physics course. This situation can be considered as a limitation for this study. Therefore, the application developed within the scope of the research can be seen as a situation that may be important in terms of revealing the reliability of the application for different courses and at different grade levels. Subsequent studies can be conducted with a focus on these recommendations.

ACKNOWLEDGE

Part of this study was presented as a paper named Development of Smart Mobile Device Application on Heat and Temperature at the conference named 3rd International Congress on 3D Printing (Additive Manufacturing) Technologies and Digital Industry 2018 on date 19 April 2018.

REFERENCES

[1] APK ? from: *www.chip.com.tr/haber/apk-dosyasi-nedir-ne-ise-yarar_73277.html#rf.* 27. 08 2018.

[2]Atmaca, U. İ., Uygun, N. G. ve Çağlar, M. F. (2014). Haberleşme Mühendisliği için Mobil Öğrenme Uygulaması. VII. URSI-Türkiye Bilimsel Kongresi, Elazığ, Türkiye.

[3]Bahçeci, F. ve Elçiçek, M. (2015). Meslek Yüksekokulu Öğrencilerinin Mobil Öğrenmeye Yönelik Tutumlarının incelenmesi. *Sakarya Üniversitesi Eğitim Fakültesi Dergisi*, 30,17-33.

[4]Büyüköztürk, Ş. (2011). Deneysel desenler: Öntest-sontest kontrol grubu desen ve veri analizi. (3. bs.), Ankara: *Pegem Akademi*.

[5]Büyüköztürk, Ş., Çakmak, E. K., Akgün, Ö. E., Karadeniz, Ş. ve Demirel, F. (2012). Bilimsel araştırma yöntemleri (13. bs.), Ankara: *Pegem Akademi*.

[6]Carfi, G. (2014). Afyonkarahisar il merkezindeki 12. Sınıf öğrencilerinin ısı ve sıcaklık konusundaki kavram yanılgıları (Yüksek Lisans Tezi, Afyonkarahisar Kocatepe Üniversitesi, Fen Bilimleri Enstitüsü, Afyon). , *https://tez.yok.gov.tr/UlusalTezMerkezi/*

[7]Cohen, J. (1992). A power primer, Psychological Bulletin, 112(1), 155–159.

[8]Cohen, L., Manion, L. & Morrison, K.(2007). Research methods in education (6. bs.), London: Routledge.

[9]Çakır, H. (2011). Mobil Öğrenmeye İlişkin Bir Yazılım Geliştirme ve Değerlendirme. *Çukurova Üniversitesi Eğitim Fakültesi Dergisi*, 40(2), 1-9.

[10]DeVellis, R. F. (2012). Scale development: theory and applications (3. bs.), London: SAGE.

[11]Egi, S. ve Çakır, H. (2015). Mobil Cihazlara Yönelik Uzaktan Eğitim Sisteminin Geliştirilmesi. *Düzce Üniversitesi Bilim ve Teknoloji Dergisi*, 3(2),439-450.

[12]Field, A. P. (2013). Discovering statistics using IBM SPSS statistics (4. bs.), London: Sage.

[13]Gök, V. (2014). Fatih projesi kapsamında fizik dersi ısı ve sıcaklık konusunda akıllı cihaz uygulaması geliştirme (Yüksek Lisans Tezi, Afyonkarahisar Kocatepe Üniversitesi, Fen Bilimleri Enstitüsü, Afyon). *https://tez.yok.gov.tr/UlusalTezMerkezi/*

[14]Göktaş, Y., Küçük, S., Aydemir, M., Telli, E., Arpacık, Ö., Yıldırım, G. ve Reisoğlu, İ. (2012). Türkiye'de eğitim teknolojileri araştırmalarındaki eğilimler: 2000-2009 dönemi makalelerinin içerik analizi. *Kuram ve Uygulamada Eğitim Bilimleri Dergisi*, 12(1), 177–199.

[15]Güven, G. ve Sülün, Y. (2012). Bilgisayar destekli öğretimin 8. sınıf fen ve teknoloji dersindeki akademik başarıya ve öğrencilerin derse karşı tutumlarına etkisi. *Türk Fen Eğitimi Dergisi*, 9(1), 68-79.

[16]Güzelyazıcı, Ö., Dönmez, B., Kurtuluş, G. ve Hacıosmanoğlu, Ö. (2014). Yeni Yüzyıl Üniversitesinde Mobil Öğrenme. *Electronic Journal of Vocational Colleges*, 4, (2), 1-7.

[17]Ho, R. (2013). Handbook of univariate and multivariate data analysis with IBM SPSS, Second Edition (2 edition). Boca Raton, New York: Chapman and Hall/CRC.

[18]Levine, T. R. (2013). A Defense of Publishing Nonsignificant (ns) Results. Communication Research Reports, 30 (3), 270-274.

[19]Mooi, E. & Sarstedt, M. (2011). A concise guide to market research: The process, data, and methods using IBM SPSS statistics. Berlin: Springer.

[20]Pallant, J. (2010). SPSS survival manual a step by step guide to data analysis using SPSS (4. bs.). Maidenhead: Open University Press/McGraw-Hill.

[21]Saran, M., Seferoglu, G. ve Cagiltay, K. (2009). Mobile assisted language learning: English pronunciation at learners' fingertips. *Eurasian Journal of Educational Research*, 34(1), 97-114.

[22]Şimşek, A., Özdamar, N., Becit, G., Kılıçer, K., Akbulut, Y. ve Yıldırım, Y. (2008). Türkiye'deki eğitim teknolojisi araştırmalarında güncel eğilimler, *Selçuk Üniversitesi Sosyal Bilimler Enstitüsü Dergisi*, 19, 440-458.

[23]Tarımer, İ., Şenli, S. ve Doğan, E. (2010). Mobil İletişim Cihazları İle Öğrenim Materyallerine Erişim Sağlayan Bir Yazılım Tasarımı. *Bilişim Teknolojileri Dergisi*, 3(3),1-6.

[23]Yertürk, İ. (2013). Fatih Fizik Öğretiminde Bilgisayar Destekli Öğretimin Öğrenci Başarısına ve Tutumuna Etkisi: Elektrik Akımı Örneği, Yüksek lisans tezi, Van Yüzüncü Yıl üniversitesi, Eğitim Bilimleri Enstitüsü, Van.

Research Article

EVALUATION OF NOISE FROM JACQUARD AND DOBBY IN THE WEAVING FACILITY THE IN TERMS OF OCCUPATIONAL HEALTH AND SAFETY

Authors: Murat KODALOĞLU

To cite to this article: Kodaloğlu, M. (2021). EVALUATION OF NOISE FROM JACQUARD AND DOBBY IN THE WEAVING FACILITY THE IN TERMS OF OCCUPATIONAL HEALTH AND SAFETY. International Journal of Engineering and Innovative Research, 3(3), p: 222-235, DOI: 10.47933/ijeir.931425

DOI: 10.47933/ijeir.931425

To link to this artice: https://dergipark.org.tr/tr/pub/ijeir/archive

International Journal of Engineering and Innovative Research

http://dergipark.gov.tr/ijeir

EVALUATION OF NOISE FROM JACQUARD AND DOBBY IN THE WEAVING FACILITY THE IN TERMS OF OCCUPATIONAL HEALTH AND SAFETY

Murat KODALOĞLU[*]

[*]Isparta University of Applied Sciences, Vocational School of Technical Sciences, Occupational Health and Safety Program, Isparta, Turkey.

[*]Corresponding Author: muratkodaloglu@isparta.edu.tr

https://doi.org/10.47933/ijeir.931425

(**Received:** 02.05.2021; **Accepted:** 16.06.2021)

ABSTRACT: Noise is an important problem affecting workers' health and quality of life in countries where industrialization is experienced effectively. Workers are in noisy areas in different environments of working life. The people who are harmed by the noise are the workers working in the workplace where there is a high rate of noise. Of noise; It is known to negatively affect worker health physiologically and psychologically. Noise causes loss of productivity as a result of the fact that workers complain about their activities and negatively affects the productivity of the workers. It was aimed to examine the noise exposure status of workers in changing noisy working environments in factories. The noise level of the jacquard and dobby weaving sections of the weaving mill was determined by measuring. The noise sound pressure level values emitted by weaving machines to the environment were measured. During the measurement; It was observed that the nominal day conditions determined in the job analysis were not exceeded. The tasks were carried out within the specified periods and all noise sources were studied within the determined periods.

Keywords: Noise, Jacquard, Dobby, Exposure

1. INTRODUCTION

One of the machine effects that negatively affects work efficiency with mechanization is noise. Noise causes high damage to the workers who use the machines in the environment where there are more than one work equipment. High noise levels negatively affect workers' health and performance. It is necessary to determine the negative effects of the noise generated by the machines used in the weaving mill on the worker health and the noise level emitted by the machines to the environment. The noise level in the weaving mill was measured and its effects on the worker were examined.

Sound is a measurable objective concept that does not change depending on the individual. Noise is a subjective concept. Noise can be defined as "disturbing sound". The acceptance of sound as noise may differ depending on the individual [12].
In a person whose hearing is damaged, a weakening of the hearing ability, called hearing loss, is seen. Hearing loss can be temporary or permanent. Hearing loss being permanent or temporary and the degree of hearing loss; It depends on the level of noise, the frequency of

the noise, the time the worker is exposed to the noise. [5]

The exposure time of the noise includes the time the person is affected by the continuous noise and the years when the person is affected by the noise from time to time. Staying for a while under the influence of a certain level of sound causes hearing loss[2] . Noise limit values in industrialized countries are the longest exposure to a certain level of noise in a day or a week. The frequency of the noise, the duration of its stay in the environment, the age of the worker exposed to the noise, the physiological and psychological condition, and the distribution of noise in the environment over time are important factors in the perception of noise as a disturbance by the receiver[11] . The negative effects of noise on the individual are mostly physiological and psychological[1].

Hearing loss is the main physiological effect. It is possible to categorize the hearing effects caused by noise in the ear in three groups as acoustic trauma, temporary and permanent hearing loss [13]. Noise-induced hearing loss is one of the common causes that negatively affect the quality of life in developed societies[4]. Physiological problems include increased blood pressure, rapid heartbeat, muscle reflexes, and sleep disorders. Do not be affected by noise for hours; adrenaline may cause deterioration in blood pressure with the increase of circulatory stress hormones [10]. The psychological effects of noise emerge as anxiety, tension, anger, concentration disorder, and perception difficulty [6].

Various collective and personal protective measures are taken in order to reduce the effects of noise on employee health. First of all, determining the factors causing noise and reducing the effects on worker health comes first. However, laws have been enacted in most countries to reduce the effects of noise.

In this factory located in Denizli Organized Industrial Zone, there are 350 employees in total. In the factory, which operates 24 hours, in three shifts, in the measurement section of the factory A total of 48 weaving machines are in service. Thirty "A" brands of machines The jacquard model produced in 2000, the dobby model of the 18 brand "A" produced in 2000, machines are operated at a speed of 300-600 rpm.

2. MATERIAL AND METHOD

2.1. Material Model

In experimental studies, noise measurements were made on looms used in the weaving factory.

2.1.1. Noise

Noise; It is an important environmental pollutant consisting of unwanted sounds with a random spectrum that negatively affects the hearing health and sense of people, disrupts the physiological and psychological balance, reduces work performance, reduces or destroys the pleasantness and calmness of the environment. [7,8,13]

2.1.1.1 Technical Abbreviations in the Report

dB: Decibel
dBA: A Weighted Decibel

Leq: Equivalent Noise Level
Lmax: Maximum Noise level
Lmin: Minimum Noise Level
m: Meter
mm: Millimeter
m^2: Square meter
Kg: Kilogram
% : Percent
μ Pa: Micro Pascal

2.1.1.2. They are The Negative Effects of Noise on Hearing

They are the negative effects of noise on hearing. It can be examined temporarily and permanently in two parts. The most common transient effects are temporary loss of hearing sensitivity known as temporary hearing threshold shift and hearing fatigue. Hearing loss is permanent in cases where the effect is too high and the hearing system is affected by noise again when it regains its former characteristics. [13]

2.1.1.3. Physiological Effects of Noise

These are changes that occur in the human body. Major physiological effects; muscle strains, stress, increase in blood pressure, changes in heart rate and blood circulation, pupil dilation, respiratory acceleration, circulatory disorders and sudden reflexes.

2.1.1.4. Psychological Effects of Noise

In the press of the psychological effects of noise; nervous breakdown, fear, discomfort, anxiety, fatigue and mental effects slow down. Suddenly rising noise levels can create fear in people. [9]

2.1.1.5. Effects of Noise on Performance

It is the effects of noise such as reducing work efficiency and not understanding the sounds heard. The blocking of functions such as the perception and comprehension of speech is largely related to the level of background noise. Studies on the effects of noise on work efficiency and productivity have shown that the environment where complex works are performed is quiet, and the environments where simple works are performed need to be a little noisy. In summary, if the background noise determined for a certain job or function in the environment is excessive, work efficiency decreases.[13]

2.1.2. Principles Regarding Personal Exposure Noise Measurement

A) Care is taken not to generate any noise that will affect the measurements of the device during noise measurements.
B) The measuring device should be positioned so that it does not interfere with the selected personnel while being mounted on it.
C) It should be paid attention that the measurement is made for eight hours during the working hours of the personnel.

2.1.3. Method and Device Used in Personal Exposure Noise Measurement

The exposure noise measurements made in the facility were made with a dosimetric noise measurement device, within the scope of the Regulation on the Protection of Employees from Noise Related Risk, Determination of the Noise Exposed at the Workplace Estimation of the Hearing Loss Caused by This Noise was made according to the method of TS 2607 ISO 1999. Three personal noise exposure measurements between 600-300 cycles were performed on jacquard and dobby weaving looms in the facility.[13]

Table 1.Meter features

Device	Brand	Model
Personal Noise Meter	Pulsar	22-R
	Pulsar	Dosebadge-22

Table 2: Ambient Conditions During Measurement

Temperature	Pressure(mbar)	Moisture (%)	Air Flow Velocity (m/s)
22,1	1.005,7	64,1	0,1
22,0	1.005,0	64,0	0,1

3. EXPERIMENTAL RESULTS

Measuring results for jacquard and dobby 600-300 revolutions in table 3-10

Table 3. Jacquard 600 rpm

Measurement Date	Measurement Start Time	Measurement Time	Peak Level dB(C)	*8 Hourly Exposure LegA Value*
April 2021	09:30	01:51.29	138,4	60,2

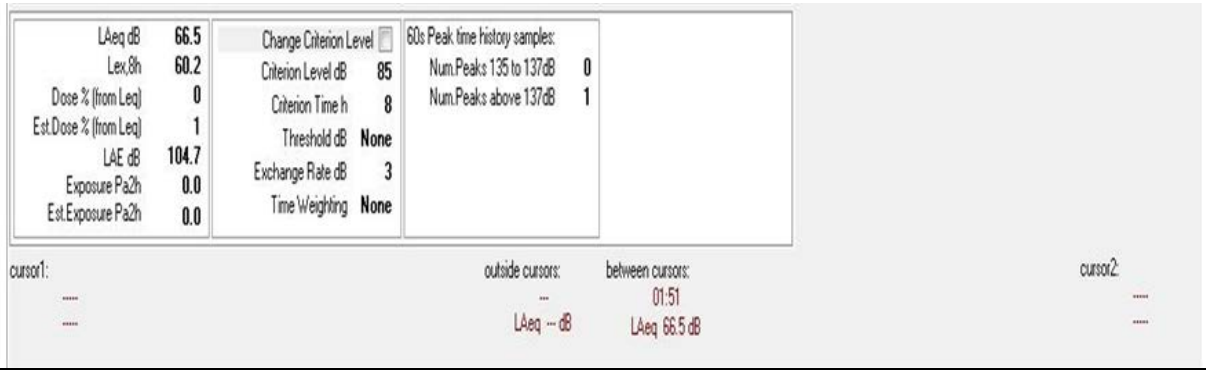

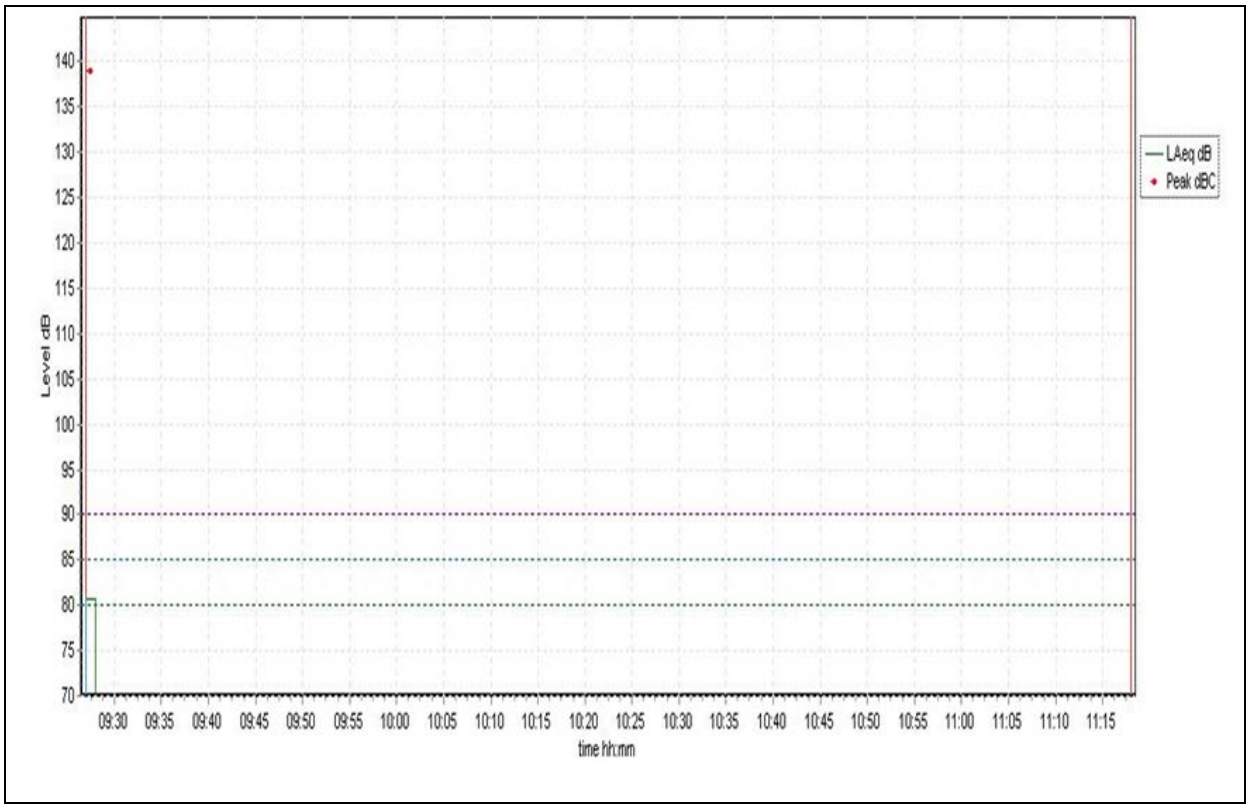

Table 4. Jacquard 500 rpm

Measurement Date	Measurement Start Time	Measurement Time	Peak Level dB(C)	*8 Hourly Exposure LegA Value*
April 2021	09:45	01:54.48	135,6	59,6

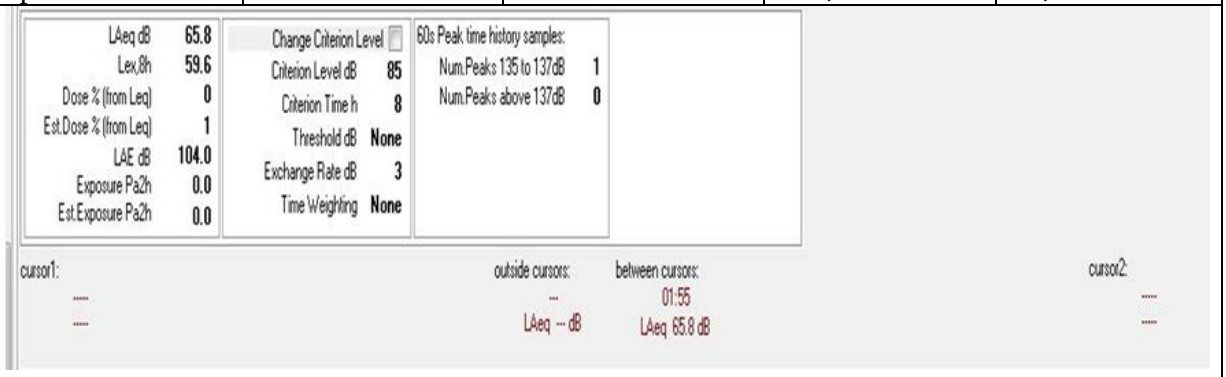

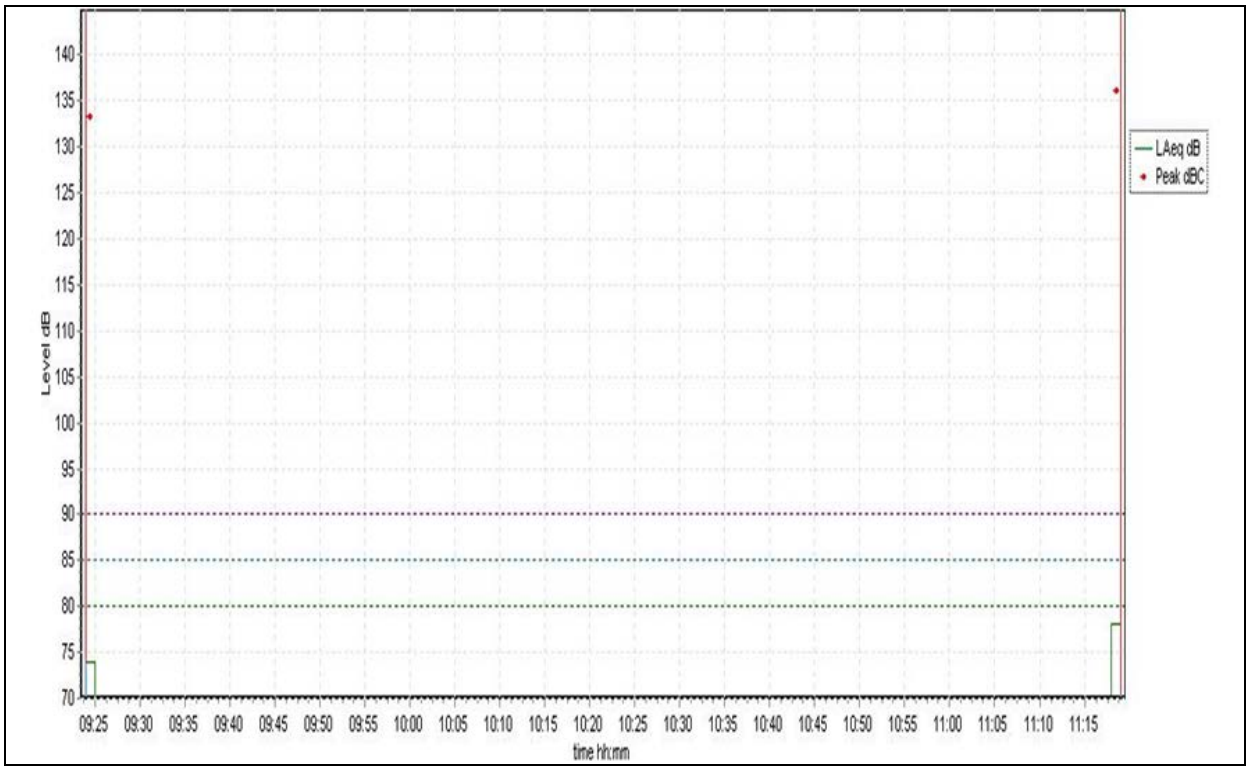

Table 5. Jacquard 400 rpm

Measurement Date	**Measurement Start Time**	**Measurement Time**	**Peak Level dB(C)**	***8 Hourly Exposure LegA Value***
April 2021	10:00	01:55.25	141,0	59,3

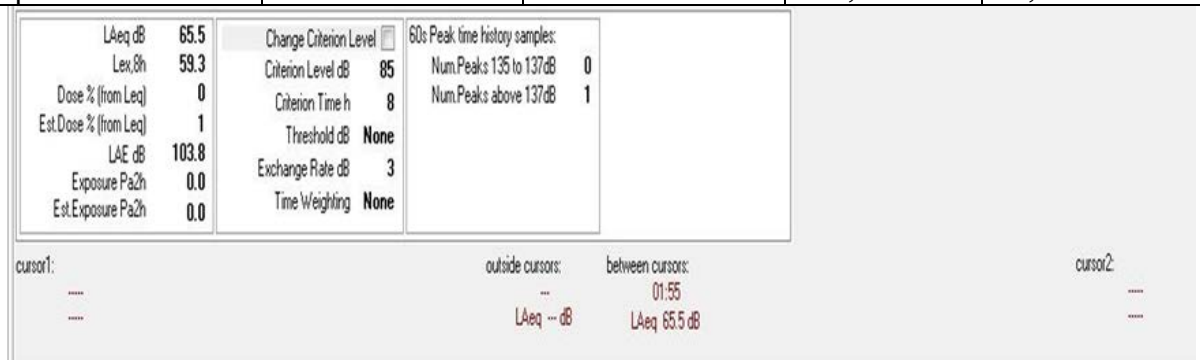

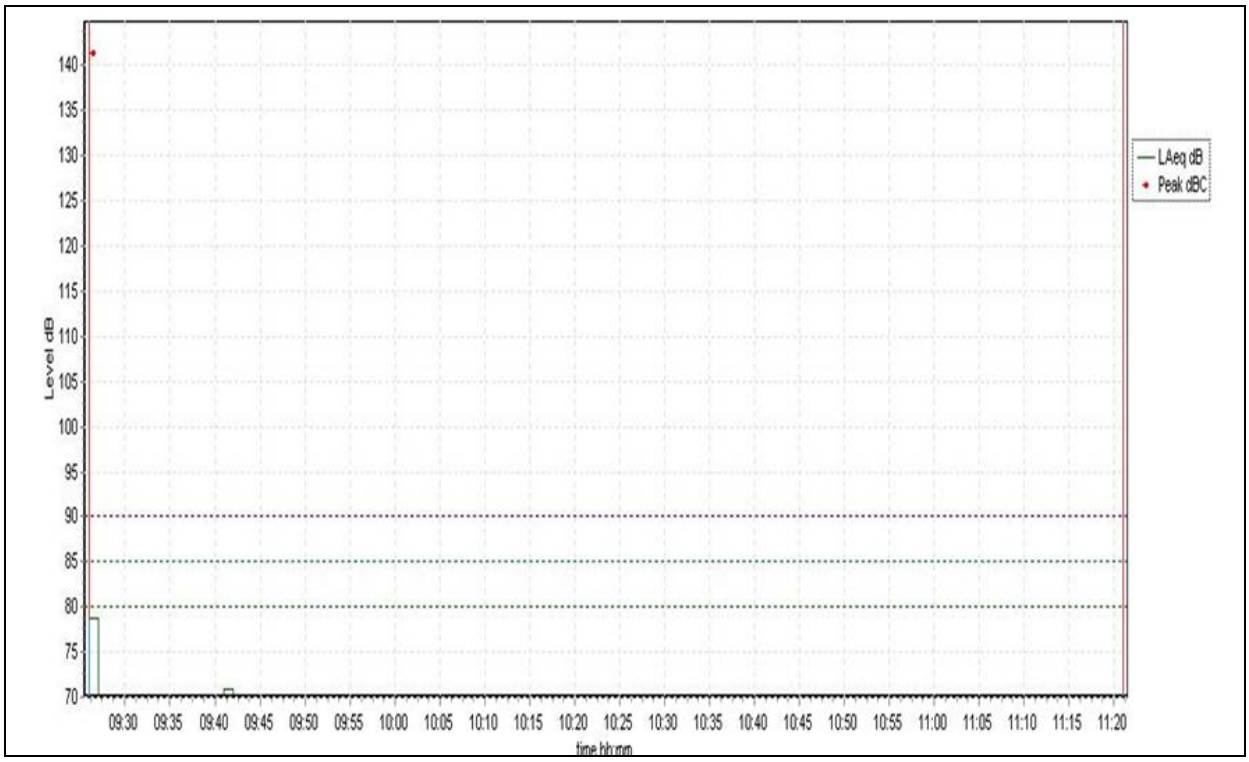

Table 6. Jacquard 300 rpm

Measurement Date	**Measurement Start Time**	**Measurement Time**	**Peak Level dB(C)**	***8 Hourly Exposure LegA Value***
April 2021	10:15	01:59.20	130,5	58,4

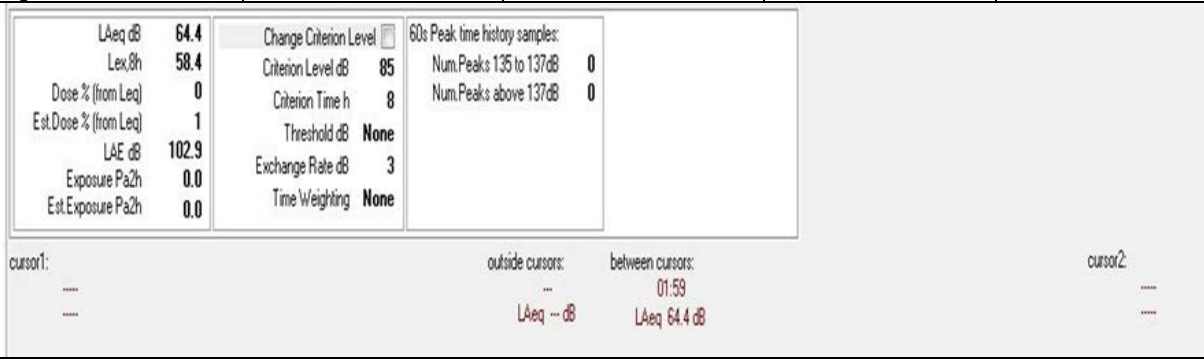

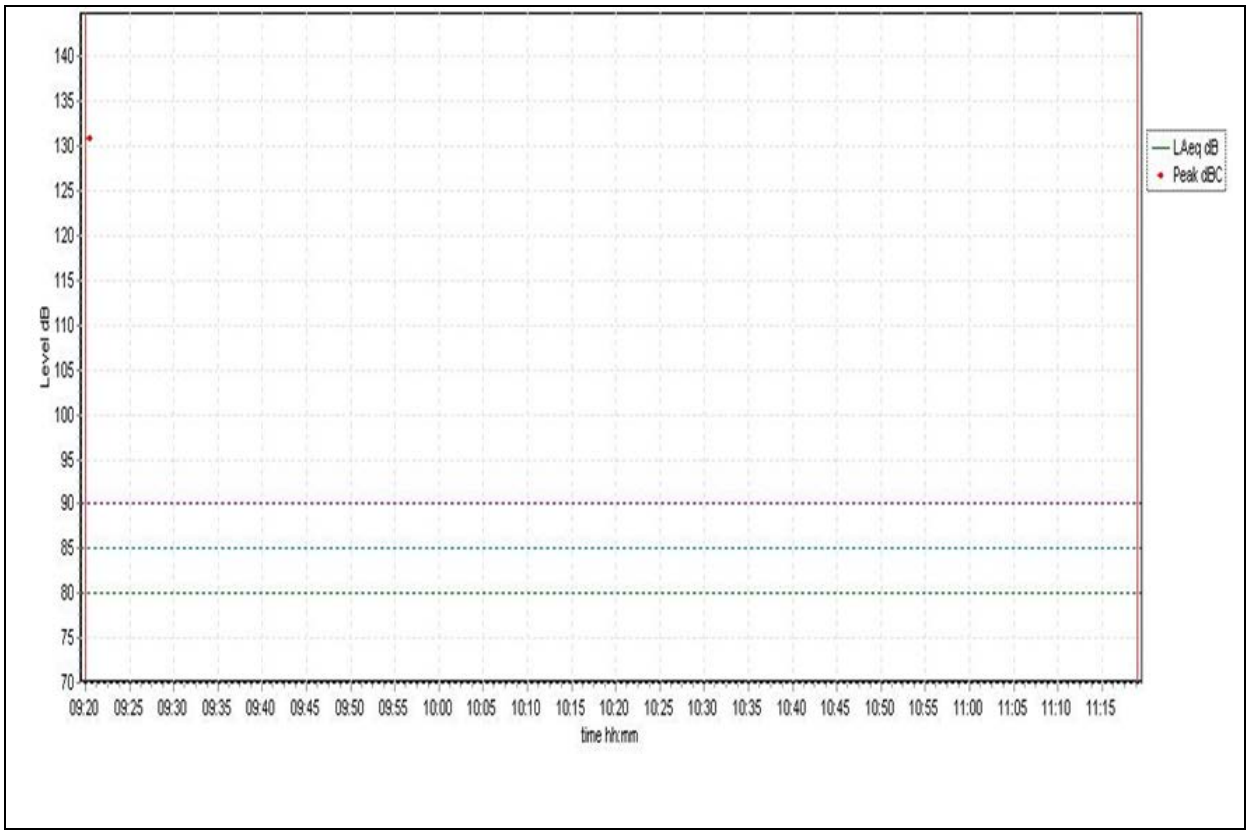

Table 7. Dobby 600 rpm

Measurement Date	Measurement Start Time	Measurement Time	Peak Level dB(C)	*8 Hourly Exposure LegA Value*
April 2021	10:30	01:55.37	122,1	59,9

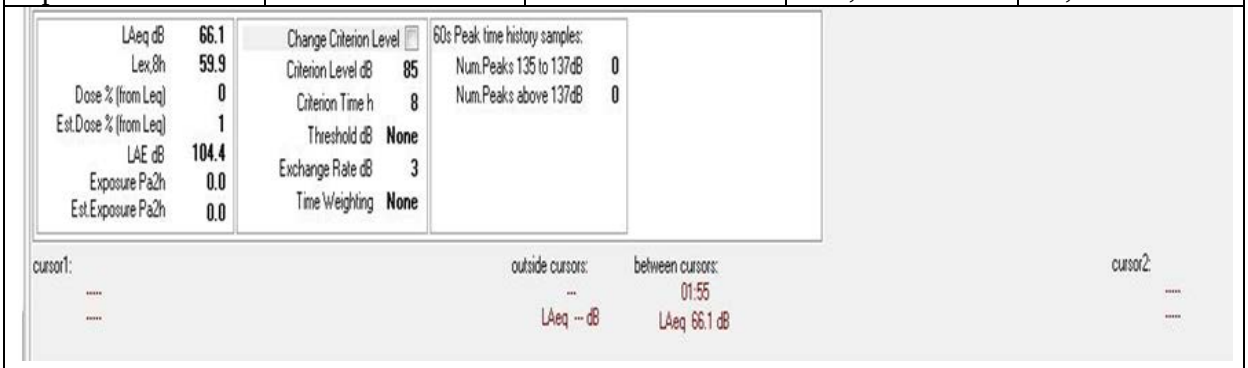

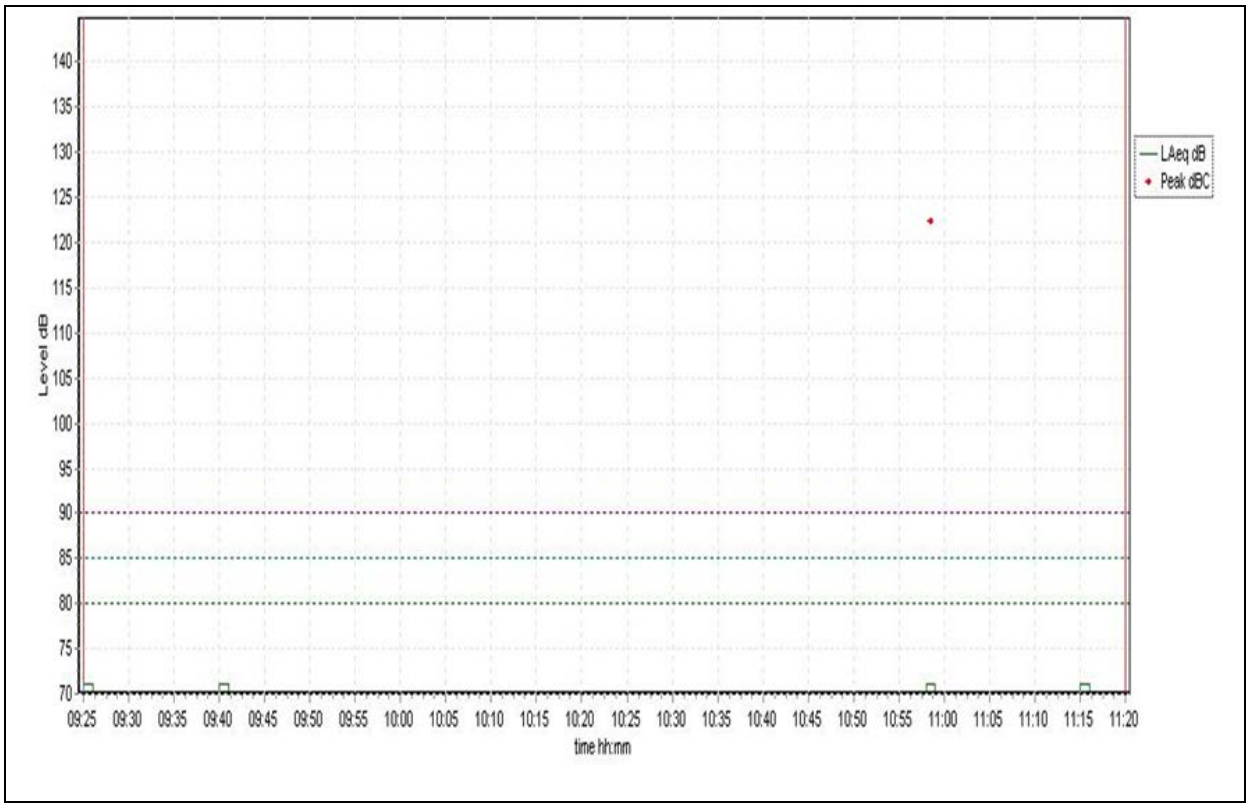

Table 8. Dobby 500 rpm

Measurement Date	**Measurement Start Time**	**Measurement Time**	**Peak Level dB(C)**	***8 Hourly Exposure LegA Value***
April 2021	10:45	02:06.09	137,1	59,6

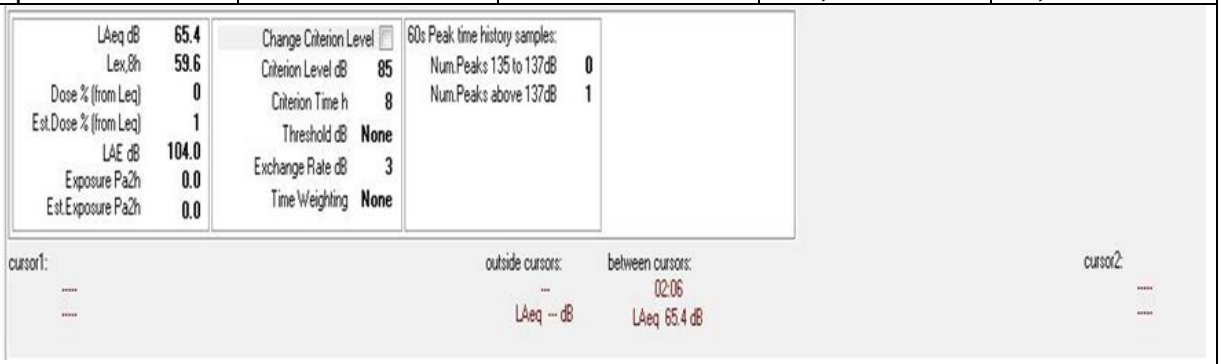

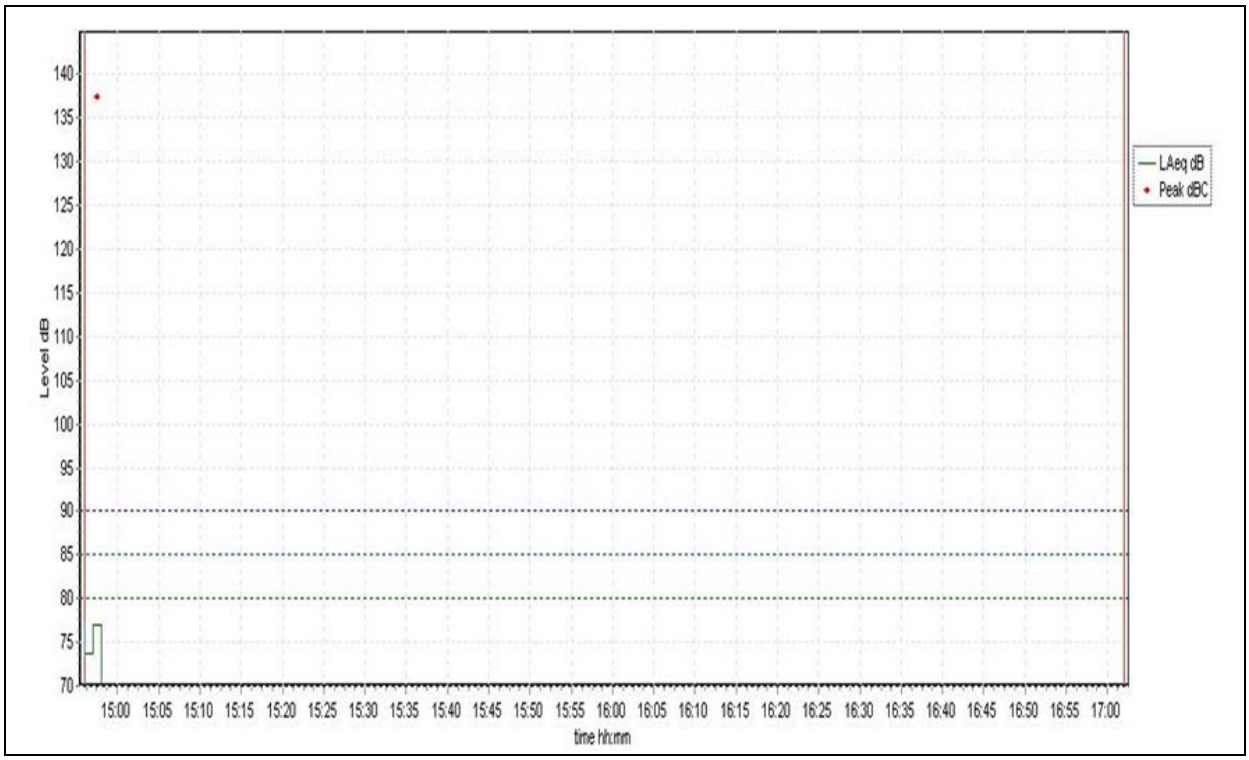

Table 9. Dobby 400 rpm

Measurement Date	Measurement Start Time	Measurement Time	Peak Level dB(C)	*8 Hourly Exposure LegA Value*
April 2021	11:00	02:09.09	128,9	59,7

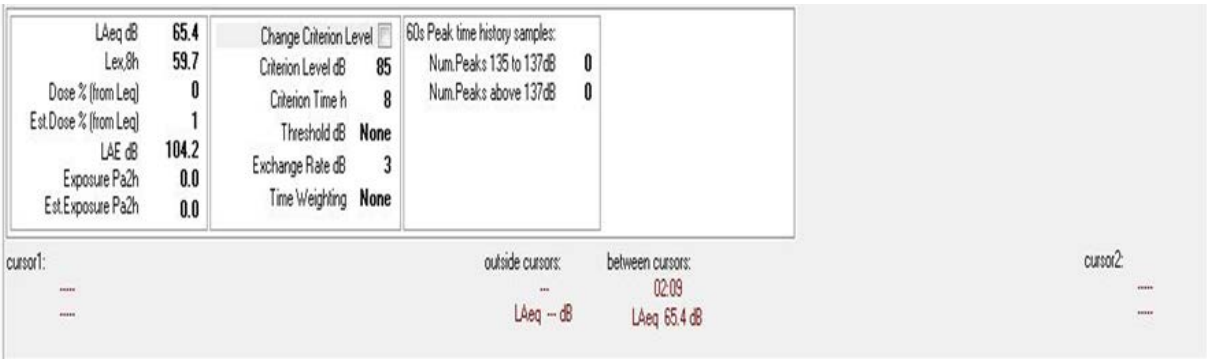

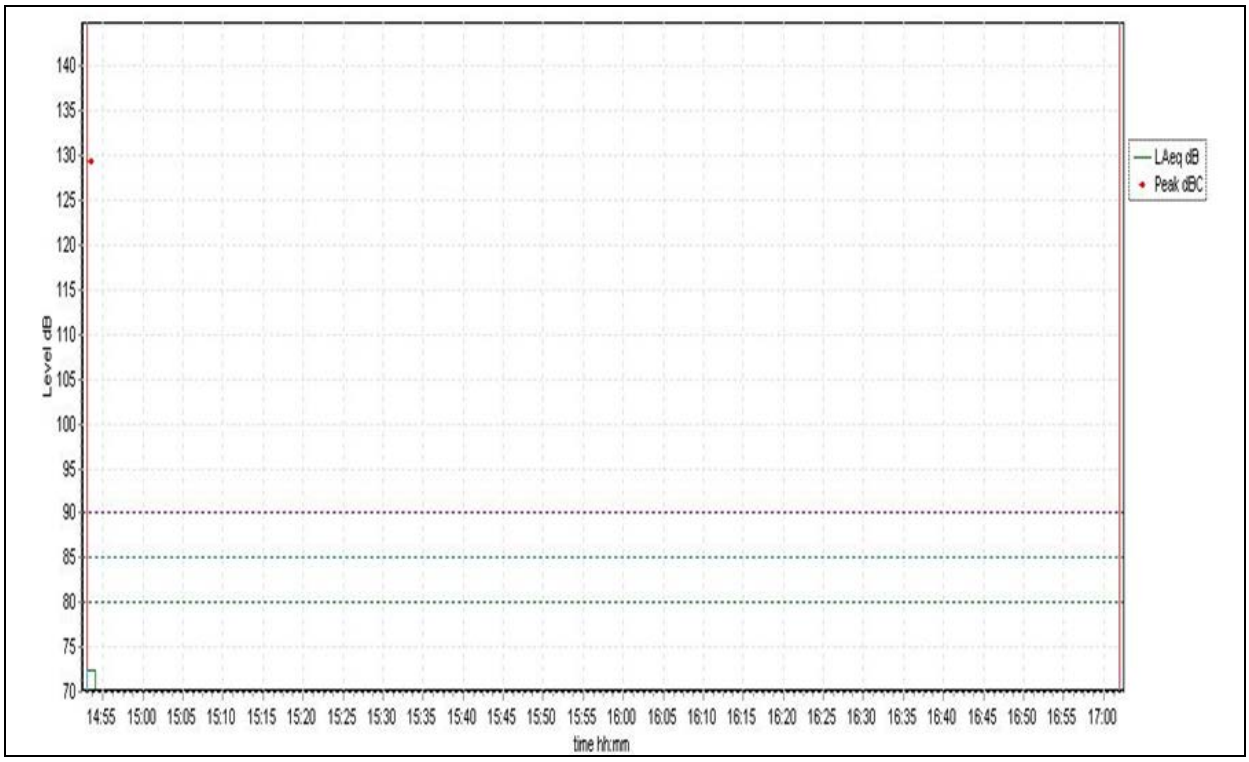

Table 10. Dobby 300 rpm

Measurement Date	Measurement Start Time	Measurement Time	Peak Level dB(C)	*8 Hourly Exposure LegA Value*
April 2021	11:16	02:11.56	132,8	59,6

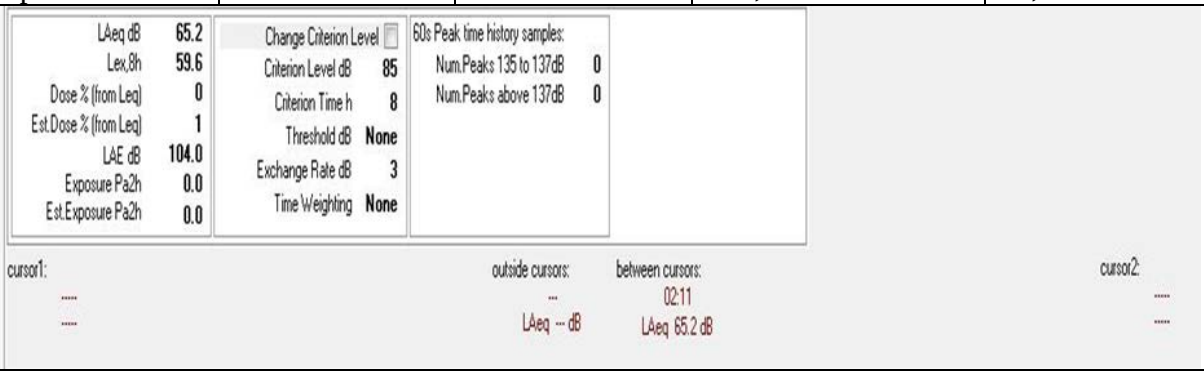

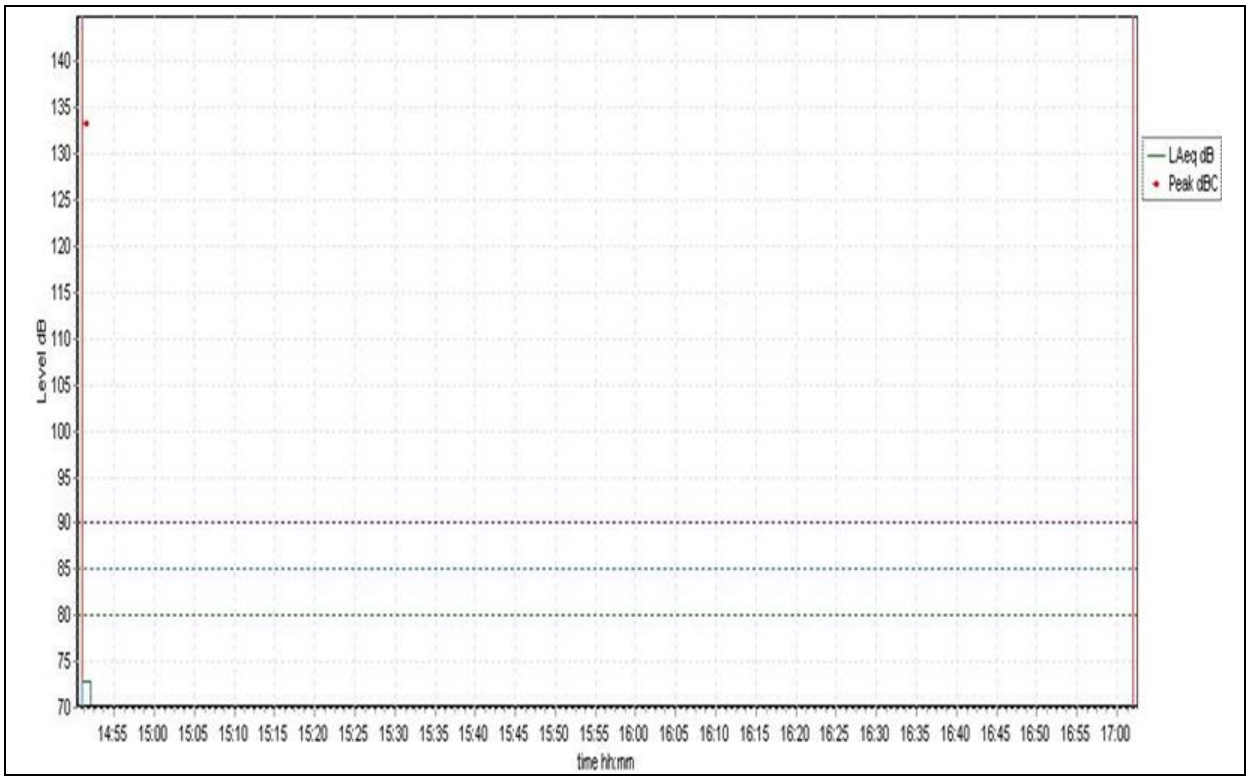

4. RESULT AND DISCUSSION

It is a fact that the noise that negatively affects the health of the employee and causes unrecoverable results must be controlled. It is necessary to raise the awareness of employees, especially young workers, about noise, which has increased effects on employee health. The solution to all problems arising from the workplace environment will be provided by training.

The physiological effects of noise on the worker vary depending on the amount of noise affected. These are permanent hearing problems due to noise, respiratory disorders, blood pressure, heart diseases. The negative physiological effects and psychological effects of noise on the working individual also occur. The most common of these is the low efficiency due to noise seen in workers in noisy environments, which can be directly correlated with the rate of noise exposure. Among the negative effects of noise on worker health are health problems affecting workers; They are permanent hearing problems due to noise due to their high prevalence among workers. These hearing losses will significantly increase the quality of life of the employee. In advanced levels of hearing loss, which increases with the effect of noise, speech is affected, and negative situations arise in communication between employees in the workplace.

Noise is a very important occupational health and safety element in the textile industry as in all other sectors. In this study, the personal noise exposure values of the weaving mill employees serving in the weaving branch of the textile industry were examined. Accordingly, measurements were made in a total of eleven weaving mills located in four provinces of Turkey, including eight fabric and towel factories and three carpet weaving factories. As a result of the measurements made, the personal noise exposure value in all factories has exceeded the limit values specified in our legislation. This shows that; In terms of the risks associated with noise, weaving mill workers are at a very serious risk.

Table 11. Results of the Measurement

Number of Revolutions (rpm)	**Episode**	**Calculated Value LEX, 8saat (dBA)**
600	Jacquard	60,2
600	Jacquard	60,0
600	Jacquard	60,1
500	Jacquard	59,6
500	Jacquard	59,5
500	Jacquard	59,5
400	Jacquard	59,3
400	Jacquard	59,2
400	Jacquard	59,4
300	Jacquard	58,4
300	Jacquard	58,6
300	Jacquard	58,3
600	Dobby	59,9
600	Dobby	59,5
600	Dobby	59,2
500	Dobby	59,8
500	Dobby	59,6
500	Dobby	58,5
400	Dobby	59,7
400	Dobby	59,2
400	Dobby	59,3
300	Dobby	59,1
300	Dobby	59,6
300	Dobby	59,9

Personal exposure emitted by jacquard weaving machines is between 600 rpm 60.0-60.2, 500 rpm 59.6-59.5, 400 rpm 59.4-59.3, 300 rpm 58.6-58.3 dB.

Personal exposure emitted by dobby weaving machines is between 600 rpm 59.9-59.2, 500 rpm 59.6-58.5, 400 rpm 59.7-59.2, 300 rpm 59.9-59.1 dB.

Earphones, etc., which reduce the effect of noise, are used by the workers in the workplaces where noise, which has a direct effect on human health, occurs. Personal protectors should be used. The first priority in preventing the noise caused by the Jacquard and Dobby weaving machine from spreading to the environment is the protection at the source, which is a collective protection method. Before personal precautions, it is necessary to reduce the noise levels at the source and effectively protect the workers from noise. In enterprises, noise should be considered during the construction phase of the workplace as a design criterion; Arrangements should be made to minimize noise during the placement of work equipment. In line with the provisions of the "Regulation on the Protection of Employees from Noise Related Risks", the highest exposure action value of 85 dBA has not been exceeded by any person.

REFERENCES

[1]. Atmaca, E. ve Peker, İ., 1999; "Sivas ili Araç Gürültüsü", Ekoloji Çevre Dergisi, Cilt 8, Sayı 30, s.3-8.

[2]. Ege, F., Sümer, K.,Sabancu, A., 2003. Tekstil işletmelerinde Gürültü Düzeyi ve etkileri, Türk tabipler Birliği Mesleki sağlık ve Güvenlik Dergisi,

[3]. ISO 11202. 1995. Makine ve Ekipmanlardan Yayılan Akustik Gürültü-Bir İş İstasyonunda ve Belirtilen Diğer Konumlarda Emisyon Ses Basıncı Seviyelerinin Ölçülmesi-Yerinde Anket Yöntemi ISO 11202, Switzerland

[4]. Funda, Y.O., 2012; "Gürültü Maruziyetin İşitme Üzerindeki Etkisini, Sigara Kullanımı ve Kotinin ile İlişkisinin İncelenmesi", Abant İzzet Baysal Üniversitesi Uzmanlık Tezi, s.103.

[5]. İlgürel ,N., Sözen, M., 2005. Sanayi İşletmelerinde Gürültünün Nesnel, Öznel ve Yönetmelikler Bağlamında İncelenmesi, Cilt 1, sayı 1 , MMGARON YTÜ Mim. Fak. E-Dergsi

[6]. Kodaloğlu M. (2020). "Yalvaç Oto Tamir Esnafının Sorunları ve İş Güvenliği Açısından Bazı Öneriler" Yalvaç Kent Araştırmaları. KONYA, (pp. 379-384). Çizgi Kitabevi Yayınları.

[7]. Kodaloğlu M., Delikanlı K. (2021). Battaniye İşletmesinde Maruz Kalınan Gürültünün İş Sağlığı ve Güvenliği Açısından Değerlendirilmesi. Teknik Bilimler Dergisi, 11, 33-38.

[8]. Kodaloğlu M. Günaydın Karakan G.(2021). Evaluation Of Dust Exposure Measurements Regarding To Occupational Health And Safety In A Warp Knitting Facility. International Journal of Engineering and Innovative Research, 3, 1-11.

[9]. Kodaloğlu M., Delikanlı K. (2021). Denizli O.S.B. Bir İplik&Dokuma İşletmesinde Partikül Madde ve Maruziyet Ölçümlerinin İş Sağlığı ve Güvenliği Açısından Değerlendirilmesi. Teknik Bilimler Dergisi, 12

[10].Maschke C., Rupp T. ve Hecht K., 2000; "Stresörlerin biyokimyasal reaksiyonlar üzerindeki etkisi - gürültülü mevcut bilimsel bulguların bir incelemesi", Int J Hyg Environ Health, Cilt 203, s.45-53.

[11].Nacar Koçer, C., Uslu, G., Işık, H. ve Hanay, Ö., 2007; "Elazığ'da Gürültü Üzerine Endüstrinin Etkisi", 7. Ulusal Çevre Mühendisliği Kongresi, 24-27 Ekim, İzmir.

[12]Özgüven, N. 1986. Endüstriyel Gürültünün Kontrolü, OTÜ, TMMOB Makina Mühendisleri Odası, Yayın No: 118, Ankara.

[13].Yılmaz, H. ve Özer S., 1997; "Gürültünün Peyzaj Yönünden Değerlendirilmesi ve Çözümü" Ziraat Fakültesi Dergisi, Cilt 28, Sayı 3, s.515-531.

[14].Özmen, A., Çalışanların Gürültü İle İlgili Risklerden Korunmalarına Dair Yönetmelik Hükümlerinin Örneklerle ve Saha Uygulamalarıyla Açıklanması, İş Sağlığı ve Güvenliği Uzmanlık Tezi, T.C. Çalışma ve Sosyal Güvenlik Bakanlığı İş Sağlığı ve Güvenliği Genel Müdürlüğü, Ankara, 2014

Research Article

TRANSIT FREQUENCY OPTIMIZATION USING FIREFLY ALGORITHM AND EVALUATION OF THE PARAMETERS

Authors: İlyas Cihan AKSOY , Mehmet Metin MUTLU Yalçın ALVER

To cite to this article: Aksoy, İ. C. , Mutlu, M. M. & Alver, Y. (2021). Transit Frequency Optimization Using Firefly Algorithm and Evaluation of the Parameters . International Journal of Engineering and Innovative Research ,3(3),p: 236-247 . DOI: 10.47933/ijeir.897839

DOI: 10.47933/ijeir.897839

International Journal of Engineering and Innovative Research

http://dergipark.gov.tr/ijeir

TRANSIT FREQUENCY OPTIMIZATION USING FIREFLY ALGORITHM AND EVALUATION OF THE PARAMETERS

İlyas Cihan AKSOY[*], Mehmet Metin MUTLU[2] Yalçın ALVER [3]

[1] Karamanoğlu Mehmet Bey University, Department, Karaman, TURKEY.
[2] Adnan Menderes University, Department, Aydın, TURKEY.
[3] Ege University, İzmir, TURKEY.

[*]Corresponding Author: icihanaksoy@kmu.edu.tr

https://doi.org/10.47933/ijeir.897839

(**Received:** 16.03.2021; **Accepted:** 26.04.2021)

ABSTRACT: Over the last few decades, rapidly growing cities in terms of population and land use have led to many transportation-based problems such as longer travel times, traffic congestion, traffic crashes, and air and noise pollution. Increasing the modal share of transit systems appears to be one of the most effective methods to solve transportation-based problems. However, transit systems, particularly in countries having limited resources, should be used efficiently to achieve sustainable urban mobility. Even only adjusting frequencies of transit lines, with no infrastructure investment cost requirements, can provide a more efficient transit system. In this paper, a transit frequency setting model based on the Firefly Algorithm (FA), which is a relatively new metaheuristic for the transportation network design problems, is presented to minimize total user cost under a fleet size constraint. The proposed model is performed on a 10-route Mandl's Test Network using different combinations of parameters to demonstrate the effect of parameter values on the solution quality. After that, the best solution of 30 solutions obtained by the calibrated parameter values is compared to the existing frequency set of the 10-route transit network. The results show that the FA can obtain better frequency sets by selecting the proper values for the parameters.

Keywords: Transit network frequency setting problem, Firefly algorithm, Bi-level optimization.

1. INTRODUCTION

Transportation-based problems, which arise from increased population, mobility, and vehicles, have become a challenging issue for decision-makers in the last decades. Transit systems, a backbone for cities in terms of mobility needs, can mitigate transportation-based problems by enhancing their modal share in the total number of trips. However, considering the potential costs of transit systems, transit systems must be utilized more efficiently, especially in countries with limited sources.

Urban Transportation Network Design Problem (UTNDP), which is related to the planning, design, and management of transportation, includes mainly Road Network Design Problem (RNDP) and Public Transportation Network Design Problem (PTNDP) [1]. PTNDP is a set of interdependent problems that must be considered for an efficient transit system. The sub-problems of PTNDP span network design, frequency setting, transit network timetabling, vehicle scheduling problem, and driver scheduling problem [2]. Ideally, all of the strategic,

tactical, and operational problems regarding the transit system must be solved simultaneously. However, such complex problems can only be tackled by dividing them into sub-problems due to their computational difficulty.

Transit Network Frequency Setting Problem (TNFSP) is solely to determine the number of vehicle departures in a given line within a given planning period or to determine the time interval of subsequent vehicles in transit lines. Determining transit service frequency is considered a tactical decision and is related to more efficient use of sources. Moreover, generally, no monetary investment is required. The demand for the transit system may vary depending on the hours of days, days of the week, and the different seasons of the year. Although a preliminary setting is determined in the strategic decision phase, a comprehensive study should be conducted in the tactical decision process [3].

Transportation network users are willing to reach their destinations by minimizing their total travel costs that consist of total trip duration (i.e., access/egress time, wait time, in-vehicle travel time) and monetary costs. Operators also desire to minimize the operating costs such as fleet cost, personnel costs, maintenance, and repair costs of vehicles. A higher level of service is likely to lead to lower user costs and higher operator costs. Conversely, lower operator costs cause a lower level of service for users or higher user costs. Transit planning should be handled in consideration of both user and operator costs considering this trade-off.

Solving TNFSPs using exact solution methods is very difficult because of NP-Hard nature with a combinatorial optimization structure, where obtaining an optimal solution is too time-consuming, especially for those having a vast search space [4]. Another challenge is the non-convexity of the problem [5]. Thus, metaheuristic algorithms, which can obtain a near-optimal solution in reasonable times, are convenient methods in solving such complex problems.

Transportation network design problems diverge slightly from the problems in other disciplines since any changes on the network influence the travel choice of the users. Thus, transportation network design problems are generally formulated as a bi-level problem. The upper level is the problem of decision-maker who designs or manages networks by forecasting the travel behaviors of users in the face of changes in the network. On the other hand, the lower level is the problem of users who plans their travel choices according to the changes in the network. Hence, the bi-level structure enables to design the network in terms of both users and operators.

TNFSP has been tackled many times in the literature employing various objective functions, constraints, transit assignment methods. [6] determines the optimal bus frequencies to minimize the total travel time of passengers subject to the constraint of the fleet size of each operator on the transit network, employing an iterative solution approach which consists of a Genetic Algorithm and a label-marking method. Using a gradient projection method, [7] presents a transit frequency setting algorithm that aims to maximize demand on variable-demand networks with the constraints of the fleet size and frequency bounds. They test the optimization model onto a small test network. [8] proposes a frequency setting model to minimize the weighted sum of the operator and user costs. The optimization algorithm is based on the parallel genetic algorithm, in which a coarse-grained strategy and a local search algorithm based on Tabu search are embedded to increase the performance of the Genetic Algorithm. The model proposed by [9] obtains both optimal frequencies and optimal bus sizes by minimizing the sum of the total user cost and operator cost. The algorithm determines a set of frequencies using the Hooke-Jeeves algorithm while performing the congested transit assignment using ESTRAUS simulation software. The proposed algorithm is performed on the Santander transit system with

a 19-line network and a fleet of six different bus sizes. The results provide a reduction of 6% of the total cost when compared with the current frequency set and bus sizes. [10] develops a transit frequency setting model minimizing the sum of the user's travel time, operator cost, and variance in user travel time onto a real-size network by Genetic Algorithm. [3] compares the exact and approximated solution approaches on TNFSP. The exact and approximated approaches use CPLEX and Tabu Search Algorithm, respectively. [11] presents a solution method facilitating the coordination between bus rapid transit and feeder bus systems with the objective of minimizing the total cost, which consists of the bus operator and users' costs, using Genetic Algorithm. [12] develops a transit frequency setting model to maximize wait time savings under the constraints of the budget, fleet size, vehicle load, and policy headway, implementing the proposed model on the Chicago Transit network for the morning-peak hours. In the work of [13], a multi-objective frequency setting model, which aims to minimize the total travel time of all users and required fleet size for the operators by Tabu Search, is performed over a real medium-sized network in terms of two data sets corresponding to morning-peak and off-peak periods. In a recent study, [14] compares two different frequency determination methods named optimum frequency and demand-based frequency methods. Frequencies are determined for two methods on the routes obtained by Ant Colony Optimization. Finally, [15] presents a frequency setting model based on a novel objective function, which aims to slow the spread of COVID-19 caused by crowding at public transportation stops. The proposed model minimizes the total infection risk cost occurring at stops under a limited fleet size, using the Differential Evolution algorithm.

The recent researches tackle frequency setting in TNDFSP in which determines the frequency of each transit line besides route design. The work of [16] addresses the problem of determining the frequencies and routes of buses in the multi-modal transit network to minimize the sum of the operator cost, user's cost, and penalty cost for unsatisfied demand. In the proposed TNDFSP model, the frequencies are obtained by an iterative frequency setting procedure, while the transit assignment is simulated using EMME software. The model is applied to the Rome transit network. [17] determines the frequencies by a proposed descent direction method in the TNDFS study. The proposed algorithm is applied to a small-scale network and the real-size bus network of Tin Shui Wai, Hong Kong. [18] aims to obtain a set of routes and their associated frequencies simultaneously using Bee Colony Algorithm. The work determines the frequency set with the objective of minimizing the total travel time for all users and minimizing the required fleet size utilizing a Pareto optimality optimization method to optimize both objectives. To minimize the weighted sum of total travel time and the total number of transfers for all users, [19] handles TNDFSP utilizing a Memetic Algorithm in which local search operators are embedded to Genetic Algorithm to obtain better solutions. [20] presents a TNDFS model to determine the optimal set of transit routes and their associated frequency simultaneously. The proposed algorithm, which is based on the Differential Evolution, generates Pareto-optimal solutions for the minimizations of the total travel time and the required fleet size. [21] assigns the frequency values to the transit lines in consideration of minimizing the passenger time and operating cost employing the Multi-Objective Particle Swarm Optimization algorithm. [22] address a TNDFSP in which both the total travel time of network users and the CO2 emission are minimized. The model employs a Memetic Algorithm considering a heterogeneous fleet.

The studies mentioned above concerning TNFSP, tackle the problem using exact, heuristic, and metaheuristic solution approaches. However, recent studies focus intensively on the use of metaheuristics due to their time-saving advantages. [1] expresses that the Genetic Algorithm (GA) and Simulated Annealing (SA) have been frequently used for TNDFSP studies and emphasize that recently developed metaheuristic like Firefly Algorithm (FA) should be applied

to TNDFSP. Similarly, [23] states that most of the transit scheduling studies are based on well-known metaheuristics such as GA, Tabu Search (TS), and that there is no investigation on novel population-based metaheuristics like FA.

FA is one of the well-known metaheuristics, which has been composed of inspiring fireflies' behavior. Its natural feature enables to converge fast and to lead to obtaining optimal solution early since each firefly moves towards the brighter firefly in each searching step [24]. [25] states that since fireflies gather more closely around each optimum (local or global) without jumping around, FA is more successful than other metaheuristics. For these reasons, we employ FA in the proposed transit frequency setting model.

There are two major motivations for this study. The first one is that, to the best of our knowledge, there is no work concerning transit frequency setting problems employing FA. Thus, the performance evaluation of FA in TNFSP is open for research. The second one is that the planners may be interested in exploring different solution methods concerning the transit frequency setting problem.

In this study, we present a bi-level TNFSP model that aims to minimize the total user cost subject to a constraint of a fleet size utilizing FA. The proposed model is tested on 10-route Mandl Test Network with the different combinations of parameter values of FA to evaluate the effect of the algorithm parameter values. After that, the best solution among the 30 solutions generated by the calibrated parameter values is compared with the existing frequency sets of the 10-route network. The structure of this article is as follows: Section 2 presents the mathematical model and passenger assignment method of this study, while Section 3 describes the solution algorithm based on FA. Section 4 gives the results of computational experiments. Finally, Section 5 presents concluding remarks and future researches.

2. PROBLEM DESCRIPTION

This paper proposes a bi-level TNFSP whose upper level determines the optimal frequency values of transit lines. The lower level is the transit assignment process that defines the path choice model of the users. Section 2.1 below explains the mathematical models, that is, the objective function and the constraint, utilized in obtaining the optimal frequency values, while Section 2.2 describes extensively how users are assigned to the transit network.

2.1. Mathematical Model

The proposed model determines a frequency set for transit lines, which minimizes total user cost subject to a fleet size constraint. User cost is a generalized cost that consists of waiting time, in-vehicle time, and transfer penalty. The expected wait time for lines is calculated as half of the line headways, assuming random arrivals of passengers. To better represent the perception of waiting time and making transfers, coefficients are applied to the costs of relevant trip stages. The objective function of the optimization model can be formulated as follows:

$$min\ F = \sum_{u \in U} IVT_u + c_{wt} \times WT_u + c_{t1} \times \delta_u^1 + c_{t2} \times \delta_u^2 \quad (1)$$

U : the set of transit users
u : index of the transit user
IVT_u : in-vehicle travel time of user u

WT_u : total waiting time of user u
δ_u^1 : binary variable, 1 if user u makes the first transfer during the trip, 0 otherwise
δ_u^2 : binary variable, 1 if user u makes the second transfer during the trip, 0 otherwise
c_{wt} : coefficient of total wait duration
c_{t1} : penalty of the first transfer
c_{t2} : penalty of the second transfer

In order to obey the fleet size constraint, the number of vehicles exceeding the fleet size is multiplied by an enormous penalty coefficient. Thus, it is guaranteed that the algorithm suppresses the number of required vehicles below the allowed fleet size. To determine the number of vehicles exceeding the fleet size constraint, the required fleet size necessary to operate the transit system is calculated as follows:

$$RF = \sum_{l \in L} round\left(\frac{t_l}{h_l}\right) \quad (2)$$

RF : required fleet size to operate transit network
L : the set of transit lines
l : index of the transit line
t_l : roundtrip time of line l
h_l : headway of line l

2.2. Transit Assignment

The transit assignment process is necessary to calculate the total user travel costs. In this study, we adopt a transit assignment method similar to the recent transit network design studies such as [18], [20], [21], [26]-[28]. The transit assignment method of this study is as follows: Users search for paths of three categories to fulfill their transportation demands. Initially, users search for direct trip paths between their origin and destination nodes. In case that there is no direct trip, users search for a one-transfer path. Further, if users do not have any one-transfer path, they try to find a two-transfer path. Users, who cannot find paths in these three categories are called unserved demand. In case users find multiple paths in a category, it is assumed that they select the path based on the logit model, as presented in Eq. (3). The utility of each path is calculated as presented in Eq. (4).

$$p_{i,j,k} = \frac{e^{-U_{i,j,k} \times R}}{\sum_{k \in P_{i,j}} e^{-U_{i,j,k} \times R}} \quad \forall i \in N, \forall j \in N \quad (3)$$

$$U_{i,j,k} = IVT + c_{wt} \times WT + c_{t1} \times \delta^1 + c_{t2} \times \delta^2 \quad (4)$$

N : set of nodes
$P_{i,j}$: set of paths between the origin i and the destination j
$p_{i,j,k}$: probability to choose the path k between the origin i and the destination j
$U_{i,j,k}$: cost/disutility of path $p_{i,j,k}$ between the origin i and the destination j
R : coefficient of path cost (disutility)
IVT : total in-vehicle time of path $p_{i,j,k}$
WT : total waiting time of path $p_{i,j,k}$

3. SOLUTION ALGORITHM

In this study, we employ the FA developed by [29] to solve complex problems, which is a relatively new metaheuristic, especially in solving transportation problems. FA is a swarm intelligence-based optimization algorithm inspired by the behavior of fireflies that produce flashes to attract mating partners. In FA, three idealized rules are followed: (1) All fireflies are attracted to each other regardless of their sex, (2) attractiveness is proportional to a fireflies' brightness; less bright fireflies will move toward the brighter fireflies, and if there is no brighter firefly, they will move randomly, (3) the brightness is determined by the landscape of objective function.

In FA, it is assumed that the brightness of a firefly determines its attractiveness. The attractiveness value, β, is relative to each firefly couple. Attractiveness depends on the distance between firefly i and firefly j, r_{ij}, as presented in Eq. (5).

$$\beta = \beta_0 e^{-\gamma {r_{ij}}^2} \tag{5}$$

Where β_0 the light intensity, typically set to 1 in literature. γ is the coefficient of light absorption, which is essential in determining the speed of convergence. γ ranges between 0.1 and 10.0. r is the Cartesian distance between any two fireflies, which can be calculated by the following equation.

$$r_{ij} = |x_i - x_j| = \sqrt{\sum_{k=1}^{d} \left(x_{i,k} - x_{j,k}\right)^2} \tag{6}$$

Where $x_{i,k}$ is the spatial coordinate of firefly i on dimension k, d is the number dimensions (*i.e.*, variables of the decision vector). If the firefly j is brighter, the position of the firefly i after moving toward firefly j is calculated by;

$$x_i = x_i + \beta_0 e^{-\gamma r^2}\left(x_j - x_i\right) + \alpha \epsilon_i \tag{7}$$

The second term of Eq. (7) is related to attractiveness. The third term is the randomization term consists of the randomization parameter α and the vector of random numbers ϵ_i drawn from the Gaussian distribution.

The parameter α takes a value between 0 and 1, and ϵ_i ranges in $rand(0,1) - 1/2$ where *rand* is a random number generation function used with boundary value parameters. The steps of FA associated with the proposed transit frequency setting model are as follows:

Step 0: *Initialization.* Set stopping criteria and values of parameters α, γ, β_0, *nPop*, z and generate a frequency set $\mathbf{f_i} = \{f_{i,1}, f_{i,2}, \dots, f_{i,d}\}\ \forall d \in L, i \in \{1,2, \dots, nPop\}$ for each firefly in the population with size *nPop*, and calculate the cost c_i of each frequency set $\mathbf{f_i}$.

Step 1: *Loop.* Compare each frequency set $\mathbf{f_i}$ with other frequency sets $\mathbf{f_j}, j \in \{1,2, \dots, nPop\}, i \neq j$

Step 1.1: *Update Frequency Set.* Update the frequency set $\mathbf{f_i}$ if $c_i < c_j$

Step 1.2: *Transit Assignment.* Assign users to the network using updated frequency set $\mathbf{f}_i$ to calculate the total user cost and the required fleet size.

Step 1.3: *Cost Calculation.* Calculate the objective function cost, c_i, as a result of updated frequency set $\mathbf{f}_i$.

Step 2: *Termination.* If maximum generation number *z* is reached, stop and output the best solution. Otherwise, return to Step 1.

4. COMPUTATIONAL EXPERIMENTS

The proposed model is performed on Mandl's Test Network, using the 10-route bus network found as the best solution in the TNDFSP study of [24]. Mandl's Test Network, which has been used in many studies by researchers, consists of 15 nodes and 21 bi-directional links. The travel time of links and transit demand between each node pair at peak hour is depicted in Fig. 1. The details of the 10-route bus network, which needs a fleet of 76 buses to operate the transit system, are given in Table 1.

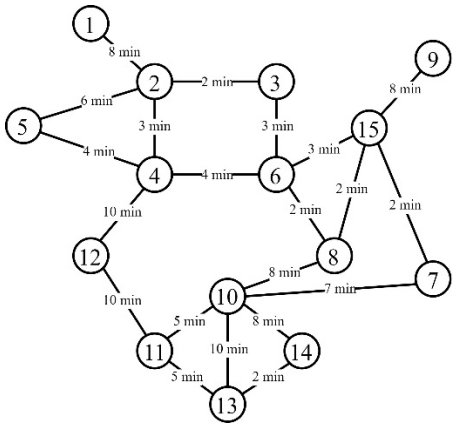

O/D	1	2	3	4	5	6	7	8	9	10	11	12	13	14	15
1	0	400	200	60	80	150	75	75	30	160	30	25	35	0	0
2	400	0	50	120	20	180	90	90	15	130	20	10	10	5	0
3	200	50	0	40	60	180	90	90	15	45	20	10	10	5	0
4	60	120	40	0	50	100	50	50	15	240	40	25	10	5	0
5	80	20	60	50	0	50	25	25	10	120	20	15	5	0	0
6	150	180	180	100	50	0	100	100	30	880	60	15	15	10	0
7	75	90	90	50	25	100	0	50	15	440	35	10	10	5	0
8	75	90	90	50	25	100	50	0	15	440	35	10	10	5	0
9	30	15	15	15	10	30	15	15	0	140	20	5	0	0	0
10	160	130	45	240	120	880	440	440	140	0	600	250	500	200	0
11	30	20	20	40	20	60	35	35	20	600	0	75	95	15	0
12	25	10	10	25	15	15	10	10	5	250	75	0	70	0	0
13	35	10	10	10	5	15	10	10	0	500	95	70	0	45	0
14	0	5	5	5	0	10	5	5	0	200	15	0	45	0	0
15	0	0	0	0	0	0	0	0	0	0	0	0	0	0	0

Figure 1. (a) Mandl's transit network, (b) Demand matrix at peak hour.

Table 1. Details of the 10-route transit network

Route No	Initial Node	Arrival Node	Node Number	Node Order	Fleet Size	Travel Time (min)	Frequency (/h)
1	1	13	8	1-2-3-6-8-10-11-13	12	66	10.91
2	9	12	6	9-7-15-7-10-11-12	9	64	8.44
3	7	5	8	7-15-8-6-3-2-4-5	4	36	6.67
4	2	14	8	2-4-6-8-10-11-13-14	9	58	9.31
5	13	4	8	13-14-10-8-6-3-2-4	8	56	8.57
6	1	12	5	1-2-5-4-12	3	56	3.21
7	11	1	8	11-10-7-15-6-3-2-1	13	60	13.00
8	5	11	6	5-4-6-8-10-11	9	46	11.74
9	13	1	7	13-11-12-4-5-2-1	5	86	3.49
10	9	12	8	9-15-8-6-3-2-4-12	4	60	4.00

Metaheuristics are known to be sensitive to parameter values. In problems having vast search space, improper parameter values can lead to failure in finding the global optimum solution. Hence, to better demonstrate the effect of different parameter values on the performance of FA, the optimization model is executed with the various combinations of parameter values.

It is expected that the increase in *nPop* and *z* values will affect the quality of the solutions positively. The light intensity parameter β_0 is usually taken as 1.0, and the effect of the parameters γ and α on the transit frequency setting problem is focused in this study. The parameters γ and α values are chosen from the sets $\boldsymbol{\gamma}$ ={0.1, 0.5, 1.0, 5.0 10.0 } and $\boldsymbol{\alpha}$={0.00, 0.25, 0.50, 0.75, 1.00}, respectively.

In this study, we execute three independent runs for 25 parameter combinations, which results in 75 runs of optimizations. Population size *nPop*, and the maximum number of generations *z* is set to 50 and 20, respectively. Both FA and transit assignment algorithms are coded in MATLAB. The tests are performed on an Intel Core i7 computer with 3.4 GHz CPU and 16 GB of RAM. The average execution time is approximately 10 min per run. The parameters used in the experiments are given in Table 2.

Table 2. Details of the 10-route transit network

Parameter	Value
Number of fireflies (*nPop*)	50
Light intensity (β_0)	1
Maximum generation (z)	20
Coefficient of path disutility (R)	0.1
Bus capacity (C)	50 passengers/bus
The penalty of the first transfer (c_{t1})	30 min/transfer
The penalty of the second transfer (c_{t2})	70 min/transfer
Coefficient of waiting time (c_{wt})	2
The minimum frequency allowed for lines (f_{min})	1/h
The maximum frequency allowed for all lines (f_{max})	60/h
The maximum fleet size allowed	76 buses

Fig. 2 presents the results of 75 solutions belonging to the parameter optimization, showing that FA is not successful enough in obeying the fleet size constraint. Due to the trade-off structure between the user cost and the fleet size, the user cost reduces as the fleet size increases or vice versa. Only 20 solutions are equal or below the constraint of 76 buses, while the remaining solutions are unsuccessful in mitigating the fleet size constraint. All optimization runs of the combinations {α=0.75, γ=1}, {α=1, γ=0.1}, {α=1, γ=1}, and {α=1, γ=5} can reach acceptable solutions not exceeding the fleet size constraint. However, the best combination of parameter values is {α=1, γ=1}, with a minimum average user cost of 271,503.

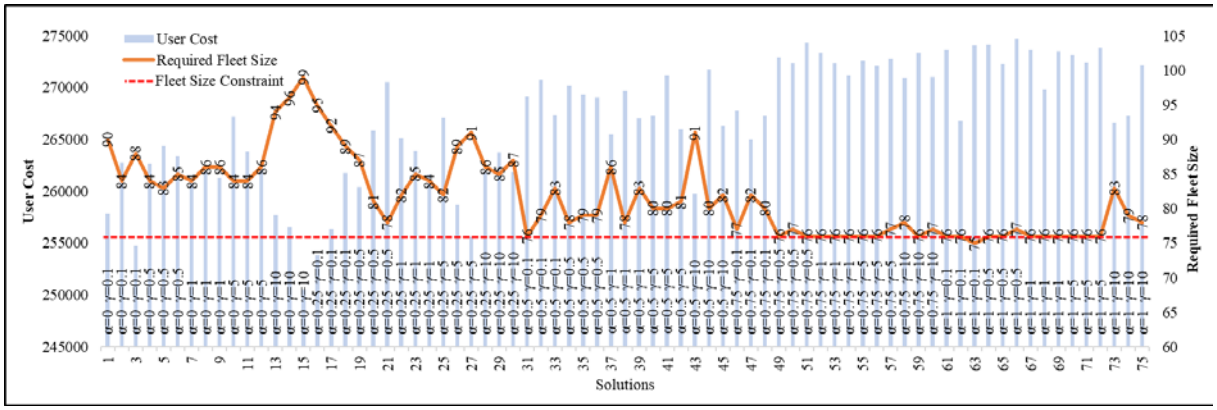

Figure 2. Comparative results of all parameter combinations in terms of required fleet size and user cost.

Fig. 3 illustrates the average fleet size and user cost values with respect to the values of α and γ. The increase in parameter α improves the quality of the solutions by decreasing the vehicle number exceeding the constraint. On the other hand, parameter γ obtains better solutions when defined as 0.5. Considering that the best combination of parameters is {α=1, γ=1}, Figs. 2 and 3 show significantly that parameter values should be treated as a combination, not individually.

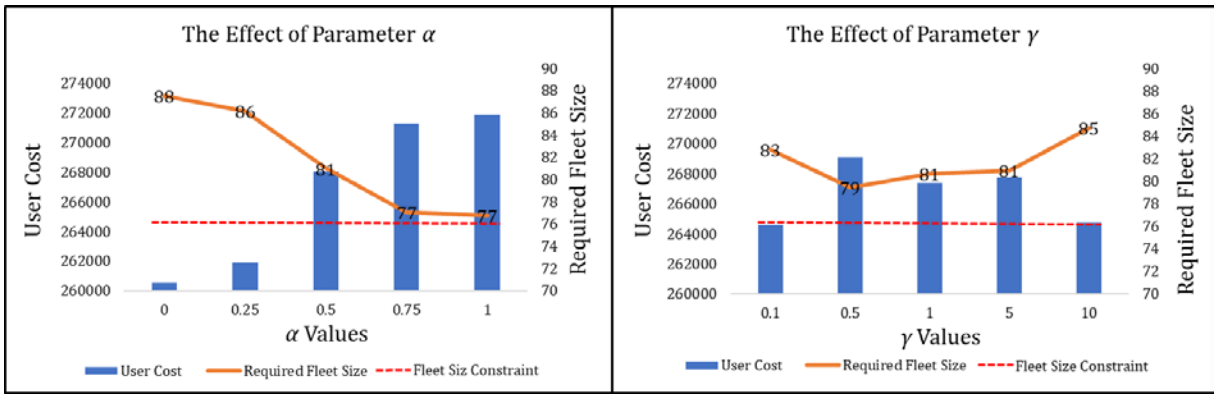

Figure 3. The effects of parameters α and γ on the quality of solutions.

To demonstrate the proposed algorithm's improvement by the calibrated parameter values in terms of stability and robustness, 30 independent optimization runs are executed by the calibrated parameter values {α=1, γ=1}. The findings of 30 runs are depicted in Fig. 4. The results clearly show that all solutions fulfill to obey the fleet constraint the contrary to the solutions in parameter optimization in Fig. 2. The best solution is obtained in 9th run with the user cost of 265,505. All 30 runs have an average user cost of 274,972, a standard deviation of 3,103, and a coefficient of variation of 1%. Details for the best solution obtained among 30 optimization runs are given in Table 3, proving that passenger loads, even in the busiest segments, do not exceed the line capacities.

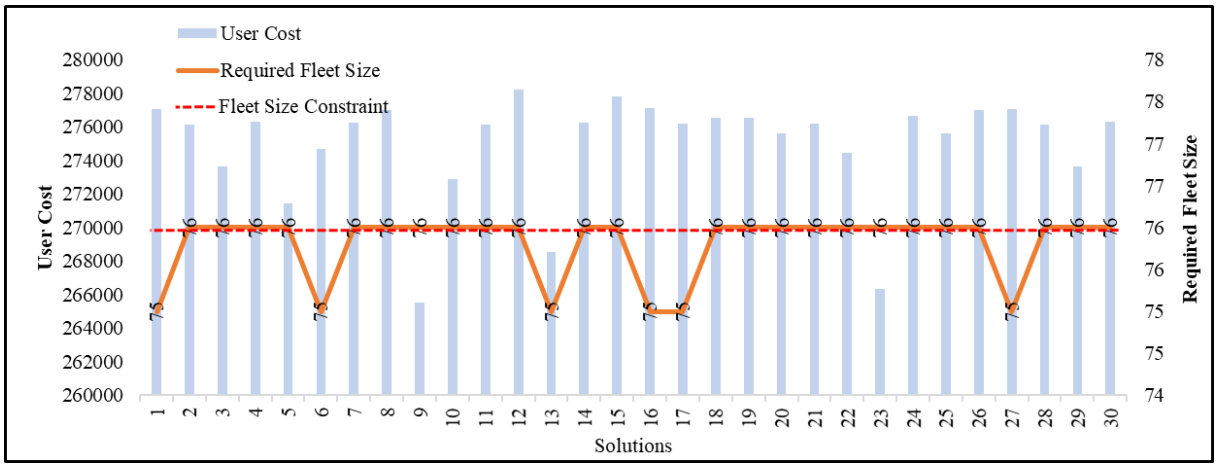

Figure 4. 30 independent runs with the calibrated parameter values.

Table 3. The corresponding details of the best frequency set obtained the calibrated parameter values

Route No	Frequency (/h)	Headway (min)	Required Buses Number	Line Capacity	Peak Segment	Max. Occupancy Rate (%)	Peak Load
1	13.78	4.35	15	689	6-8	96	665
2	8.82	6.80	9	441	10-11	96	425
3	5.73	10.47	3	286	3-2	96	276
4	1.00	60.00	1	50	6-7	34	17
5	12.96	4.63	12	648	10-8	90	581
6	5.08	11.81	5	254	1-2	81	207
7	12.52	4.79	13	626	15-6	99	624
8	16.22	3.70	12	811	8-10	94	764
9	2.36	25.42	3	118	11-12	81	95
10	3.36	17.86	3	168	6-3	81	137

Table 4 presents a comparison between the best frequency set obtained by the proposed model and the frequency set of the existing network. It should be noted that the user cost and fleet size

values of Arbex and Cunha solution are obtained by our transit assignment model and that the assignment methods of both studies are quite similar. The best frequency set generated by the proposed model provides a reduction of 4% in the user cost using the same fleet size. The results show that the frequency optimization model proposed in this study can slightly improve the solution quality. The significant changes occur in the frequency values of lines 1, 4, 5, and 8.

Table 4. Comparison of the best solutions

Solution	User Cost	Fleet Size	L1	L2	L3	L4	L5	L6	L7	L8	L9	L10
Existing frequency set	276,433	76	10.91	8.44	6.67	9.31	8.57	3.21	13.00	11.74	3.49	4.00
The best of our proposed model	265,505	76	13.78	8.82	5.73	1.00	12.96	5.08	12.52	16.22	2.36	3.36

Table 5 compares the performance outputs concerning the best frequency set of the proposed model with the performance outputs related to the frequency set of the existing network, in terms of required buses number, peak segments, line capacity, and peak load for each line. The left side of the slash gives the outputs belonging to the best frequency set of the proposed model, while the right side gives the outputs regarding the existing frequency set. The findings show a remarkable difference in the required bus number of line 4 between the solutions. The peak segments of lines are about the same for both solutions except for lines 3, 4, 7, and 9. Also, the significant difference in capacity values of lines 4, 5, and 8, which stems from frequency values, takes attention.

Table 5. Comparison of the best solutions

Lines	Required buses number	Line Capacity	Peak Load	Peak Segment
L1	15/12	689/546	665/574	6-8/6-8
L2	9/9	441/422	425/406	10-11/10-11
L3	3/4	286/334	276/287	3-2/6-3
L4	1/9	50/466	17/464	6-7/8-10
L5	12/8	648/429	581/402	8-10/8-10
L6	5/3	254/161	207/117	1-2/1-2
L7	13/13	626/650	624/607	15-6/10-7
L8	12/9	811/587	764/597	8-10/8-10
L9	3/5	118/175	95/141	11-12/1-2
L10	3/4	168/200	137/150	6-3/6-3

5. CONCLUSION AND FUTURE RESEARCH

In this study, we present an optimization model for TNFSP employing the Firefly Algorithm, which is a relatively new metaheuristic for transportation network design problems. The objective of the optimization model is to minimize the total user cost under a fleet size constraint. The proposed model is applied to Mandl's Network with 10 routes, by different combinations of parameters to show the effect of different parameter values on the quality of the solutions. The best of 30 solutions obtained by the calibrated parameter values is compared with the existing frequency set of the 10-route network.

The results show that the FA is not successful enough to satisfy the fleet size constraint in every optimization run by the randomly chosen parameter values. However, the FA can reach better solutions by selecting proper parameter values without exceeding the fleet size constraint. The best solutions are obtained with the combination of parameter values $\alpha = 1$ and $\gamma = 1$. The best

frequency set found by the proposed model slightly decreases the user cost by about 4% using the same fleet size compared to the existing frequency set of the 10-route bus network.

For future research, we plan to compare the efficiency of FA in the transit frequency setting problem with other well-known metaheuristics such as the Genetic Algorithm, Differential Evolution algorithm, and Particle Swarm Optimization algorithm. Moreover, we will use a real-sized network to test the applicability of the proposed model.

REFERENCES

[1] Farahani RZ, Miandoabchi E, Szeto WY, Rashidi H (2013). "A review of urban transportation network design problems". *European Journal of Operational Research*, 229(2), 281–302.

[2] Ceder A (2007). *Public Transit Planning and Operation: Modeling, Practice and Behavior*. Elsevier, Oxford, UK.

[3] Martinez H, Mauttone A, Urquhart ME (2014). "Frequency optimization in public transportation systems: Formulation and metaheuristic approach". *European Journal of Operational Research*, 236 (1), 27-36.

[4] Magnanti TL, Wong RT (1984). "Network Design and Transportation Planning: Models and Algorithms". *Transportation Science*, 18 (1), 1-55.

[5] Luo Z, Pang J, Ralph D (1996). *Mathematical Programs with Equilibrium Constraints*. Cambridge University Press, Cambridge, UK

[6] Yu B, Yang Z, Yao J (2010). "Genetic Algorithm for Bus Frequency Optimization". *Journal of Transportation Engineering*, 136 (6), 576-583.

[7] Yoo GS, Kim DK, Chon KS (2010). "Frequency design in urban transit networks with variable demand: Model and algorithm". *KSCE Journal of Civil Engineering*, 14 (3), 403-411.

[8] Yu B, Yang Z, Sun X, Yao B, Zeng Q, Jeppesen E (2011). "Parallel genetic algorithm in bus route headway optimization". *Applied Soft Computing Journal*, 11 (8), 5081-5091.

[9] Dell'Olio L, Ibeas A, Ruisanchez F (2012). "Optimizing bus-size and headway in transit networks". *Transportation*, 39 (2), 449-464.

[10] Huang Z, Ren G, Liu H (2013). "Optimizing bus frequencies under uncertain demand: Case study of the transit network in a developing city". *Mathematical Problems in Engineering*, 2013 (1).

[11] Wu J, Song R, Wang Y, Chen F, Li S (2015). "Modeling the coordinated operation between bus rapid transit and bus". *Mathematical Problems in Engineering*, 2015(1).

[12] Verbas IO, Mahmassani HS (2015). "Integrated Frequency Allocation and User Assignment in Multimodal Transit Networks". *Transportation Research Record: Journal of the Transportation Research Board*, 2498(1), 37-45.

[13] Giesen R, Martinez H, Mauttone A, Urquhart ME (2016). "A method for solving the multi-objective transit frequency optimization problem". *Journal of Advanced Transportation*, 50 (8), 2323-2337.

[14] Gholami A, Tian Z (2019). "The comparison of optimum frequency and demand based frequency for designing transit networks". *Case Studies on Transport Policy*, 7(4), 698–707.

[15] Mutlu MM, Aksoy İC, Alver Y (2021)." COVID-19 transmission risk minimization at public transportation stops using Differential Evolution algorithm". *European Journal of Transport and Infrastructure Research*, 21(1), 53-69.

[16] Cipriani E, Gori S, Petrelli M (2012). "Transit network design: A procedure and an application to a large urban area". *Transportation Research Part C: Emerging Technologies*, 20 (1), 3-14.

[17] Szeto WY, Jiang Y (2014). "Transit route and frequency design: Bi-level modeling and hybrid articial bee colony algorithm approach". *Transportation Research Part B: Methodological*, 67, 235-263.

[18] Nikolic M, Teodorovic D (2014). "A simultaneous transit network design and frequency setting: Computing with bees". *Expert Systems with Applications*, 41(16), 7200-7209.

[19] Zhao H, Xu W, Jiang R (2015). "The Memetic algorithm for the optimization of urban transit network". *Expert Systems with Applications*, 42 (7), 376-3773.

[20] Buba AT, Lee LS (2018). "A differential evolution for simultaneous transit network design and frequency setting problem". *Expert Systems with Applications*, 106, 277-289.

[21] Jha SB, Jha JK, Tiwari MK (2019). "A multi-objective meta-heuristic approach for transit network design and frequency setting problem in a bus transit system". *Computers and Industrial Engineering*, 130, 166-186.

[22] Duran J, Pradenas L, Parada V (2019). "Transit network design with pollution minimization". *Public Transport*, 11(1), 189-210.

[23] Uvaraja V, Lee LS (2017). "Metaheuristic approaches for urban transit scheduling problem: A review". *Journal of Advanced Review on Scientic Research*, 34 (1), 11-25.

[24] Bidar M, Sadaoui S, Moudhoub M, Bidar M (2018). "Enhanced Firefly Algorithm Using Fuzzy Parameter Tuner". *Computer and Information Science*, 11(1), 26-51.
[25] Gandomi AH, Yang XS, Talatahari S, Alavi AH (2013). "Firefly algorithm with chaos". *Commun Nonlinear Sci Numer Simulat*, 18, 89-98.
[26] Baaj MH, Mahmassani H (1991). "An AI-Based Approach for Transit Route System Planning and Design". *Journal of Advanced Transportation*, 25 (2), 187-209.
[27] Afandizadeh S, Khaksar H, Kalantari N (2013). "Bus fleet optimization using genetic algorithm a case study of Mashhad". *International Journal of Civil Engineering*, 11 (1), 43-52.
[28] Arbex RO, da Cunha CB (2015). "Effcient transit network design and frequencies setting multi-objective optimization by alternating objective genetic algorithm". *Transportation Research Part B*, 81, 355-376.
[29] Yang XS (2010). *Engineering Optimization An Introduction with Metaheuristics Applications*. Wiley, NJ, USA.

Research Article

SIGNATURE VERIFICATION USING SIAMESE NETWORK BASED ON ONE-SHOT LEARNING

Authors: Merve VAROL ARISOY

To cite to this article: Varol Arısoy, M. (2021). SIGNATURE VERIFICATION USING SIAMESE NEURAL NETWORK ONE-SHOT LEARNING. International Journal of Engineering and Innovative Research ,3(3), p: 248-260. DOI: 10.47933/ijeir.972796

DOI: 10.47933/ijeir.972796

To link to this artice: https://dergipark.org.tr/tr/pub/ijeir/archive

International Journal of Engineering and Innovative Research

http://dergipark.gov.tr/ijeir

SIGNATURE VERIFICATION USING SIAMESE NETWORK BASED ON ONE-SHOT LEARNING

Merve VAROL ARISOY[1*]

1Mehmet Akif Ersoy University, Department of Informatics, Burdur, Turkey.

*Corresponding Author: mvarisoy@mehmetakif.edu.tr

https://doi.org/10.47933/ijeir.972796

(**Received:** 30.05.2021; **Accepted:** 04.07.2021)

ABSTRACT: With the acceleration of digitalization in all areas of our lives, the need for biometric verification methods is increasing. The fact that biometric data is unique and biometric verification is stronger against phishing attacks compared to password-based authentication methods, has increased its preference rate. Signature verification, which is one of the biometric verification types, plays an important role in many areas such as banking systems, administrative and judicial applications. There are 2 types of signature verification, online and offline, for identifying the identity of the person and detecting signature forgery. Online signature verification is carried out during signing and temporal dynamic data are available regarding the person's signature. Offline verification is applied by scanning the image after signing, and this verification is limited to spatial data. Therefore, the offline signature verification process is considered a more challenging task.

In this study, offline signature verification, independent of the writer, based on One-Shot Learning, was performed using Siamese Neural Network. Due to the fact that the Deep Convolution Neural Network requires a large amount of labeled data for image classification, real and fake signature distinction has been achieved by using the One-Shot Learning method, which can perform a successful classification by using less numbers of signature images. As a result of the experiments conducted on signature datasets, using the Siamese architecture, the proposed approach achieved percentage accuracy of 93.23, 90.11, 89.99, 92.35 verification in 4NSigComp2012, SigComp2011, 4NSigComp2010 and BHsig260 respectively.

Keywords: Offline Signature Verification, Siamese Neural Network, One-Shot Learning, Machine Learning, Deep Learning.

1. INTRODUCTION

Depending on the rapid development of technology, many transactions have become realizable through the use of the internet. These transactions include personal transactions such as banking and e-state transactions. During the execution of such transactions, it is absolutely necessary to make sure that the transactions are carried out with the right person. And this verification can be carried out by using biometric and behavioral verification techniques.

Biometric and behavioral features are used especially in cases where authentication and security are required to be in a high level. Biological features such as face, fingerprint, palm, iris, retina

and behavioral features such as signature and voice can be given as examples for them. Especially with the development of GPUs and accordingly the developments in artificial intelligence algorithms, the use of biometric and behavioral features for authentication purposes in every field has become widespread. In the upcoming period, the application and usage areas of these verification techniques will expand further with the developments in quantum programming and, accordingly, in quantum machine learning topics.

At this point, signature, which is a type of behavioral biometric verification, is used at many points in daily life for authentication and confirming that the related person does the relevant job. For this reason, being able to distinguish between real and fake signature is highly important in terms of both verifying the identity of the related person and confirming that the related person does the relevant work. Signature verification is divided into online and offline signature verification. In offline signature verification, verification is performed by comparing an existing signature with reference signatures previously obtained from the relevant person. At this point, the document, on which the person has put the signature at that moment, is first scanned and converted into image format, then the signature is defined and verified from within this document. Two approaches are used for offline signing. These are writer-dependent and writer-independent approaches. In the writer-dependent approach, a separate model is created for each author, whereas in the writer-independent approach, it is used by creating a single model for all authors. In online signature verification, the signature is put on a tablet or monitor; therefore, features such as pen pressure and pen slope angle can also be analyzed. Therefore, in online signature verification, first of all, individuals' signatures are recorded in the system at the registration stage, with data preprocessing and feature extraction methods. Afterwards, when the user puts the signature again, the same attributes are extracted and compared with the reference signature features. If the difference is below a specified threshold value, it is accepted, otherwise it is rejected [7].

With the development of technology and the increase in security needs, the authentication methods have also differentiated. One of the authentication methods to be used is offline and online signature verification methods. Identifying these signatures, with high accuracy, in all transactions that people will make by using their signatures will be of great importance in terms of the correct progress of the process in all areas of life. Therefore, One-Shot Learning based Siamese Neural Network is proposed in this study for offline signature verification, and the performance of this method has been tested on four different datasets and the results have been shared.

In the following sections of the article, literature review, smart city applications, machine learning, Siamese network and One-Shot Learning-based signature verification mechanism and conclusion section, respectively, are included.

2. RELATED WORKS

Signature verification, which is one of the types of biometric verification, plays an important role in many areas such as banking systems, administrative and judicial applications, where users are required to have their authentication made. Signatures of individuals are unique to them, as in the example of fingerprints, and only by means of the signature, it can be determined who owns an official document or by whom it has been approved. However, although the way of signing is unique to the individual, a person's signature can be imitated as a result of a

sufficient number of attempts. Machine learning and deep learning methods were used so as to prevent this threat and also to distinguish between real and fake signatures.

Signature verification can be carried out online and offline. There are studies related to the both methods in the literature. In study [1], they examined the spatial-temporal adaptation of the Siamese neural network. According to this, they extracted spatial features using 1-dimensional CNN (Convolutional Neural Network) and also included the input in the temporal field by using LSTM (Long Short-Term Memory) networks. Similarly, in [2], they also used this method in the process of signature verification because the Siamese network provides effective classification results with a small number of learning inputs.

In the work of [3], a time-based recurring neural network approach for the solution of the online signature verification problem is proposed. They combined Dynamic Time Warping with the RNN network to create powerful models that can better distinguish fake signatures. On the other hand in study [4], they created an architecture, independent from convolutional neural network-based language, for the signature verification process. Their architecture, named sCNN (Shallow Convolutional Neural Network), has three convolutional layers and one fully connected layer. The model, which they trained, is quite simple in terms of the number of base layers, unlike other advanced methods; therefore, they optimized fewer number of weight parameters. The model includes few numbers of layers and parameters that reduced the time to be spent on training and testing. They stated that the sCNN model gave better results in terms of accuracy and error rate compared to other methods.

In the work of [5], they developed an application on offline signature verification by establishing the Siamese Network, in which the Convolutional Neural Network used as a subnet. In the Siamese network, they aimed to make the real-fake signature distinction more accurately by adding some statistical features to the embedding vector, which is the mathematical expression of each signature image. In the study of [6], it is shown that the RNN network could be used for the solution the online signature verification problem. They used the model, which they established, in online signature verification by combining RNN LSTM and Siamse Network. By extracting the similarity metric between the two signature samples, they enabled the model to learn this. They were also able to classify a signature image which was previously unlearned by their system. Similarly, in [7] and in [8], the Siamese network is also applied in the field of offline signature verification.

In study [9], offline signature verification and signature identification by comparing 2 different models of RNN and CNN, is examined. The RNN models, were based on LSTM and BLSTM. These two models outperformed the model, which they created with CNN. In the work of [10], they proposed combining EEG signals and offline signature samples by using a multimoded Siamese Neural Network (mSNN) for enhanced user verification. mSNN networks learn distinctive temporal and spatial features from EEG signals by using an EEG encoder and from offline signatures by using a video encoder. These two encoders were combined in a common feature field for further procedures. They used a distance measure based on similarity and difference of input features to generate validation results in the Siamese network.

In [11], it is determined that the desired success rate could not be achieved on account of the insufficient dataset required for training in the signature verification process. Therefore, they proposed a new use of Cycle-GAN, which is a data augmentation method, in their study. They tested the data augmentation methods on CNN-based VGG16, VGG19, ResNet50 and DenseNet121 models, which are widely used in the literature. As a result of experiments, they

observed that data augmentation methods increased the success of all CNN models in the offline signature database. In the work of [12], it is focused on offline signature verification by using the artificial neural network approach. They used geometric features for offline verification of signatures. Among these features, there are such functions as Baseline Slope Angle (BSA), Aspect Ratio (AR) and Normalized Area (NA) and Center of Gravity Extraction.

In the study of [13], it is aimed to learn difference metrics from signature image pairs by combining writer-independent online signature verification systems, RNN network with Siamse architecture. Furthermore, they tried Short-Term Memory (LSTM) and Gated Recurrent Unit (GRU) systems with Siamse architecture in order to measure the effectiveness of different network structures. As a result of their studies, they determined that the Siamese network outperformed state-of-the-art online signature verification systems using the same database.

In [14] they developed a deep learning-based online signature verification system. They used Legendre polynomial coefficients as a feature in order to model the signatures. They classified the signature images with a deep feedforward neural network and used the stochastic gradient descent algorithm with momentum as a deep learning algorithm. As a result of their studies during which they used the SigComp2011 dataset, they observed a decrease in the error rate and an increase in the accuracy rate.

In the study [15], they proposed a new single-template strategy that uses averaging templates and local stability weighted dynamic time warping (LS-DTW) to simultaneously improve the speed and accuracy of online signature verification in order to meet the latest demands for automated security systems. In this method, which is called Euclidean centroid-based DTW centroid average, it was adopted to obtain an effective average template set for each feature while maintaining intra-user variability among reference samples. Afterwards, the local stability of the average template set was estimated by using the matching points between the average template set and references. Later, they increased the discrimination ability at the verification stage by using the LS-DTW distance measure between the average template set and a query signature. According to the results they obtained, they reported that their method was effective in both random and fraud scenarios.

In the study [16], they proposed a system that uses a score-level combination of complementary classifiers using different local features (histogram of oriented gradients, local binary patterns, and scale-invariant feature transformation descriptors) for offline signature verification. They adopted two different approaches for the classification task; these were universal and user-dependent classifiers. While user-dependent classifiers are trained individually for each user to learn to distinguish a user's real signature from other signatures, the universal classifiers are trained with the difference vectors of the query and reference signatures of all users in the training set to learn the differences. With the fusion of all classifiers, they achieved an equal error rate of 6.97% in qualified forgery tests. In [17], it is pointed out that there were not enough studies on providing model training using small-scale sampling in offline signature recognition. Therefore, in their studies, they presented a new convolutional neural network (CNN) structure called Large-Scale Signature Network (LS2Net) with collective normalization to overcome the large-scale training problem. They also proposed the Class Center Based Classifier (C3) algorithm based on KNN. They stated that they got better results when special designs were made for datasets in their networks, where they used the Leaky ReLU structure.

In [18], a new grid-based template matching scheme for offline signature analysis and verification is proposed. Their method is based on efficient encoding of the geometric structure

of signatures with grid templates that are properly partitioned into subsets. In [19], they developed an online signature verification approach based on writer-specific features, and an again on writer-specific classifier. Which features would best suit the author and which classifier would be used to verify the author were taken according to the error rate obtained with the training samples. Experimental results indicated the effectiveness of the features they had used for online signature verification, depending on the author. Moreover, they also noted that the error rate was lower, when compared to many existing contemporary studies, on online signature verification, especially when the number of existing training examples for each author was sufficient.

Machine learning methods are also used in signature verification systems. In machine learning-based signature verification processes, first of all, the model is trained with real and fake signature samples. Then, the similarity ratio between the fake signature being questioned and any signature sample in the training set is tried to be determined. In the continuation of the article, studies carried out using machine learning algorithms are given.

In the study of [20], a method which based on learning and encoding of rare words as a tool in providing feature field for offline signature verification is propsed. They used the K-SVD dictionary learning algorithm to create a writer-oriented dictionary. When they tested their sparse representation-based methods with the SVM classifier, they obtained successful results for the validation problem.

In [21] they created a writer-independent signature verification system by using single-class SVM. Upon noticing that SVM-based classification could make accurate classification in the presence of a large sample and that that success decreased when they reduced the sample size, they carefully adjusted the optimum threshold by combining the different distances between the signature samples, thus, they tried to achieve correct classification success with less samples.

In [22] they conducted an application to identify attacks developed against offline signature verification systems. In their applications, they aimed to determine the threats to offline handwriting signature verification with Contradictory Machine Learning method and to find the effect of conflicting samples on biometric systems. In study of [23], an online and offline signature verification model based on pixel density levels were proposed. For the signature verification process, a comparative analysis was performed using classifiers such as decision tree, Naive Bayes and KNN. As a result of their studies in which they used the DWT method for feature extraction, they achieved a classification success of 99.90% with decision trees, 99.82% with Naive Bayes and 98.11% with KNN.

In [24] they proposed a system that is made of combination of signature verification, machine learning, IoT and blockchain technologies so as to cope with the risk of identity theft that may occur during online trading. In their system, the signals of roll, slope and deviation values received from the MPU6050 sensor (Inertial Measurement Unit) are analyzed by using Digital Time Wrapping in order to obtain the DTW minimum distance in authentication of the user. When it comes to cryptocurrencies, they mention about a system design in which the private key is not stored, but the same unique private key assigned to the user by the Blockchain is generated each time by using a method involving biometrics and machine learning.

In [25] they applied the AlexNet, which is a convolutional neural network algorithm, so as to recognize the offline Chinese signature. Depending on the writer, they managed to distinguish

between real and fake signatures. They concluded that classification success of AlexNet's was higher than that of SVM.

In study [26], they mentioned a small 3-layer deep convolutional neural network, trainable parameters of which are several times less than those of previously reported in the literature, so as to verify the offline signature. They used these networks with 2 different configurations. In the first one, they used it for a feature extractor function in a hybrid classifier. And in the second one, they used it as an end-to-end classifier in a Siamese network. In the hybrid classifier scheme, they used the support vector machine in order to verify the authenticity of the signature.

In [27], a new approach for online signature verification based on machine learning method is presented. In the method they proposed, they considered the average values of the attributes for validation. They enabled that features such as x and y coordinates, timestamp, pen ups and downs, azimuth, elevation and pressure, which they used, were learned by different classifiers (Naive bayes, J48, MLP, PART, Bayes Net, random forest and random tree).

3. Methods

In this section, CNN and Siamese Network, One-Shot Learning, pre-processing steps carried out on signature images, architecture formed for offline signature verification problem, respectively, are mentioned.

3.1. CNN (Convolutional Neural Networks, CNN) and Siamese Network

CNN is among the most successful and widely used architectures in the deep learning community, especially for computer vision tasks. CNN architecture usually consists of 3 layers. The first one is the convolutional layer, in which a kernel (or filter) of the weights is convoluted so as to extract the features. The second one is the nonlinear layer, which applies an enable function to the feature maps, thereby enabling the network to model nonlinear functions. And the third one is the pooling layer, which reduces spatial resolution by replacing neighborhoods in a feature map with some statistical information about these neighborhoods (average, max, etc.). The neural units in the layers are locally interconnected. Each layer of the CNN carries the input to an output of neuron activation, thus creating fully connected layers. After all these things, the input data is matched to a 1-dimensional feature vector [30-31].

The Siamese neural network is a network architecture that includes 2 identical subnets. Twin CNN's have an equal configuration, where the same parameters and shared weights are combined with a distance metric. In the event of a parameter update, this case is reflected in both subnets. In this architecture type, one of the twin networks takes a real signature image as input and the other one takes a signature image that is requested to be verified by the model as input. Afterwards, each twin network does a feature extraction based on the given input. Finally, the difference (similarity-difference) of the features extracted by each of the twin networks is found by calculating the distance metric with the loss function applied in the last output layer. The contrastive loss, which is a loss function mostly used in Siamese networks, is defined in (1) [35]. Since the Siamese architecture yields successful results in the scenarios of comparing the similarities of the picture images, this architecture has been specially preferred.

$$L(s_1, s_2, y = \propto (1-y)D_w^2 + \beta y \max(0, m - D_w)^2) \quad (1)$$

The s1 and s2 values included here represent the signature images in the input and y is a binary indicator function that indicates whether two examples belong to the same class or not. α and β are two constants, and m is the numerator. $D_w = ||f(s_1; w_1) - f(s_2; w_2)||_2$ is the Euclidean distance. f is the embedding function that matches a signature image with a real vector space through CNN. w1, w2 are the learned weights for a particular layer of the network [35].

According to the Siamese network, it is expected that feature vectors of image pairs belonging to the same class are closer to each other, while feature vectors of image pairs belonging to different classes are far from each other. In the last stage of this architecture, a threshold value is determined in the distance metric calculated and it is decided whether the 2 images belong to the same class or not [35].

3.2. One-Shot Learning

The Siamese network supports the One-Shot way of learning. In one-shot learning, learning can be done from a single input image and a single target image [35]. While most machine learning-based object classification algorithms require making training by using a large number of sample images, in One-Shot learning, it is aimed to obtain information about classes with one or more images from each object category [36].

In order to create a model in one-shot assisted image classification, first of all, a neural network that can distinguish the class identities of image pairs must be learned. This step constitutes the image validation step. The validation model learns the probability that the input pairs belong to the same class or to different classes, in other words, the similarity-difference ratios. Later, it is subjected to one-shot classification by using the network that is successful in the verification process. In the one-shot phase, an image pair is created with the test image and the image belonging to the new class and evaluated by the previously learned model, and it is decided whether the image is a real-fake signature [37].

In the network architecture established in this study, first of all, image vectors were learned with a supervised metric-based approach, and then the features of this network were re-used with on-shot learning without the need for retraining. The method adopted for the solution of the signature verification problem is given in Figure 1.

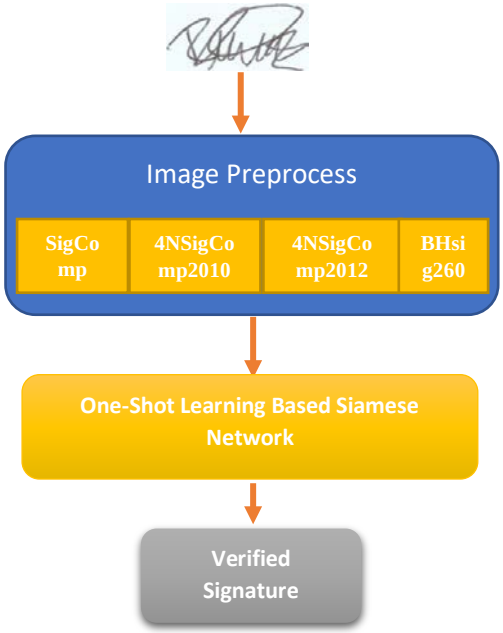

Figure 1. Solution Steps of the Signature Verification Problem

3.3. Pre-processing

Primarily, the "bounding box" method, known as the bounding box, and enabling the excess background images to be clipped, was applied on the used image set. Since in the generated neural network, training in the form of a stack is made, it is essential that the images to be used as input be standard in size. Therefore, sizing process was performed on the signature images. In order for the learning algorithm to better understand the features of the picture, the "binary thresholding" method, which converts the signature images into binary, was applied to each pixel in the signature image. Afterwards, the images were inverted so that the pixel values of the background could be 0. In the normalization process performed on the image, the standard deviation of the pixel values was achieved as a result of dividing these values. The pre-processing step was carried out on both the test and training set. Figure 2 shows the preprocessing steps.

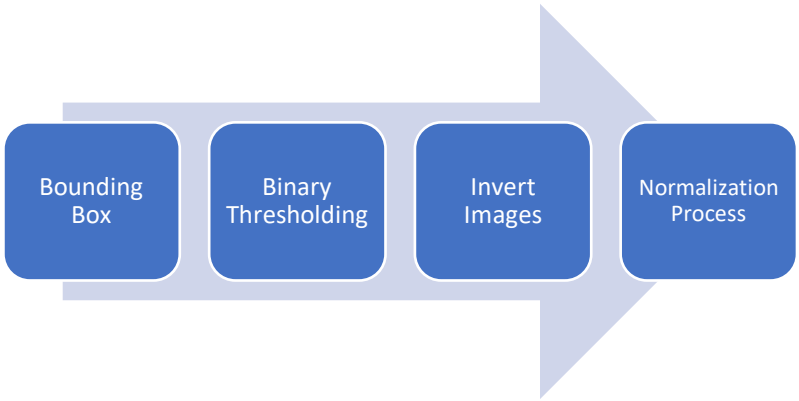

Figure 2. Preprocess Steps of Images

3.4. Network Architecture

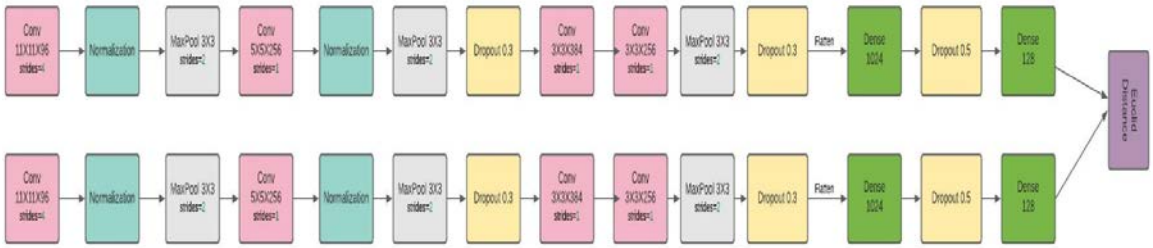

Figure 3. Siamese Network Architecture

In the established network architecture, a basic CNN was created with 4 convolution layers and then 2 fully-connected layers. Nuclei and neuron numbers are shown in Figure 3. Relu (Rectified Linear Units) is used as the activation function in all convolutional and fully-connected layers throughout the network. Each layer has a valid padding. Also, each block of convolutional layers is followed by a max-pooling layer with a filter size and stride of 2. The fully-connected layer in the last step represents the 128-neuron embedding vector of the input signature image. The 2 pairs of images given to the network are labelled with 1 if they are in the same class and labelled with 0 if they are in different classes. This situation is stated in the equation in (2).

$$f(x) = \begin{cases} 1 \ldots if\ (s1, s2)\ (Genuine, Genuine) \\ 0 \ldots if\ (s1, s2)\ (Genuine, Forged) \end{cases} \quad (2)$$

4. Experiments

The developed signature verification algorithm has been tested on SigComp2011, BHSig260, 4NSigComp2010 and 4NSigComp2012 datasets.

4.1. SigComp2011

This dataset was published for the International Signature Verification Competition (SVC) at the ICDAR 2011 conference. The dataset includes online and offline signatures of Chinese and Dutch writers. In the study performed, the offline signatures of the SigComp2011 dataset belonging to the Chinese writers were used for both training and testing purposes. In the sub-dataset consisting of Chinese signatures, the training set contains 576 images for 10 identities, approximately 25 real signatures for each identity and 30 fake ones. The Chinese test set of the SigComp2011 dataset consists of 2 subsets as “reference” and “questioned”. Here, the reference set consists of real signatures and the questioned set consists of both real and fake signatures [32]. 576 signatures of this dataset, consisting of both real and fake signatures, 80% were used for training and 20% for verification. The signatures reserved for testing, 10% of those in both the "reference" and "questioned" folders were used for testing purposes.

4.2. BHsig260

The BHSig260 signature dataset contains the signatures of 260 persons, among them 100 subsets of the set consist of Bengali signatures and 160 subsets consists of Hindi signatures. There are 6240 real signatures and 7800 qualified fake signatures in the whole set. Each identity has 24 real and 30 qualified fake signatures. Also, for each of the signers, 24 genuine and 30

forged signatures are available. This results in 100x24 = 2400 genuine and 100x30 = 3000 forged signatures in Bengali, and 160x24 = 3840 genuine and 160x30 = 4800 forged signatures in Hindi [38]. In the conducted study, both Hindi and Bengali signatures were used separately for training and testing. Real and fake signatures of all authors in both the Bengali dataset and the Hindi dataset were used for training and testing purposes. In other words, some of the authors were not allocated for training and the rest for testing. Accordingly, 70% of the 2400 real signatures in the Bengali dataset were used for training, 20% for verification and the rest for testing. This separation format is also adopted for the Hindi dataset.

4.3. 4NSigComp2010

This dataset consists of offline signature images. The signature collection for education includes 209 images. Signatures consist of 9 reference (real) signatures and 200 queried signatures belonging to the same writer. In 200 query signatures, there are 76 real signatures written by the reference writer and 104 simulated/fake signatures (written by 27 fraudsters freely copying the reference writer's signature features). The remaining 20 signatures are masked signatures written by the reference writer. Masking process involves an attempt to deliberately alter the signature of the reference writer so as to avoid being identified. The simulation/forgery process involves an attempt by a person to imitate the reference signature features of a genuine original writer.

This dataset contains 125 signature collections for testing. The signatures consist of 25 reference signatures and 100 queried signatures, this time belonging to another writer, apart from the writer for training. Of 100 query signatures, there are 3 real signatures written by the reference writer in normal signature style and 90 simulated signatures (freely typed by 34 fraudsters copying the reference writer's signature features). Moreover, there are 7 masked signatures written by the reference writer [33]. Of the part of this dataset reserved for training, 70% was used for training and 30% was used for validation. 20% of the part reserved for testing was used for testing purposes.

4.4. 4NSigComp2012

The training set of this dataset consists of the training and test set of 4NsigComp2010. In total, it includes the signatures of two examples writers. The first writer has 9 reference signatures and 200 queried signatures. Of these 200 queried signatures, 76 are real, 104 are forgery/fake and 20 are masked. And for the second writer, there are 25 reference signatures and 100 queried signatures. Of these 100 queried signatures, 3 are real, 90 are forgery/fake and 7 are masked.

The test set includes signature samples of belonging to 3 different writers. Query signatures consists of a mixture of real signatures, disguised signatures, and qualified frauds [34]. 90% of the part of this dataset reserved for training was used for training and 10% for validation. 20% of the part reserved for testing was used for testing purposes.

5. Results

In Table 1, the success results, which were obtained as a result of the One-Shot Learning-based Siamese Network method applied in solving the writer-independent offline signature verification problem, are given. Trials were applied separately for each dataset. Furthermore, real and fake signature pairs were used both when calculating accuracy and when comparing the similarity of 2 signature images. In the training conducted on each dataset, random signature pairs belonging to that dataset were selected. The performance evaluation of the offline signature verification task is not case having a standard. Because the way the training set given to the model is created, in other words, how much of it will be reserved for real and fake signatures, or how different datasets will be combined so as to obtain a new dataset is a completely personal application, the signature verification process is not a uniform task.

Table 1. Dataset values

Dataset	Accuracy	FAR	FRR
4NSigComp2010	89.99	10.22	8.33
SigComp2011	90.11	7.89	6.42
4NSigComp2012	93.23	6.77	7.02
BHsig260-Bengali	91.17	9.83	8.27
BHsig260-Hindi	92.35	8.92	7.65

Table 2 shows the accuracy of our proposed work together with other state-of-the-art methods on different datasets discussed in subheadings of Section 4.

Table 2. Comparison of the proposed work with the state-of-the-art methods on various signature databases

Databases	***State of art Methods***	***Accuracy***
SigComp2011	Ref [12]	82.5%
SigComp2011	Ref [39]	88%
SigComp2011	**Our proposed work**	**90.11%**
Bengali	Ref [7]	86.11%
Hindi		84.64%
Bengali	Ref [38]	66.18%
Hindi	Ref [38]	75.53%
Bengali	Ref [40]	84.90%
Hindi	Ref [40]	85.90%
Bengali	Ref [26]	75.06%
Hindi	Ref [26]	89.33%
Bengali	**Our proposed work**	**91.17%**
Hindi	**Our proposed work**	**92.35%**
4NSigComp2012	Ref [41]	88%
4NSigComp2012	**Our proposed work**	**93.23%**

5.1. Evaluation Protocol

A threshold value was used so as to detect whether signature pairs belong to the same class or not. Provided that the difference (dissimilarity ratio) between the two images is less than the threshold value (0.42), these two signatures are considered real-real, but provided that the difference is greater than the threshold value, these two signatures are considered real-fake. Performance assessment of the model was carried out by using accuracy (accuracy), FAR (False Acceptance Rate), FRR (False Rejection Rate) metrics. According to this, FAR and FRR calculations are as they are shown in (3) and (4), respectively.

$$FAR = \frac{Number\ of\ forged\ Pairs\ accepted\ as\ a\ geniune\ pairs}{T\ otal\ number\ of\ Forged\ Pairs\ submitted} \times 100 \quad (3)$$

$$FRR = \frac{Number\ of\ Geniune\ Pairs\ rejected}{Total\ number\ of\ Geniune\ Pairs\ submitted} \times 100 \quad (4)$$

6. Conclusion

In this study, an effective writer-independent offline signature verification task was performed by establishing a One-Shot Learning-based Siamese network. The aim of the study is to distinguish between real and fake signatures. Experiments were conducted on the 4NSigComp2010, SigComp2011, 4NSigComp2012, BHsig260 datasets. The model was also able to be distinguishing for new signatures without the need for any re-training. High accuracy rates were obtained on all datasets that were used. The largest of these ratios is the one on the 4NSigComp2012 dataset. As a new study in the future, through GAN (Generative Adversarial Neural Networks) architecture, which will be created by using the same datasets, it is planned to distinguish between real signatures and those signatures produced in a forged way.

REFERENCES

1. Ghosh, S., Ghosh, S., Kumar, P., Scheme, E., Roy, P.P. (2021). A novel spatio-temporal Siamese network for 3D signature recognition. Pattern Recognition Letters. 144, 13-20.
2. Jain, S., Khanna, M., Singh, A. (2021). Comparison among different CNN Architectures for Signature Forgery Detection using Siamese Neural Network. In: 2021 International Conference on Computing, Communication, and Intelligent Systems (ICCCIS), pp. 481-486. IEEE Press, Greater Noida, India
3. Tolosana, R., Vera-Rodriguez, R., Fierrez, J., Ortega-Garcia, J. (2021). DeepSign: Deep On-Line Signature Verification. Ieee Transactions On Biometrics, Behavior, And Identity Science. 3, 229-239
4. Jain, A., Singh, S.K., Singh, K.P. (2020). Handwritten signature verification using shallow convolutional neural network. Multimed Tools Appl. 79, 19993-20018.
5. Jagtap A.B., Sawat D.D., Hegadi R.S., Hegadi R.S. (2019). Siamese Network for Learning Genuine and Forged Offline Signature Verification. In: Recent Trends in Image Processing and Pattern Recognition. RTIP2R 2018, pp. 131-139.
6. Tolosana, R., Vera-Rodriguez, R., Fierrez, J., Ortega-Garcia, J. (2017). Biometric Signature Verification Using Recurrent Neural Networks. In: 14th IAPR International Conference on Document Analysis and Recognition (ICDAR), pp. 652-657. Kyoto, Japan
7. Dey, S., Dutta, A., Toledo, J.I., Ghosh, S.K., Llados, J., Pal, U. (2017). SigNet: Convolutional Siamese Network for Writer Independent Offline Signature Verification. Pattern Recognition Letters. 1-7.
8. Ruiz, V., Linares, I., Sanchez, A., Velez, J.F. (2020). Off-line handwritten signature verification using compositional synthetic generation of signatures and Siamese Neural Networks. Neurocomputing. 374, 30-41.
9. Ghosh, R. (2021). A Recurrent Neural Network based deep learning model for offline signature verification and recognition system. Expert Systems with Applications. 168.
10. Chakladar, D.D., Kumar, P., Roy, P.P., Dogra, D.P., Scheme, E., Chang, V. (2021). A multimodal-Siamese Neural Network (mSNN) for person verification using signatures and EEG. Information Fusion. 71, 17-27.
11. Yapıcı, M.M., Tekerek, A., Topaloğlu, N. (2021). Deep learning-based data augmentation method and signature verification system for offline handwritten signature. Pattern Anal Applic. 24, 165-179.
12. Tahir, N.M., Ausat, A.N., Bature, U.I., Abubakar, K.A., Gambo, I. (2021). Off-line Handwritten Signature Verification System: Artificial Neural Network Approach. 1, 45.57.
13. Tolosana, R., Vera-Rodriguez, R., Fierrez, J., Ortega-Garcia, J. (2018). Exploring Recurrent Neural Networks for On-Line Handwritten Signature Biometrics. in IEEE Access. 6, 5128-5138
14. Hefny, A., Moustafa, M. (2019). Online Signature Verification Using Deep Learning and Feature Representation Using Legendre Polynomial Coefficients. In: n book: The International Conference on Advanced Machine Learning Technologies and Applications AMLTA, pp. 689-697.

15. Okawa, M.: Time-series averaging and local stability-weighted dynamic time warping for online signature verification. Pattern Recognition. 112, (2021)
16. Yılmaz, M.B., Yanıkoğlu, B. (2016). Score level fusion of classifiers in off-line signature verification. Information Fusion. 32, 109-119.
17. Calik, N., Kurban, O.C., Yilmaz, A.R., Yıldırım, T., Durak, A.L. (2019). Large-scale offline signature recognition via deep neural networks and feature embedding. Neurocomputing, 359, 1-14.
18. Zois, E.N., Alewijnse, L., Economou, G. (2016). Offline signature verification and quality characterization using poset-oriented grid features. Pattern Recognition. 54, 162-177.
19. Manjunatha, K.S., Manjunath, S., Guru, D.S., Somashekara, M.T. (2016). Online signature verification based on writer dependent features and classifiers. Pattern Recognition Letters. 80, 129-136.
20. Zois, E.N., Theodorakopoulos, I., Tsourounis, D., Economou, G. (2017). Parsimonious Coding and Verification of Offline Handwritten Signatures. In: 2017 IEEE Conference on Computer Vision and Pattern Recognition Workshops (CVPRW), pp. 636—645. Honolulu, HI, USA.
21. Guerbai, Y., Chibani, Y., Hadjadji, B. (2015). The effective use of the one-class SVM classifier for handwritten signature verification based on writer-independent parameters. Pattern Recognit., 48, 103-113.
22. Hafemann, L.G., Sabourin, R., Oliveira, L.S. (2019). Characterizing and Evaluating Adversarial Examples for Offline Handwritten Signature Verification. IEEE Transactions on Information Forensics and Security. 14, 2153-2166.
23. Shah, A.S., Khan, M.A., Subhan, F., Fayaz, M., Shah, A. (2016). An offline signature verification technique using pixels intensity levels. International Journal of Signal Processing, Image Processing and Pattern Recognition. 9, 205-222.
24. Jain, V., Chaudhary, G., Luthra, N., Rao, A., Walia, S. (2019). Dynamic handwritten signature and machine learning based identity verification for keyless cryptocurrency transactions. Journal of Discrete Mathematical Sciences and Cryptography. 22, 191-202.
25. Wencheng, C., Xiaopeng, G., Hong, S., Limin, Z. (2018). Offline Chinese Signature Verification Based on AlexNet. In: International Conference on Advanced Hybrid Information Processing ADHIP 2017: Advanced Hybrid Information Processing, pp. 33-37.
26. Rateria, A., Agarwal, S. (2018). Off-line Signature Verification through Machine Learning. In: 2018 5th IEEE Uttar Pradesh Section International Conference on Electrical, Electronics and Computer Engineering (UPCON), Gorakhpur, India.
27. Chandra, S. (2020). Verification of dynamic signature using machine learning approach. Neural Comput & Applic. 32, 11875-11895.
30. Minaee, S., Boykov, Y., Porikli, F., Plaza, A., Kehtarnavaz, N., Terzopoulos, D. (2020). Image Segmentation Using Deep Learning: A Survey. arXiv.
31. Voulodimos, A., Doulamis, N., Doulamis, A., Protopapadakis, E. (2018) Deep Learning for Computer Vision: A Brief Review. Comput Intell Neurosci.
32. Liwicki, M., Blumenstein, M., Heuvel, E., Berger, C.E.H, Stoel, R.D., Found, B., Chen, X., Malik, M.I. (2011). Sigcomp11: signature verification competition for on- and offline skilled forgeries, In: 11th Int. Conf. Document Anal Recognit.
33. Malik, M.I. (2010). ICFHR 2010 Signature Verification Competition (4NSigComp2010).
34. Liwicki, M., Malik, M.I., Alewijnse, L., Heuvel, E., Found, B. (2012). ICFHR 2012 Competition on Automatic Forensic Signature Verification (4NsigComp 2012). In: 2012 International Conference on Frontiers in Handwriting Recognition, pp. 823-828. Bari, Italy.
35. Jagtap, A.B., Sawat, D.D., Hegadi, R.S. et al. (2020). Verification of genuine and forged offline signatures using Siamese Neural Network (SNN). Multimed Tools Appl. 79, 35109-35123.
36. One-shot learning, https://en.wikipedia.org/wiki/One-shot_learning
37. Koch, G., Zemel, R., Salakhutdinov, R. (2015). Siamese neural networks for one-shot image recognition. In: ICML deep learning workshop.
38. Pal, S., Alaei, A., Pal, U., Blumenstein, M. (2016). Performance of an Off-Line Signature Verification Method Based on Texture Features on a Large Indic-Script Signature Dataset. In: 2016 12th IAPR Workshop on Document Analysis Systems (DAS), pp. 72-77.
39. Alvarez, G., Sheffer, B., Bryant, M. (2016). Offline Signature Verification with Convolutional Neural Networks. In: Technical Report. Stanford University, Stanford.
40. Dutta, A., Pal, U., Llad´os, J. (2016). Compact correlated features for writer independent signature verification, In: ICPR, pp. 3411–3416.
41. Butt, U.M., Masood, F., Unnisa, Z., Razzaq, S., Dar, Z., Azhar, S., Abbas, I., Ahmad, M. (2020). A Deep Insight into Signature Verification Using Deep Neural Network. IntelliSys.